Validation of innovative digital microscopes for the diagnosis of schistosomiasis and other helminthiases

Meulah Tcheubousou, B.

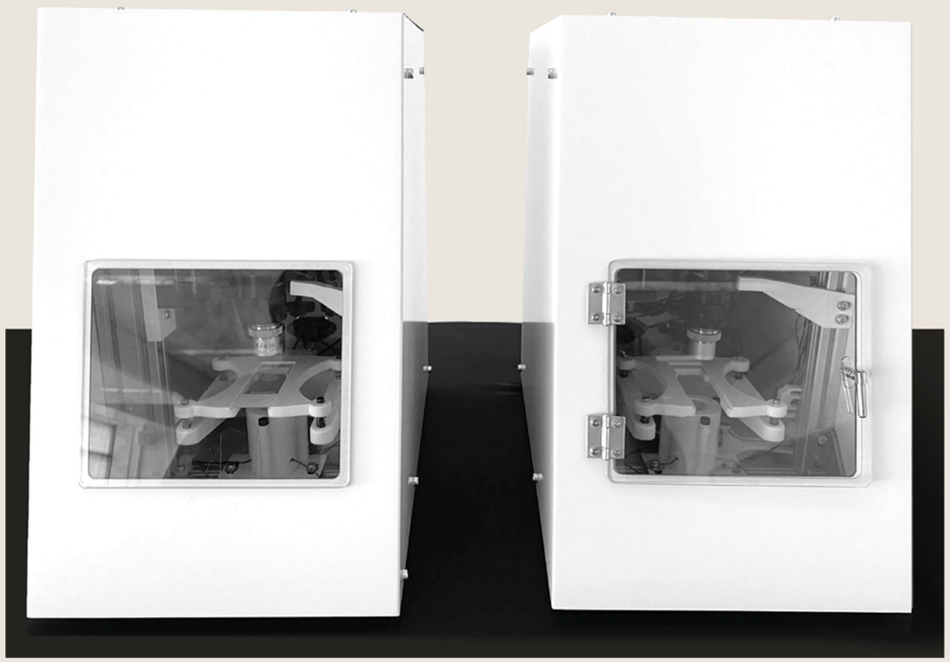

VALIDATION OF INNOVATIVE DIGITAL MICROSCOPES FOR THE DIAGNOSIS OF SCHISTOSOMIASIS AND OTHER HELMINTHIASES

BRICE MEULAH 2024

Validation of innovative digital microscopes for the diagnosis of schistosomiasis and other helminthiases

Brice Meulah Tcheubousou

Validation of innovative digital microscopes for the diagnosis of schistosomiasis and other helminthiases

Brice Meulah Tcheubousou

ISBN: 978-94-90858-90-2
Cover Design Brice Meulah T.
Lay-out Brice Meulah T.
Printing: Drukkerij Mostert, Leiden

Validation of innovative digital microscopes for the diagnosis of schistosomiasis and other helminthiases

Proefschrift

ter verkrijging van
de graad van doctor aan de Universiteit Leiden,
op gezag van rector magnificus prof.dr.ir. H. Bijl,
volgens besluit van het college voor promoties
te verdedigen op donderdag 5 december 2024
klokke 16.00 uur

door

Brice Meulah Tcheubousou
geboren te Buea, Kameroen

Promotor:

Prof. Dr. C.H. Hokke
Prof. Dr. ir. J.C. Diehl (Technology University of Delft)

Co-promotor:

Dr. E.A. van Lieshout

Leden promotiecommissie:

Prof. dr. A. Geluk
Prof. dr. M. Staring
Prof. dr. T. Rinke de Wit (Department of Global Health, Amsterdam UMC)
Dr. J.J van Hellemond (Dept. Medical Microbiology & Infectious Diseases, Erasmus MC)

TABLE OF CONTENTS

1.

General introduction

Adapted and extended from: A review on innovative optical devices for the diagnosis of human soil-transmitted helminthiasis and schistosomiasis: From research and development to commercialisation

Brice Meulah, Michel Bengtson, Lisette Van Lieshout, Cornelis Hendrik Hokke, Andrea Kreidenweiss, Jan-Carel Diehl, Ayola Akim Adegnika, and Temitope Ebenezer Agbana.

Parasitology. 2023;150(2):137-149.

Neglected tropical diseases

Neglected tropical diseases (NTDs) are a diverse group of infectious and non-infectious diseases mostly affecting people in tropical and subtropical regions around the world. One feature all NTDs have in common is that, they overwhelmingly affect the poorest and most marginalised communities, most are chronic, slowly developing and becoming progressively worse if undiagnosed on time, some can cause severe life-long disability, and people with NTDs are often stigmatised [1]. However, the impact of NTDs has been overlooked by the Global Health Communities compared to other infectious diseases like HIV/AIDS, tuberculosis and malaria, hence the name "neglected". The World Health Organization (WHO) has identified a number of NTDs caused by and not limited to a variety of pathogens such as helminths, protozoans, bacteria and viruses and developed a road map to ending the neglect [2, 3]. These pathogens are spread through vectors such as snails, faecal-oral route or contaminated soil, flies and mosquitoes. Timely diagnosis of NTDs, which is often lacking in endemic settings, is crucial for test and treatment, disease control, and prevention of the irreversible life-long disabilities associated with the diseases [4].

Schistosomiasis and soil-transmitted helminth infections

Schistosomiasis and soil-transmitted helminth (STH) infections for example, are two major NTDs that affect approximately 1.5 billion people, predominantly in low- and middle-income countries (LMICs) [5]. Infection with schistosomes occurs when the human skin comes in contact with fresh water contaminated with *Schistosoma* cercariae. The cercariae released from the intermediate snail host penetrates the skin, migrate to the vascular system, and mate as female and male mature worms. Female worms then start producing eggs which can be released in urine or stool into the environment and are the main cause of the disease pathology (Figure 1). The major species in Africa causing urogenital (urine) and intestinal (stool) schistosomiasis in humans are *S. haematobium* and *S. mansoni* respectively. Both species are prevalent in Africa with *S. haematobium* impacting the urogenital system. This leads to symptoms such as hematuria, bladder and kidney failure, along with genital schistosomiasis manifestations like vaginal discharge and postcoital bleeding in women, and hematospermia in men. Chronic infections can lead to risk of miscarriage and infertility, and potentially increase susceptibility to sexually transmitted diseases like HIV [6]. *S. mansoni* infection leads to symptoms such as abdominal pain, diarrhoea as well as blood in stool. When chronic can lead to enlargement of the liver and spleen. The disabilities arising from this disease has a negative effect on the social and economic status of affected individuals in LIMCs with an overall impact on the country's economic growth.

The transmission of STHs generally follows a common pattern. Adult worms of the STHs residing in the intestines mate, produce eggs which are passed out in human stool and deposited in the environment. Infection occurs through accidental ingestion of eggs (*A. lumbricoides*, *T. trichiura* and to some extent also hookworm) or penetration of the skin (hookworm larvae) which then migrate and develop into adult worms in the intestine (Figure 2). These STH infections have a considerable public health impact when left untreated and can lead to anaemia, malnutrition with opposing effects on both physical and cognitive development in children and

adolescents [7, 8]. The disability caused by STH infections measured as disability adjusted life years has a significant impact on the economy [9].

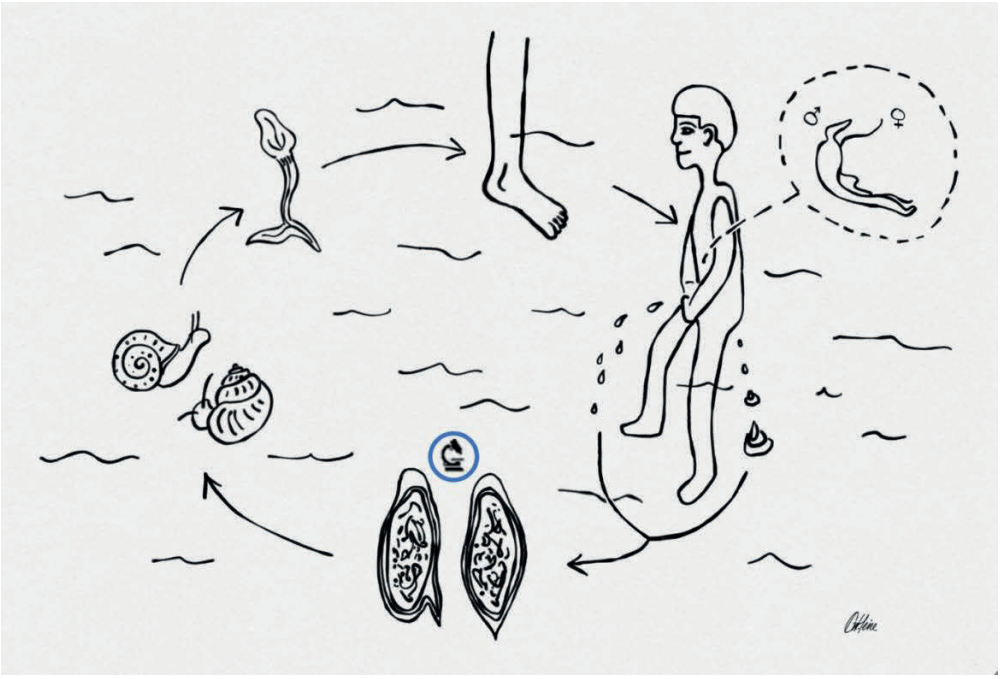

Figure 1: Diagrammatic representation of the lifecycle of *Schistosoma* spp. The stage with the sign is a diagnostic stage of the parasite and the main focus of this thesis (by C. R. Heine).

Diagnostics methods in field settings

The diagnosis of schistosomiasis and STH infections in LMICs so far relies mainly on conventional microscopy. With this diagnostic technique, parasite-derived products (in particular eggs) in stool and urine can be identified and quantified. This technique applied on urine filtration and Kato-Katz slides for detection and quantification of schistosome and STHs eggs is laborious, requires well-trained personnel as well as infrastructure which is often lacking in resource-limited settings [10, 11]. Alternatives to conventional microscopy for schistosomiasis diagnosis include the urine-based point-of-care test to detect circulating cathodic antigens (POC-CCA) extensively validated in settings endemic for *S. mansoni* infections and endorsed by the WHO [12]. Also, reagent strip tests for detection of microhaematuria as a marker for *S. haematobium* infection have been employed for epidemiological surveys [13-15]. However, this test has a limited specificity [16].

The up-converting particle lateral flow (UCP-LF) assay has been developed to detect circulating anodic antigen (CAA) in urine and serum, which is an antigen produced by all *Schistosoma* spp [17-20]. Nucleic acid amplification tests (NAATs), involve the amplification and detection of parasite's specific nucleic acid sequences, typically through real-time Polymerase Chain Reaction (PCR). The real-time PCRs which have been developed for the diagnosis of

schistosomiasis and STH infections, can be used on clinical samples such as stool, urine and blood and are mainly applied in equipped research laboratory settings in LIMCs or as a laboratory tool for the diagnosis of imported infections in high-income countries [21-25]. The UCP-LF CAA and NAATs, although highly accurate methods, both require well-trained personnel and appropriate laboratory infrastructure, with the UCP-LF CAA being less laborious than NAATs. These two methods are still being validated and standardised for use in daily clinical care and medical research in resource-limited settings [18, 26-29].

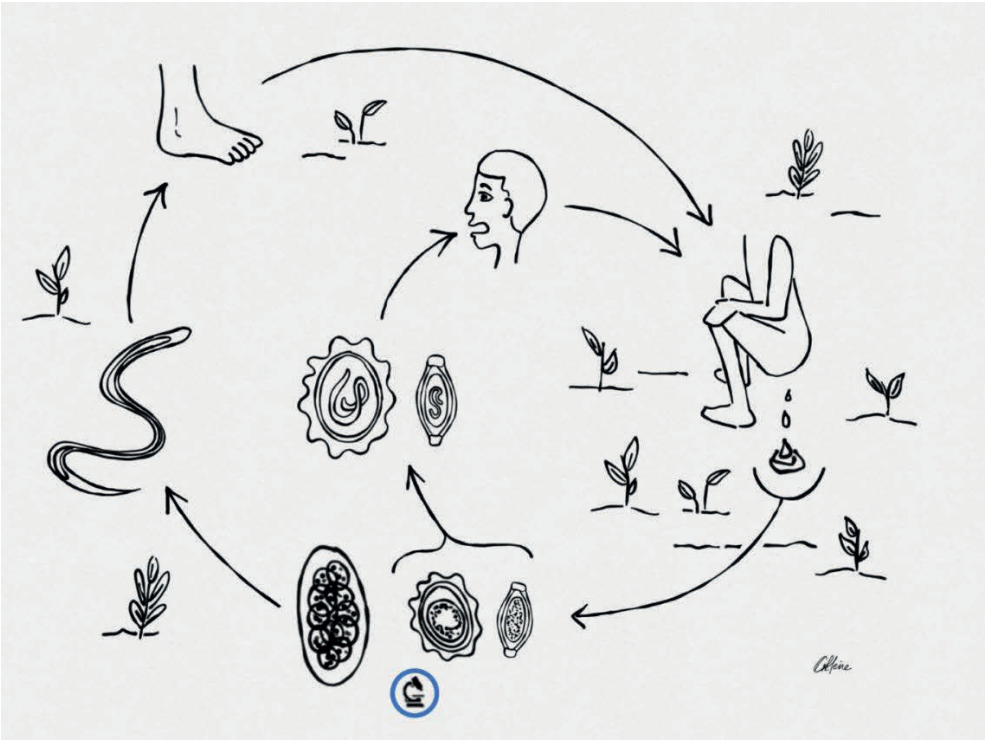

Figure 2: Diagrammatic representation of the life cycle of *Ascaris*, *Trichuris* and hookworm. The stage with the sign is a diagnostic stage of the parasites and the main focus of this thesis (by C. R. Heine).

Approach to control and challenges

In order to accelerate control of schistosomiasis and STH infections, focus is placed mainly on mass drug administration (MDA) of praziquantel to all persons above the age of 2 years and albendazole or mebendazole to school age children, respectively. In addition, approaches such as increased access to clean water and sanitation, snail control (for schistosomiasis only), education and behavioural changes are adopted, together with a multi-diagnostic approach to support monitoring and evaluation these programs [30]. Detecting and quantifying schistosome and STHs eggs with conventional microscopy has been the primary approach to determining the level of ongoing transmission, serving as a crucial tool in assessing

the effectiveness of control programs in endemic setting. Although conventional microscopy remains the most commonly used diagnostic method, it confronts challenges, particularly the need for trained personnel to meet the overwhelming diagnostic demands of control programs and test and treat in clinical settings. Novel diagnostics are needed and automating conventional microscopy could offer a viable solution to this challenge. The development of automated, easy to use digital microscopes for the detection of parasite eggs in faeces or urines, and based on low-cost platforms may provide a matching solution. The WHO has postulated a target product profile (TPP) to guide development of novel diagnostics to reliably measure the effectiveness of control programs in endemic settings [31-33] and advance towards elimination as well as for case management.

Digital optical diagnostic devices

Innovative digital optical diagnostic devices (DODDs), designed to (semi-) automatically detect helminth eggs in clinical samples have been built based on technical modifications of the optical train of a smartphone [34, 35] or mounting off the-shelf optical components [36, 37]. The integrated sensors on smartphones are commonly used for image acquisitions [38, 39]. The processing power of smartphones as well as simple computer units (e.g. Raspberry Pi, Jetson nano) have equally been exploited for the development and running of artificial intelligence (AI) algorithms. The AI algorithms are developed for analysis of registered image data. Such devices have been reported to possess the potential for (semi-) automated medical diagnosis in endemic settings [36-38, 40-42].

Over the last years, several investigators have reported the use of multiple digital devices to detect schistosomiasis and STH infections. While these devices show promise for diagnosing these diseases, they are currently underrepresented in LIMCs. The nine-level technology readiness level (TRL) scale developed by National Aeronautics and Space Administration (NASA) has been used by engineers to qualify readiness for technology applications [43]. However, the TRL scale does not consider extensive medical and design outcomes including the WHO TPP. Using an adapted version (Figure 3) of the TRL scale including the WHO TPP and context specific needs to qualify the readiness of DODDs for field applications in LIMCs, revealed that a majority (85%) are not ready [44]. Meeting the WHO TPP for the majority of these devices in field validation stage (TRL 5,6 and 7) was found to be a major bottle neck, followed by non-continuous validation after the demonstration of proof of concept, despite promising outcomes.

This clearly highlights the need for more research and development of DODDs alongside preclinical and in field validation studies in different endemic settings with diverse conditions to meet the desired TPPs.

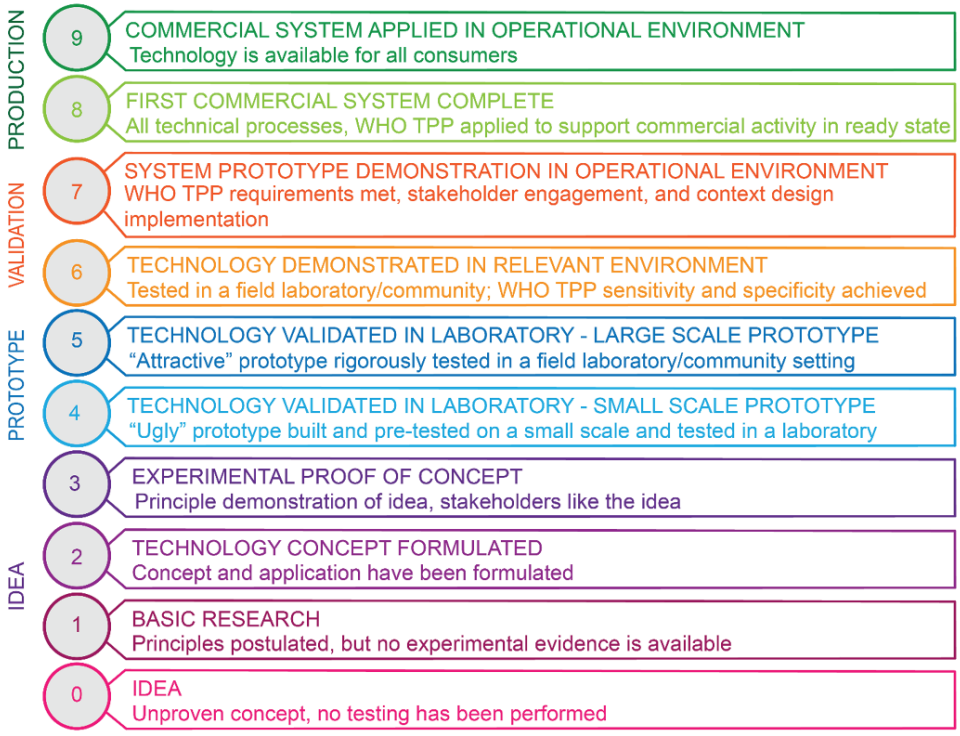

Figure 3. The nine-scale TRL classification chart. Image adapted from (43). TPP= Target product profile

The Schistoscope [36] and AiDx Assist devices are AI-powered automated slide-scanner digital microscopes developed for the diagnosis of schistosomiasis, STHs and other parasitic infections. They are both composed of a custom-designed optical bright-field illumination, x, y, x-axis movement and a condenser controlled by a custom printed circuit board but differ in their electronic and computing modules including the AI framework used. The Schistoscope consist of a Raspberry Pi 4B computer connected to a Raspberry Pi HQ camera that has a pixel size of 1.55 µm and an image resolution of 2028 × 1520 pixels. The AiDx Assist consists of a Jetson Nano computer connected to a Sony IMX 178 CMOS camera sensor with a pixel size of 2.40 µm and an image resolution of 3088 × 2076 pixels. The Schistoscope and AiDx Assist digital microscopes have a 4× objective sufficient to resolve *Schistosoma* spp, STHs eggs and microfilaria. The Schistoscope has been developed as a standalone AI-based device for diagnosing these infections, with the AI analysis result serving as the conclusive test outcome (Figure 4). In contrast, for the AiDx Assist, the AI results undergo additional verification by the operator before a final test outcome is reported. These devices have gone through multiple iterations in their development.

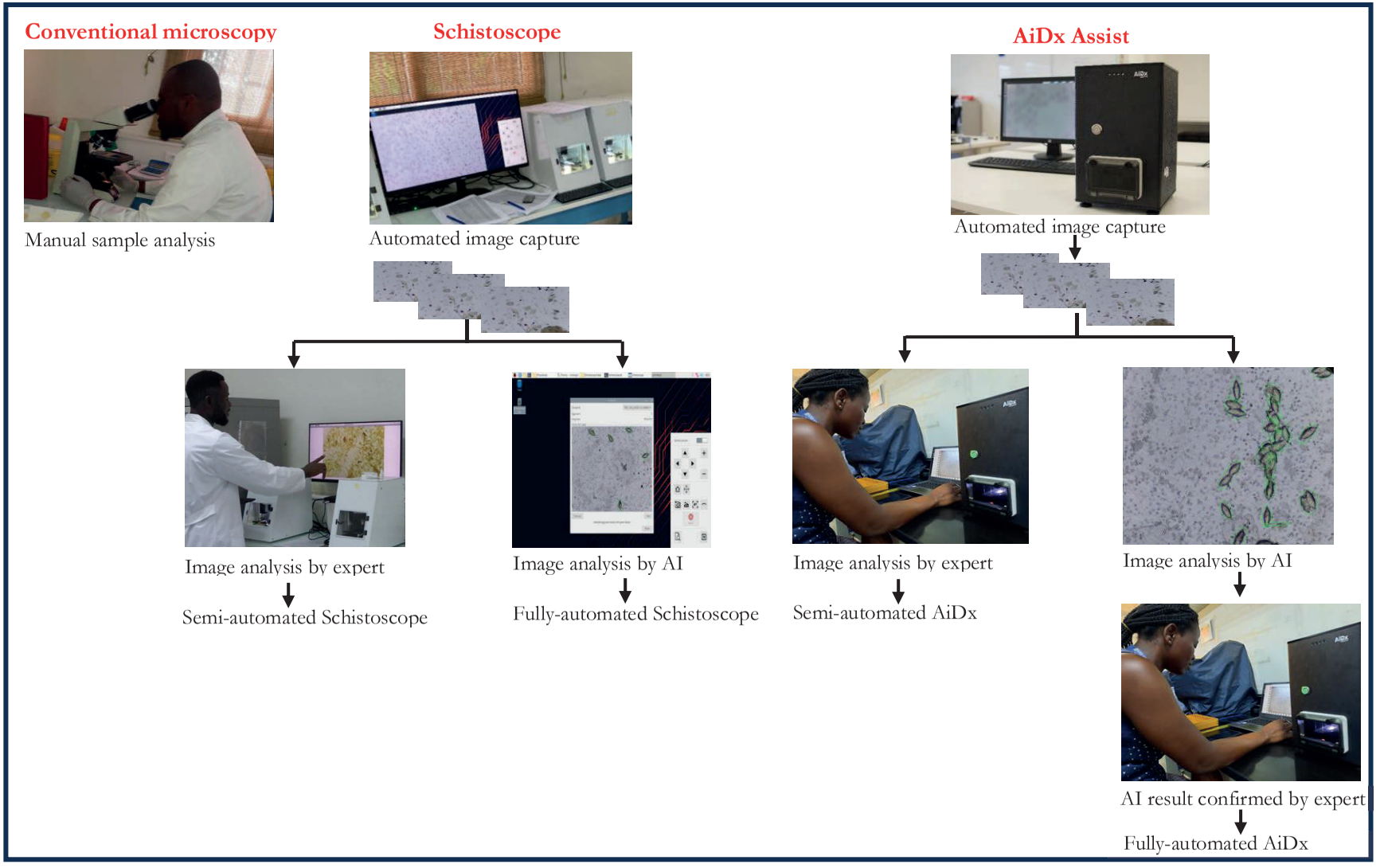

Figure 4: Comprehensive flow chart showing the use case scenario of conventional microscopy, Schistoscope and AiDx Assist for disease diagnosis

In this thesis we conducted preclinical and in-field validations of the Schistoscope and AiDx Assist at different iterations of their research and development. These devices underwent validation procedures throughout their development, beginning with preclinical validation in a technical laboratory setting using phosphate buffer saline or human biological samples spiked with parasitic worm eggs. Based on the preclinical outcomes, we proceeded to an in-field validation with the objective to achieve the WHO diagnostic TPP (with a focus on sensitivity and specificity) for the Schistoscope and AiDx Assist and to further explore their performance in comparison to conventional microscopy.

Scope and outline of this thesis

The main objective of the work described in this thesis is to validate the diagnostic performance of the Schistoscope and AiDx Assist as egg-based detection methods for schistosomiasis and the STHs through their research and development. The validation was performed through preclinical and in-field studies based on collected clinical samples of potentially infected individuals, in different endemic settings. In **Chapter 1** we present an overview of this thesis and highlight the main challenges faced with the research and development to commercialisation of DODDs as egg-based detection methods. In **chapter 2** we demonstrate context specific needs with regards to different diagnostics methods by highlighting the limitation of POC-CCA and haematuria rapid test as field friendly alternatives of conventional microscopy. In addition, we determined the need for egg-based detection (microscopy) methods in accessing the current prevalence of schistosomiasis in a particular setting in Tanzania, endemic for *S. haematobium* and *S. mansoni* infections. In **chapter 3** the Schistoscope was evaluated as a semi-automated and fully automated (with AI algorithm) microscope, compared to conventional microscopy for the detection and quantification of *S. haematobium* eggs in urine in Nigeria. **In chapter 4** we carried out improvements of the AI algorithm of the Schistoscope through a two-stage automated diagnosis framework for *S. haematobium* eggs detection and quantification with pre-clinical validation on microscopy images obtained from endemic settings**. In chapter 5** we performed a follow up validation of the Schistoscope in Lambaréné, Gabon. The detection and quantification of *S. haematobium* eggs in urine by the Schistoscope was compared to conventional microscopy and to a more sensitive composite reference standard, including real-time PCR and UCPLF-CAA data. In **chapter 6** we evaluated the AiDx Assist digital microscope as a tool for diagnosing *S. haematobium* in urine and *S. mansoni* and other STHs in stool under field conditions in Nigeria. The results are summarised and discussed in **chapter 7** highlighting the progress made in the development of DODDs, looking beyond diagnostic performance including some additional field experience with the devices, discussing the context specific diagnostic needs and the prospects of DODDs for schistosomiasis and other helminthiases in endemic settings.

References

1. Molyneux D. Neglected tropical diseases. Community Eye Health. 2013;26(82):21-4.
2. World Health Organisation. New road map for neglected tropical diseases 2021−2030: World Health Organisation.; 2023 [Available from: https://www.who.int/teams/control-of-neglected-tropical-diseases/ending-ntds-together-towards-2030.
3. Bhaumik S, Zwi AB, Norton R, Jagnoor J. How and why snakebite became a global health priority: a policy analysis. BMJ Glob Health. 2023;8(8).
4. Souza AA, Ducker C, Argaw D, King JD, Solomon AW, Biamonte MA, et al. Diagnostics and the neglected tropical diseases roadmap: setting the agenda for 2030. Transactions of The Royal Society of Tropical Medicine and Hygiene. 2020;115(2):129-35.
5. World Health Organisation. Schistosomiasis and soil-transmitted helminthiases: treating millions of people, despite the pandemic.: World Health Organisation. ; 2021 [Available from: https://www.who.int/news/item/08-12-2021-schistosomiasis-and-soil-transmitted-helminthiases-treating-millions-of-people-despite-the-pandemic.
6. Bustinduy AL, Randriansolo B, Sturt AS, Kayuni SA, Leustcher PDC, Webster BL, et al. An update on female and male genital schistosomiasis and a call to integrate efforts to escalate diagnosis, treatment and awareness in endemic and non-endemic settings: The time is now. Adv Parasitol. 2022;115:1-44.
7. Ezeamama AE, Bustinduy AL, Nkwata AK, Martinez L, Pabalan N, Boivin MJ, et al. Cognitive deficits and educational loss in children with schistosome infection-A systematic review and meta-analysis. PLoS Negl Trop Dis. 2018;12(1):e0005524.
8. Pabalan N, Singian E, Tabangay L, Jarjanazi H, Boivin MJ, Ezeamama AE. Soil-transmitted helminth infection, loss of education and cognitive impairment in school-aged children: A systematic review and meta-analysis. PLoS Negl Trop Dis. 2018;12(1):e0005523.
9. Montresor A, Mwinzi P, Mupfasoni D, Garba A. Reduction in DALYs lost due to soil-transmitted helminthiases and schistosomiasis from 2000 to 2019 is parallel to the increase in coverage of the global control programmes. PLoS Negl Trop Dis. 2022;16(7):e0010575.
10. Ajibola O, Gulumbe BH, Eze AA, Obishakin E. Tools for Detection of Schistosomiasis in Resource Limited Settings. Med Sci (Basel). 2018;6(2):39.
11. Khurana S, Singh S, Mewara A. Diagnostic Techniques for Soil-Transmitted Helminths – Recent Advances. Research and Reports in Tropical Medicine. 2021;Volume 12:181-96.
12. World Health Organisation. World Health Organization.; 2021 [Available from: https://www.who.int/publications/i/item/9789240031104.
13. Ephraim RK, Abongo CK, Sakyi SA, Brenyah RC, Diabor E, Bogoch II. Microhaematuria as a diagnostic marker of Schistosoma haematobium in an outpatient clinical setting: results from a cross-sectional study in rural Ghana. Tropical Doctor. 2015;45(3):194-6.
14. King CH, Bertsch D. Meta-analysis of urine heme dipstick diagnosis of Schistosoma haematobium infection, including low-prevalence and previously-treated populations. PLoS neglected tropical diseases. 2013;7(9):e2431.
15. Knopp S, Ame SM, Hattendorf J, Ali SM, Khamis IS, Bakar F, et al. Urogenital schistosomiasis elimination in Zanzibar: accuracy of urine filtration and haematuria reagent strips for diagnosing light intensity Schistosoma haematobium infections. Parasites & Vectors. 2018;11(1):552.
16. Krauth SJ, Greter H, Stete K, Coulibaly JT, Traoré SI, Ngandolo BNR, et al. All that is blood is not schistosomiasis: experiences with reagent strip testing for urogenital schistosomiasis with special consideration to very-low prevalence settings. Parasites & Vectors. 2015;8(1):584.
17. Hoekstra PT, van Dam GJ, van Lieshout L. Context-Specific Procedures for the Diagnosis of Human Schistosomiasis – A

Mini Review. Frontiers in Tropical Diseases. 2021;2.
18. Corstjens P, de Dood CJ, Knopp S, Clements MN, Ortu G, Umulisa I, et al. Circulating Anodic Antigen (CAA): A Highly Sensitive Diagnostic Biomarker to Detect Active Schistosoma Infections-Improvement and Use during SCORE. Am J Trop Med Hyg. 2020;103(1_Suppl):50-7.
19. Hoekstra PT, Madinga J, Lutumba P, van Grootveld R, Brienen EAT, Corstjens P, et al. Diagnosis of Schistosomiasis without a Microscope: Evaluating Circulating Antigen (CCA, CAA) and DNA Detection Methods on Banked Samples of a Community-Based Survey from DR Congo. Trop Med Infect Dis. 2022;7(10).
20. van Lieshout L, Polderman AM, Visser LG, Verwey JJ, Deelder AM. Detection of the circulating antigens CAA and CCA in a group of Dutch travellers with acute schistosomiasis. Trop Med Int Health. 1997;2(6):551-7.
21. Meurs L, Brienen E, Mbow M, Ochola EA, Mboup S, Karanja DMS, et al. Is PCR the Next Reference Standard for the Diagnosis of Schistosoma in Stool? A Comparison with Microscopy in Senegal and Kenya. PLOS Neglected Tropical Diseases. 2015;9(7).
22. Obeng BB, Aryeetey YA, de Dood CJ, Amoah AS, Larbi IA, Deelder AM, et al. Application of a circulating-cathodic-antigen (CCA) strip test and real-time PCR, in comparison with microscopy, for the detection of Schistosoma haematobium in urine samples from Ghana. Annals of tropical medicine and parasitology. 2008;102(7):625-33.
23. Sanprasert V, Kerdkaew R, Srirungruang S, Charuchaibovorn S, Phadungsaksawasdi K, Nuchprayoon S. Development of Conventional Multiplex PCR: A Rapid Technique for Simultaneous Detection of Soil-Transmitted Helminths. Pathogens. 2019;8(3).
24. Fuss A, Mazigo HD, Mueller A. Evaluation of serum-based real-time PCR to detect Schistosoma mansoni infection before and after treatment. Infect Dis Poverty. 2020;9(1):74.
25. Cools P, van Lieshout L, Koelewijn R, Addiss D, Ajjampur SSR, Ayana M, et al. First international external quality assessment scheme of nucleic acid amplification tests for the detection of Schistosoma and soil-transmitted helminths, including Strongyloides: A pilot study. PLoS Negl Trop Dis. 2020;14(6):e0008231.
26. Cools P, Vlaminck J, Verweij JJ, Levecke B. Quantitative PCR in soil-transmitted helminth epidemiology and control programs: Toward a universal standard. PLoS Negl Trop Dis. 2021;15(3):e0009134.
27. Casacuberta-Partal M, Hoekstra PT, Kornelis D, van Lieshout L, van Dam GJ. An innovative and user-friendly scoring system for standardised quantitative interpretation of the urine-based point-of-care strip test (POC-CCA) for the diagnosis of intestinal schistosomiasis: a proof-of-concept study. Acta Tropica. 2019;199:105150.
28. Cools P, van Lieshout L, Koelewijn R, Addiss D, Ajjampur SSR, Ayana M, et al. First international external quality assessment scheme of nucleic acid amplification tests for the detection of Schistosoma and soil-transmitted helminths, including Strongyloides: A pilot study. PLOS Neglected Tropical Diseases. 2020;14(6):e0008231.
29. Amoah AS, Hoekstra PT, Casacuberta-Partal M, Coffeng LE, Corstjens PLAM, Greco B, et al. Sensitive diagnostic tools and targeted drug administration strategies are needed to eliminate schistosomiasis. The Lancet Infectious Diseases. 2020;20(7):e165-e72.
30. Raso G, Essé C, Dongo K, Ouattara M, Zouzou F, Hürlimann E, et al. An Integrated Approach to Control Soil-Transmitted Helminthiasis, Schistosomiasis, Intestinal Protozoa Infection, and Diarrhea: Protocol for a Cluster Randomized Trial. JMIR Res Protoc. 2018;7(6):e145.
31. World Health Organisation. Diagnostic target product profiles for monitoring, evaluation and surveillance of schistosomiasis control programmes. Licence: CC BY-NC-SA 3.0 IGO. Geneva: World Health Organization. Available from: https://wwwwhoint/publications/i/item/9789240031104[cited 2022 17/03. 2021.
32. World Health Organisation. Public consultation: Target Product Profiles for

diagnostic tests to meet Schistosomiasis and Soil-transmitted Helminth programme needs. Available from: https://wwwwhoint/news-room/articles-detail/public-consultation-target-product-profiles-for-diagnostic-tests-to-meet-schistosomiasis-and-soil-transmitted-helminth-programme-needs [cited 2022 17/03]. 2021(17 March).

33. World Health Organisation. WHO GUIDELINE on control and elimination of human schistosomiasis: World Health Organisation. https://www.who.int/publications/i/item/9789240041608; 2022 [Available from: https://www.who.int/publications/i/item/9789240041608.
34. Dacal E, Bermejo-Peláez D, Lin L, Álamo E, Cuadrado D, Martínez Á, et al. Mobile microscopy and telemedicine platform assisted by deep learning for the quantification of Trichuris trichiura infection. PLoS Negl Trop Dis. 2021;15(9):e0009677.
35. Yang A, Bakhtari N, Langdon-Embry L, Redwood E, Grandjean Lapierre S, Rakotomanga P, et al. Kankanet: An artificial neural network-based object detection smartphone application and mobile microscope as a point-of-care diagnostic aid for soil-transmitted helminthiases. PLoS Negl Trop Dis. 2019;13(8):e0007577.
36. Oyibo P, Jujjavarapu S, Meulah B, Agbana T, Braakman I, van Diepen A, et al. Schistoscope: An Automated Microscope with Artificial Intelligence for Detection of Schistosoma haematobium Eggs in Resource-Limited Settings. Micromachines (Basel). 2022;13(5).
37. Ward P, Dahlberg P, Lagatie O, Larsson J, Tynong A, Vlaminck J, et al. Affordable artificial intelligence-based digital pathology for neglected tropical diseases: A proof-of-concept for the detection of soil-transmitted helminths and Schistosoma mansoni eggs in Kato-Katz stool thick smears. PLoS Neglected Tropical Diseases. 2022;16(6):e0010500. ogy. 2022:1-41.
38. Vasiman A, Stothard JR, Bogoch, II. Mobile Phone Devices and Handheld Microscopes as Diagnostic Platforms for Malaria and Neglected Tropical Diseases (NTDs) in Low-Resource Settings: A Systematic Review, Historical Perspective and Future Outlook. Adv Parasitol. 2019;103:151-73.
39. Hernández-Neuta I, Neumann F, Brightmeyer J, Ba Tis T, Madaboosi N, Wei Q, et al. Smartphone-based clinical diagnostics: towards democratization of evidence-based health care. J Intern Med. 2019;285(1):19-39.
40. Saeed MA, Jabbar A. "Smart Diagnosis" of Parasitic Diseases by Use of Smartphones. J Clin Microbiol. 2018;56(1).
41. Diehl JC, Oyibo, P. O., Agbana, T. E., Jujjavarapu, S., Van, G. Y., Vdovin, G., & Andi, W. O., editor Schistoscope: Smartphone versus Raspberry Pi based low-cost diagnostic device for urinary Schistosomiasis. Proceedings of 10th IEEE Global Humanitarian Technology Confrence IEEE; 2020; P. M. Cunningham (Ed.).
42. Sangameswaran R. MAIScope: A low-cost portable microscope with built-in vision AI to automate microscopic diagnosis of diseases in remote rural settings. arXiv preprint arXiv:220806114. 2022.
43. Bruno I LG, Covino BV, Donarelli A, Marchetti V, Panni AS and, F M, editors. Technology readiness revisited: a proposal for extending the scope of impact assessment of European public services. Proceedings of the 13th International Conference on Theory and Practice of Electronic Governance; 2020.
44. Meulah B, Bengtson M, Van Lieshout L, Hokke CH, Kreidenweiss A, Diehl J-C, et al. A review on innovative optical devices for the diagnosis of human soil-transmitted helminthiasis and schistosomiasis: From research and development to commercialisation. Parasitol

2.

Current status of schistosomiasis in school-aged children in Mwanga district Tanzania; impact of two decades of annual Mass Drug Administration programme

Jeremia J. Pyuza, Brice Meulah, Pytsje T. Hoekstra, Noel Mdende, Elizabeth Mvilli, Lisette van Lieshout, Stan T. Hilt, Paul L.A.M. Corstjens, Maria Yazdanbakhsh, Sia E. Msuya, Govert J. van Dam.

Parasitology 2024, pp.1-6..

Abstract

Schistosomiasis is a neglected tropical disease with significant health implications, particularly among children. A cross-sectional study was conducted among school-aged children (SAC) in Mwanga district, Tanzania, a region known to be co-endemic for *S. haematobium* and *S. mansoni* infection and where annual mass drug administration (MDA) has been conducted for 20 years. In total, 576 SAC from five schools provided a urine sample for the detection of *Schistosoma* circulating anodic antigen using the upconverting particle-based lateral flow (UCP-LF CAA) test. Additionally, the potential of the point-of-care circulating cathodic antigen (POC-CCA) and microhaematuria dipstick test as field-applicable diagnostic alternatives for schistosomiasis were assessed and the prevalence outcome compared to UCP-LF CAA. Risk factors associated with schistosomiasis was assessed based on UCP-LF CAA. The UCP-LF CAA test revealed an overall schistosomiasis prevalence of 20.3%, compared to 65.6% based on a combination of POC-CCA and microhaematuria dipstick. No agreement was observed between the combined POC tests and UCP-LF CAA. Factors associated with schistosomiasis included age (5-10 years), involvement in fishing, farming, swimming activities and attending two of the five primary schools. Our findings suggest a significant progress in infection control in Mwanga district due to annual MDA, although not enough to interrupt transmission. Accurate diagnostics play a crucial role in monitoring intervention measures to effectively combat schistosomiasis.

Keywords: schistosomiasis, UCP-LF CAA, POC-CCA, microhaematuria dipstick, school-aged children, diagnosis, microscopy, Mwanga, Tanzania.

Introduction

Schistosomiasis is a major neglected tropical disease disproportionately affecting sub-Saharan African countries, with 90.0% of the global disease burden occurring in this region [1]. In Tanzania, the overall prevalence of schistosomiasis is 51.5% [2], and among school-aged children (SAC) it is reported to be 53.5% [3], reaching up to about 80.0% in the northwestern zone around Lake Victoria[4, 5]. However, current prevalence estimates do not include the northern region of Tanzania, including Mwanga district in the Kilimanjaro region. This district has been known to be endemic for both *Schistosoma haematobium* and *Schistosoma mansoni* [6]. The population is at high risk of schistosomiasis possibly due to the presence of the intermediate snail host (Bulinus and Biomphalaria) as well as irrigation schemes, which are the conducive environment for the transmission the *Schistosoma* spp. The presence of the hydroelectric dam known as "Nyumba ya Mungu" (Figure 1) which ensures a constant water supply to the surrounding villages for irrigation contributes to the continues transmission of schistosomiasis in Mwanga district [6].

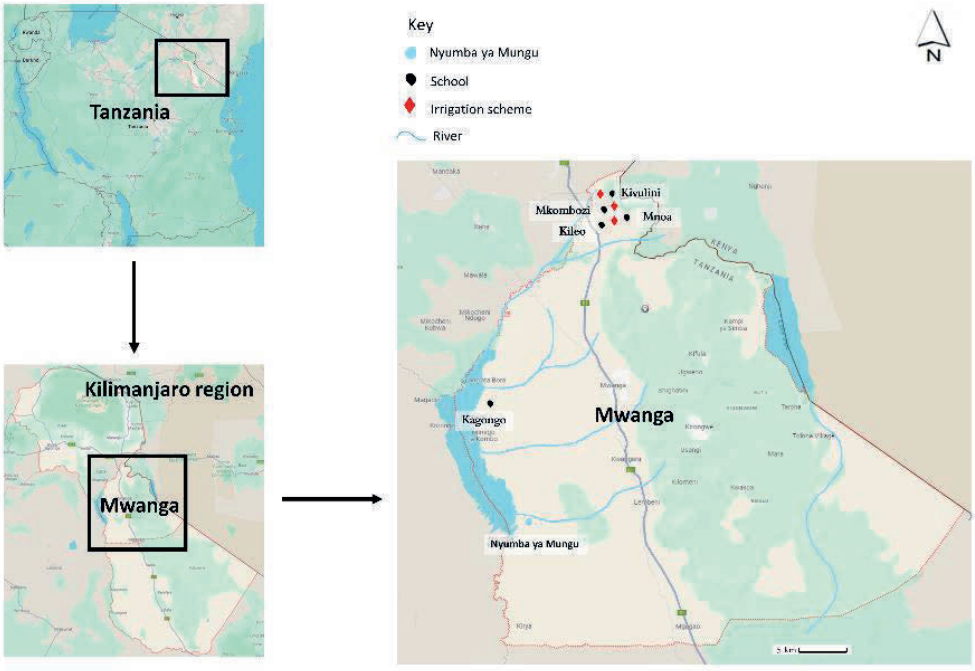

Figure 1. Map of Mwanga district Tanzania showing water sources, five primary schools and irrigation schemes

In Tanzania, including the Kilimanjaro region, mass drug administration (MDA) of praziquantel has been the major strategy to reduce the burden of schistosomiasis and has been organized annually since 2004 among SAC who are at the highest risk of infection[7]. The need to assess the success of MDA has

been highlighted by the World Health Organization and tools to enhance strategic guidance for schistosomiasis control programme in Tanzania have equally been reported [8, 9]. The most recent data on the prevalence status of schistosomiasis among SAC in Mwanga district are from 2005, indicating a prevalence ranging from 33.5 to 70.0% [6]. Conventional microscopy is the reference method to diagnose schistosomiasis in endemic settings and involves the detection of *Schistosoma eggs* in faeces or urine, depending on the species. However, microscopy requires experienced, well-trained technical personnel, is considered a time-consuming, laborious method and has limited sensitivity in low-intensity infection settings [10]. Furthermore, the availability and access to microscopy is challenging in many rural areas in Tanzania due to a lack of trained personnel and appropriate infrastructure.

Low-cost, user-friendly rapid tests could overcome such issues, but the accuracy of available point-of-care (POC) tests to determine the prevalence of schistosomiasis in regions co-endemic for *S. haematobium* and *S. mansoni* needs to be determined. The POC test for detecting *Schistosoma* Circulating Cathodic Antigen (POC-CCA) in urine has been endorsed by the WHO as an alternative to conventional microscopy, in particular for the diagnosis of *S. mansoni* infections[9]. It requires minimal training and has been validated in several field settings endemic for intestinal schistosomiasis [11, 12]. Another easy-to-use rapid test is the microhaematuria dipstick test for the detection of haematuria, which has been shown to be strongly associated with urogenital schistosomiasis, although it is considered nonspecific [13]. A quantitative Up-Converting reporter Particle Lateral Flow (UCP-LF) test detecting the genus-specific *Schistosoma* Circulating Anodic Antigen (CAA) is a highly accurate test to detect active infection of all *Schistosoma* species in urine or serum[14]. Although it requires a more advanced laboratory infrastructure, it has been shown to be 100% specific and can reach a sensitivity to detect single-worm infections [14-16].

This study aimed to determine the current prevalence of schistosomiasis in the Mwanga district Tanzania after approximately twenty years of MDA using the UCP-LF CAA test and to explore the potential of using the POC-CCA and microhaematuria dipstick as a combined POC test for diagnosing schistosomiasis in co-endemic settings in comparison to the laboratory-based UCP-LF CAA test. Furthermore, we investigated *Schistosoma* infection risk factors and associated parameters.

Materials and methods

Ethical considerations

Ethical approval for this study was obtained from Kilimanjaro Christian Medical University College (KCMUCo) research and ethical committee board (reference number: 2588). Administrative authorization was obtained from the district education officer and Mwanga District Medical Officer. Children were enrolled based on their availability, and those willing to participate were given a consent form to be signed by guardians and/or parents. Immediately after sample collection all children, including those who participated in our study, were provided with praziquantel under the yearly MDA programme at school at the recommended dose in the presence of a local clinician.

Study area and population

The study was conducted in Mwanga district, one of the seven districts of Kilimanjaro region in Tanzania. Farming, fishing, sand collection, pebble making, soil bricking and animal keeping are the major economic activities. The study was conducted in five schools, of which two were selected based on a previous study [6]. MDA of praziquantel had occurred in these schools more than 6 months prior to our study.

Sample/data collection and processing

Enrolled study participants provided consent forms from parents and were given sterile containers with unique identifiers to provide fresh urine samples. For each sample, POC-CCA and microhaematuria dipstick was done in the field for the diagnosis of *S. mansoni* and *S. haematobium*, respectively. An aliquot of 2 mL of urine was conserved (at -20 °C) per participant and was shipped on ice to Leiden University Medical Center in the Netherlands for retrospective UCP-LF CAA analysis. Following urine sample collection, a face-to-face interview using a closed-ended questionnaire in English and Swahili was conducted.

Field and Laboratory analysis

The POC-CCA test (batch 180817091) was obtained from Rapid Medical Diagnostics, South Africa (SA), and analysis was done according to the manufacturer's instructions. Briefly, two drops of urine were transferred into the sample window of the test cassette. The readout of the cassette was done in 20 minutes. Results were scored as negative, trace or positive. Microhaematuria dipstick (Mission Urinalysis, Lot no: URS8090018) test was performed by placing the strip on a flat surface and a drop of urine applied to the reagent pad. Readouts were done in 1 minute as either negative or positive according to the manufacturer's instructions.

The *Schistosoma* genus-specific UCP-LF CAA test was employed to detect CAA in urine samples and to confirm active infection with *Schistosoma* spp [14]. All urine samples were subjected to the UCAA*hT*417 wet format of the test. Briefly, 500µL of each urine sample was mixed with 100µL of 12% trichloroacetic acid, then incubated at room temperature for 5 minutes and centrifuged. The clear supernatant was then concentrated to 20µL using a 0.5 mL centrifugal device (Amicon Ultra-0.5, Millipore, Merck Chemicals B.V., Amsterdam, The Netherlands). The resulting concentrate was then applied to the lateral flow test strip. To quantify CAA concentrations and to validate the assay cutoff (0.6 pg/mL), reference standards with known CAA-levels were included. A CAA concentration above 0.6 pg/mL was considered positive. Infection intensity was categorized as low positive (>0.6-10 pg/mL), moderate positive (>10-100 pg/mL) and high positive (>100 pg/mL).

Statistical analysis

The agreement between the combination of POC-CCA an microhaematuria dipstick (combined POC test) and UCP-LF CAA was performed using Kappa (K) statistics. For POC-CCA, trace results were considered negative. Furthermore, the association between socio-demographic characteristics and risk factors associated with *Schistosoma* infection, based on the UCP-LF CAA test, was performed using chi-square statistics, binary and multiple logistic regression analyses. Statistical analysis was performed using IBM Statistical Package for Social Sciences version 29 (SPSS Inc., Chicago, United States of America). For generation of plots, GraphPad Prism version 9.3.1 for Windows (GraphPad Software, San Diego, California USA, www.graphpad.com) was used.

Results

Socio-demographic characteristics

A total of 576 children provided informed consent and subsequently provided a urine sample and were therefore included in the final analysis. In Table 1 socio-demographic characteristics of the study population are given. The children's age ranged from 5 to 16 years, with a mean age of 9.8 years (SD 2.4) and 50.7% were females. Furthermore, the majority of the children were in class range 1 to 3 (50.3%). Farming was the most common father's profession (46.7%) followed by fishing (23.4%). The most common mother's profession was farming (44.8%), followed by small businesses (34.2%).

Table 1. The prevalence of schistosomiasis across all five schools based on UCP-LF CAA, POC-CCA, microhaematuria dipstick and a combination of the POC-CCA and microhaematuria dipstick.

			Diagnostic test			
		Number of children	**UCP-LF CAA**	**POC-CCA**	**Microheamaturia dipstick**	**Combined Test***
			Positive (%)	Positive (%)	Positive (%)	Positive (%)
School	Kagongo	279	35 (12.5)	174 (62.4)	84 (30.1)	209 (74.9)
	Kileo	59	14 (23.7)	37 (62.7)	12 (20.3)	41 (69.5)
	Kivulini	57	19 (33.3)	30 (52.6)	12 (21.1)	36 (63.2)
	Mkombozi	106	31 (22.2)	35 (33.1)	23 (21.6)	43 (40.6)
	Mnoa	75	18 (24.0)	38 (50.6)	17 (22.7)	47 (62.7)
Total		**576**	**117 (20.3)**	**314 (54.5)**	**148 (25.7)**	**376 (65.3)**
	*combination of POC-CCA and/or microheamaturia dipstick positive outcome					

Prevalence and intensity of Schistosoma infection

In total 117 (20.3%) of children were found to be CAA positive (Table 1). The highest proportion of positives was observed among children attending Kivulini primary school (33.3%), followed by Mkombozi primary school (29.2%). The lowest proportion was 12.5% and was found among school children at Kagongo primary school. The majority of moderate to high intensity infections based on CAA-levels was observed in the schools in Kivulini and Mkombozi (Figure 2a). Furthermore, SAC within the age category 5-10 years were found to be more often CAA positive than those aged 11-16 years (Figure 2b). The outcome of the point-of-care tests are also summarized in Table 1. Based on POC-CCA and microhaematuria dipstick tests the prevalence of schistosomiasis were, 54.5% and 25.7% respectively. Assuming that the combination of two tests will give more clearer prevalence, combining POC-CCA and microhaematuria dipstick, the prevalence was 65.3%.

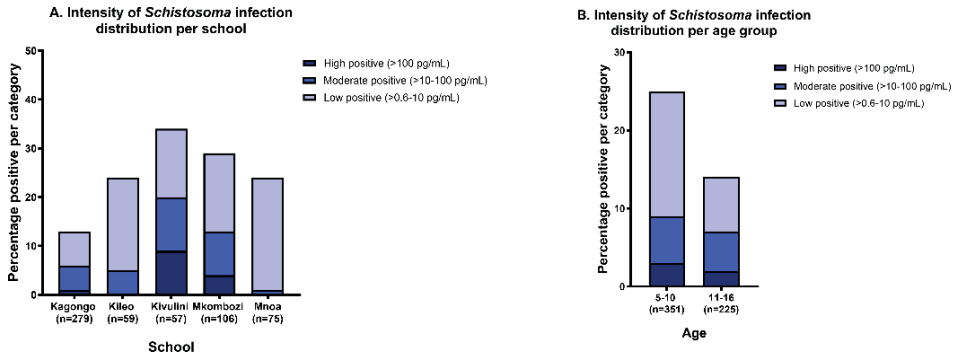

Figure 2. Prevalence and intensity of *Schistosoma* infection based on UCP-LF CAA amongst (A), five selected schools (B) the age categories.

The agreement between the combination of POC-CCA and microhaematuria dipstick and the reference test UCP-LF CAA.

The combination of POC-CCA and microhaematuria dipstick showed no agreement with the UCP-LF CAA test (Table 2). Furthermore the p-value indicates that this lack of agreement is not statistically significant, suggesting that the disagreement between tests is likely due to chance at significance level of 0.05. Analysis of the individual POC-CCA and microhaematuria dipstick tests also showed no agreement with the UCP-LF CAA test.

Table 2. The level of agreement between point-of-care circulating cathodic antigen (POC-CCA) test, microhaematuria dipstick and upconverting particle lateral flow circulating anodic antigen (UCP-LF CAA) urine test by Cohen's kappa coefficient in 576 school-aged children from Mwanga Tanzania.

Test		**UCP-LF CAA**				
		Positive	Negative	K-value	P-Value	Interpretation
POC-CCA	Positive	86	367	0.011	0.128	Poor
	Negative	31	92			
Microhaematuria dipstick	Positive	37	110	0.013	0.090	Poor
	Negative	80	349			
Combined (Microhaematuria and POC-CCA)	Positive	79	297	0.015	0.569	Poor
	Negative	38	162			

Risk factors associated with schistosomiasis

Using multivariate logistic regression analysis (adjusted odd ratio), the potential risk factors associated with *Schistosoma* infection, based on the presence of CAA, showed that children in class level 1-3 had two times higher odds of having schistosomiasis than children in higher classes. Children involved in farming and swimming activities had respectively 5.6 and 3.6 odds of being infected than those who did not farm nor swim. Furthermore, children attending Kileo, Kivulini, Mkombozi and Mnoa primary schools had 2.2, 2.6, 2.4 and 2.7 times higher odds of

CAA positive results respectively, when compared to those attending Kagongo primary school. More details can be found in Supplementary Table 1.

Discussion

Using a highly accurate diagnostic approach (UCP-LF CAA), this study indicated that after nearly two decades of MDA schistosomiasis remains highly prevalent (20%) among school-aged children in Mwanga district, Tanzania. Although POC-CCA and microhaematuria dipstick test showed an even higher prevalence than the UCP-LF CAA test, no agreement was found between these tests and the UCP-LF CAA results nor any association was observed between these tests and known risk factors for schistosomiasis, highlighting the limitation of these currently available rapid diagnostics tests (POC-CCA and microhaematuria) in accurately determining the true prevalence in this specific setting that is known to be co-endemic for *S. mansoni* and *S. haematobium*.

Different prevalence's have been observed throughout Tanzania[17-21]. As commonly known as well as shown in the current study, measurement of prevalence highly depends on the diagnostic method used. Since we have used a highly accurate diagnostic method in our study, i.e. the UCP-LF CAA test, it is difficult to directly compare our results to previously published results based on microscopy and/or POC-CCA as these methods have limited sensitivity/specificity. Our data confirm regional variation in the burden of schistosomiasis in Mwanga district, which would, extrapolated to Tanzania as a whole, argue for a more focally oriented schistosomiasis control approach.

A significant difference in infection rates among different age groups was identified. Younger children (5-10 years) exhibited a higher prevalence of schistosomiasis than the older age group (11-16 years), indicating early exposure to the infection[21]. The possible reason for older children having low prevalence is through acquired immunity due repeated infections as indicated by other previous studies for example possible presence of IgE antibodies [22, 23]. A significant association was found between schistosomiasis and children who swim in water bodies, which may be attributed to playful behavioral activities common among children [4]. The children involved in swimming activities had 3.6 times more risk of being infected, in line with recent systematic review demonstrated by Reitzug and colleagues [24]. Children's involvement in farming was found to be associated with an increased risk of being infected with schistosomiasis. Finally, children attending Kileo, Kivulini, Mkombozi and Mnoa primary schools were identified to have higher rates of *Schistosoma* infection compared to those attending Kagongo primary school. These findings are likely due to the proximity of irrigation schemes/rivers to these schools, which are perceived as safer water sources for young children and so most likely to visit compared to larger water bodies like the dams located closer to Kagongo, where parents have concerns about the risk of children drowning and so cautioned not to go there for water.

Despite of providing crucial updates on the prevalence of schistosomiasis among school children in the area, the study has several limitations. Firstly, the laboratory UCP-LF CAA test

detects all *Schistosoma* species, but it does not provide any species-specific information [14]. In control settings, where species information would be relevant, other measures can provide this, e.g. determining the presence of specific snail species, or performing egg microscopy or species-specific PCR. For treatment, species information as such is not needed, and CAA has been demonstrated to be an excellent marker for monitoring treatment efficacy [15, 25-27]. Although POC-CCA and microhaematuria rapid tests are user-friendly, kappa statistics revealed a poor agreement between these tests and the UCP-LF CAA. It was expected that the combined positivity rates of POC-CCA and microhaematuria dipstick test would reflect the UCP-LF CAA results, however this was not the case (Table 1). The poor agreement may be due to production batch differences, sexually transmitted infections (STIs), low-intensity infections, and subjectivity to test readouts, which might also affect results [28]. Furthermore, more accurate result with both tests might have been possible if the test was scored in a more quantitative manner. For example, following the recently described G-score scoring method for POC-CCA, an inclusion of control samples as a way to standardize the readout and to determine the cut-off for positivity. The microhaematuria test can be scored semi-quantitatively based on color intensity linked to the level of red blood cells. However, registering of more quantitative results was not foreseen in this study.

In conclusion, this study demonstrates a moderate prevalence of schistosomiasis in Mwanga district Tanzania, implicating that the ~ 20 years annual MDA of praziquantel in this region may have had an effect on reducing the schistosomiasis burden, but transmission is still ongoing. To improve the efficacy of MDA strategies, diagnosis at acute stages of the disease in combination with treatment could be extended not only to higher risk groups but also to all persons above two years of age as recommended by WHO [9, 29]. Apart from that, integrated approaches including improved access to WASH infrastructure, political willingness, and production of reliable data are important for controlling schistosomiasis in Tanzania [30]. The presence of persistent hotspots in countries like Tanzania where provision of MDA programme failed to provide long terms solution in some villages shows the need for such an integrated approach[31]. Furthermore, a combination of the POC-CCA and microhaematuria dipstick did not prove to be useful as a screening tool for schistosomiasis in this *S. haematobium* and *S. mansoni* co-endemic setting. However, efforts are ongoing to make CAA detection generally available, with a recent initiative focusing on the development of a more easy-to-use, accurate, affordable and visually scored CAA-RDT [32, 33]. The CAA-RDT could be of great potential in resource-poor endemic settings and assist in the development of targeted control measures and interventions to effectively combat schistosomiasis.

Acknowledgements

We gratefully acknowledge Claudia de Dood (LUMC) for her assistance in performing the CAA analysis, Dieuwke Kornelis (LUMC) for technical assistance with the POC-CCA, and George A. Masisila for assisting in data entry and POC-CCA processing.

References

1. World Health Organization. Schistosomiasis facts sheet: World Health Organization; 2023 [Available from: https://www.who.int/news-room/fact-sheets/detail/schistosomiasis.
2. Mazigo HD, Nuwaha F, Kinung'hi SM, Morona D, de Moira AP, Wilson S, et al. Epidemiology and control of human schistosomiasis in Tanzania. Parasites & vectors. 2012;5:1-20.
3. Kavana N. Prevalence of Schistosomiasis Infection among Young Children Aged 5 to 17 Years in Kilosa District, Tanzania: A 3 Year Retrospective Review. J Trop Dis. 2018;6(255):2.
4. Munisi DZ, Buza J, Mpolya EA, Kinung'hi SM. Intestinal Schistosomiasis among Primary Schoolchildren in Two On-Shore Communities in Rorya District, Northwestern Tanzania: Prevalence, Intensity of Infection and Associated Risk Factors. Journal of parasitology research. 2016;2016(1):1859737.
5. Bakuza JS, Denwood MJ, Nkwengulila G, Mable BK. Estimating the prevalence and intensity of Schistosoma mansoni infection among rural communities in Western Tanzania: The influence of sampling strategy and statistical approach. PLoS Neglected Tropical Diseases. 2017;11(9):e0005937.
6. Poggensee G, Krantz I, Nordin P, Mtweve S, Ahlberg B, Mosha G, et al. A six-year follow-up of schoolchildren for urinary and intestinal schistosomiasis and soil-transmitted helminthiasis in Northern Tanzania. Acta tropica. 2005;93(2):131-40.
7. Mwanga JR, Kinung'hi SM, Mosha J, Angelo T, Maganga J, Campbell Jr CH. Village response to mass drug administration for schistosomiasis in Mwanza region, northwestern Tanzania: are we missing socioeconomic, cultural, and political dimensions? The American Journal of Tropical Medicine and Hygiene. 2020;103(5):1969.
8. Clements AC, Lwambo NJ, Blair L, Nyandindi U, Kaatano G, Kinung'hi S, et al. Bayesian spatial analysis and disease mapping: tools to enhance planning and implementation of a schistosomiasis control programme in Tanzania. Tropical medicine & international health. 2006;11(4):490-503.
9. World Health Organisation. WHO GUIDELINE on control and elimination of human schistosomiasis: World Health Organisation. https://www.who.int/publications/i/item/9789240041608; 2022 [Available from: https://www.who.int/publications/i/item/9789240041608.
10. Hoekstra PT, Madinga J, Lutumba P, van Grootveld R, Brienen EAT, Corstjens P, et al. Diagnosis of Schistosomiasis without a Microscope: Evaluating Circulating Antigen (CCA, CAA) and DNA Detection Methods on Banked Samples of a Community-Based Survey from DR Congo. Trop Med Infect Dis. 2022;7(10).
11. Bärenbold O, Garba A, Colley DG, Fleming FM, Haggag AA, Ramzy RM, et al. Translating preventive chemotherapy prevalence thresholds for Schistosoma mansoni from the Kato-Katz technique into the point-of-care circulating cathodic antigen diagnostic test. PLoS neglected tropical diseases. 2018;12(12):e0006941.
12. Ochodo EA, Gopalakrishna G, Spek B, Reitsma JB, Van Lieshout L, Polman K, et al. Circulating antigen tests and urine reagent strips for diagnosis of active schistosomiasis in endemic areas. Cochrane Database of Systematic Reviews. 2015(3).
13. Emukah E, Gutman J, Eguagie J, Miri ES, Yinkore P, Okocha N, et al. Urine heme dipsticks are useful in monitoring the impact of praziquantel treatment on Schistosoma haematobium in sentinel communities of Delta State, Nigeria. Acta tropica. 2012;122(1):126-31.
14. Corstjens PL, de Dood CJ, Knopp S, Clements MN, Ortu G, Umulisa I, et al. Circulating Anodic Antigen (CAA): a highly sensitive diagnostic biomarker to detect active Schistosoma infections—improvement and use during SCORE. The American journal of tropical medicine and hygiene. 2020;103(1 Suppl):50.
15. Hoekstra PT, van Esbroeck M, de Dood CJ, Corstjens PL, Cnops L, Wammes LJ, et al. Early diagnosis and follow-up of acute schistosomiasis in a cluster of

infected Belgian travellers by detection of antibodies and circulating anodic antigen (CAA): a diagnostic evaluation study. Travel Medicine and Infectious Disease. 2021;41:102053.
16. Langenberg MC, Hoogerwerf M-A, Koopman JPR, Janse JJ, Kos-van Oosterhoud J, Feijt C, et al. A controlled human Schistosoma mansoni infection model to advance novel drugs, vaccines and diagnostics. Nature medicine. 2020;26(3):326-32.
17. Kajembe VR, Gasarasi DB, Tarimo DS, Lushina M, Sylvester B. Prevalence and factors associated with persistent transmission of Schistosoma haematobium among primary school children after five rounds of mass drug administration using praziquantel: A cross sectional study in Mkuranga district, Tanzania. Tropical Doctor. 2022;52(4):526-31.
18. Maganga JK, Campbell Jr CH, Angelo T, Mosha J, Mwanga JR, Kinung'hi SM. Test-treat-track-test-treat strategy for control of schistosomiasis in two low-prevalence villages in Northwestern Tanzania. The American Journal of Tropical Medicine and Hygiene. 2023;108(6):1167.
19. Mazigo HD, Uisso C, Kazyoba P, Nshala A, Mwingira UJ. Prevalence, infection intensity and geographical distribution of schistosomiasis among pre-school and school aged children in villages surrounding Lake Nyasa, Tanzania. Scientific Reports. 2021;11(1):295.
20. Mnkugwe RH, Minzi OS, Kinung'hi SM, Kamuhabwa AA, Aklillu E. Prevalence and correlates of intestinal schistosomiasis infection among school-aged children in North-Western Tanzania. PloS one. 2020;15(2):e0228770.
21. Ogweno G, Mushi V, Silvestri V, Bonaventura W, Justine NC, Noah M, et al. Burden and risk factors for Schistosoma mansoni infection among primary school children: A quantitative school-based cross-sectional survey in Busega district, Northern Tanzania. PLoS One. 2023;18(1):e0280180.
22. Oettle RC, Wilson S. The interdependence between schistosome transmission and protective immunity. Tropical Medicine and Infectious Disease. 2017;2(3):42.
23. Woolhouse M. Patterns in parasite epidemiology: the peak shift. Parasitology today. 1998;14(10):428-34.
24. Reitzug F, Ledien J, Chami GF. Associations of water contact frequency, duration, and activities with schistosome infection risk: A systematic review and meta-analysis. PLOS Neglected Tropical Diseases. 2023;17(6):e0011377.
25. Hoekstra PT, Casacuberta-Partal M, van Lieshout L, Corstjens PLAM, Tsonaka R, Assaré RK, et al. Limited efficacy of repeated praziquantel treatment in Schistosoma mansoni infections as revealed by highly accurate diagnostics, PCR and UCP-LF CAA (RePST trial). PLOS Neglected Tropical Diseases. 2022;16(12):e0011008.
26. Hoekstra PT, Chernet A, de Dood CJ, Brienen EA, Corstjens PL, Labhardt ND, et al. Sensitive diagnosis and post-treatment follow-up of schistosoma mansoni infections in asymptomatic eritrean refugees by circulating anodic antigen detection and polymerase chain reaction. The American journal of tropical medicine and hygiene. 2022;106(4):1240.
27. Sousa MS, Van Dam GJ, Pinheiro MCC, de Dood CJ, Peralta JM, Peralta RHS, et al. Performance of an ultra-sensitive assay targeting the circulating anodic antigen (CAA) for detection of Schistosoma mansoni infection in a low endemic area in Brazil. Frontiers in immunology. 2019;10:682.
28. Assaré RK, Tra-Bi MI, Coulibaly JT, Corstjens PL, Ouattara M, Hürlimann E, et al. Accuracy of two circulating antigen tests for the diagnosis and surveillance of schistosoma mansoni infection in low-endemicity settings of Côte d'Ivoire. The American journal of tropical medicine and hygiene. 2021;105(3):677.
29. Faust CL, Osakunor DN, Downs JA, Kayuni S, Stothard JR, Lamberton PH, et al. Schistosomiasis control: leave no age group behind. Trends in parasitology. 2020;36(7):582-91.
30. Abe EM, Tambo E, Xue J, Xu J, Ekpo UF, Rollinson D, et al. Approaches in scaling up schistosomiasis intervention towards transmission elimination in Africa: leveraging from the Chinese experience and lessons. Acta tropica. 2020;208:105379.

31. Kittur N, King CH, Campbell Jr CH, Kinung'hi S, Mwinzi PN, Karanja DM, et al. Persistent hotspots in schistosomiasis consortium for operational research and evaluation studies for gaining and sustaining control of schistosomiasis after four years of mass drug administration of praziquantel. The American journal of tropical medicine and hygiene. 2019;101(3):617.
32. FIND. Rapid test for precision mapping, and monitoring and evaluation of schistosomiasis control programmes 2020 [Available from: https://www.finddx.org/what-we-do/projects/rapid-test-for-precision-mapping-and-monitoring-and-evaluation-of-schistosomiasis-control-programmes.
33. GHIT. Schistosomiasis rapid diagnostic test to support control programmes in monitoring treatment impact and reassessment mapping 2020 [Available from: https://www.ghitfund.org/investment/portfoliodetail/detail/167/en

Supplementary information

Supplementary Table 1. Socio-demographic characteristics associated to *Schistosoma* infection, as determined by UCP-LF CAA, among 576 school children in Mwanga

Variables	Frequency (%)	N° CAA Positive (%)	X^2	P-Value
Total (N=576)		**117 (20.3)**		
Age (years)				
5-10	351(60.9)	86(24.5)	9.7	0.002
11-16	225(39.1)	31(13.8)		
Sex				
Male	284(49.0)	58(20.4)	1.0	0.948
Female	292(50.7)	59(20.2)		
School enrolled				
Kagongo	279(48.4)	35(12.5)	4	<0.001
Kileo	59(10.2)	14(23.7)		
Kivulini	57(9.9)	19(33.3)		
Mkombozi	106(18.4)	31(29.2)		
Mnoa	75(13.0)	18(24.0)		
Class				
1-3	290(50.3)	76(26.2)	2	0.002
4-5	166(28.8)	22(13.3)		
6-7	120(20.8)	19(15.8)		
Mother's occupation				
Farming	258(44.8)	62(24.0)	4	0.067
Fishing	4(0.7)	0(0.0)		
House wife	88(15.3)	19(21.6)		
Small business	197(34.2)	28(14.2)		
Employed	29(5.0)	8(27.6)		
Father's occupation (n=575)				
Farming	269(46.7)	69(25.7)	3	0.006
Fishing	135(23.4)	17(12.6)		
Small business	119(20.7)	18(15.1)		
Employed	52(9.0)	13(25.0)		

Supplementary Table 2. Factors associated with *Schistosoma* infection among school children in Mwanga.

Variable	N	COR	95% CI	P-Value	AOR	95% CI	P-Value
Age							
5 – 10	351	1			1		
11 – 15	225	0.5	0.31-077	0.002	0.7	0.33-1.6	0.44
Class							
1– 3	290	1			1		
4 – 5	166	0.4	0.26-0.72	0.001	0.4	0.19-0.75	0.006
6 – 7	120	0.5	0.30-0.923	0.025	0.3	0.13-0.90	0.030
Farming Involvement							
No	330	1			1		
Yes	246	5.2	3.3-8.2	<0.001	5.6	3.3-9.4	<0.001
Fishing Involvement							
No	431	1			1		
Yes	145	1.7	1.1-2.6	0.024	0.8	0.50-1.42	0.525
Father occupation							
Farming	269	1			1		
Fishing	135	0.42	0.23-0.74	0.003	1.1	0.52-2.47	0.755
Small business	119	0.52	0.29-0.92	0.023	0.9	0.32-2.24	0.745
Employed	52	0.96	0.49-1.92	0.992	0.5	0.20-1.22	0.130
Swimming							
No	147	1			1		
Yes	429	2.0	1.2-3.4	0.011	3.6	1.85-6.95	<0.001
School							
Kagongo	279	1			1		
Kileo	59	2.2	1.1-4.4	0.029	2.2	0.89-5.26	0.087
Kivulini	57	3.5	1.8-6.7	<0.001	2.6	1.13-5.85	0.025
Mkombozi	106	2.9	1.7-5.0	<0.001	2.4	1.21-4.94	0.013
Mnoa	75	2.2	1.2-4.2	0.015	2.7	1.17-6.43	0.021

COR:Crue odds ratio; AOR: Adjusted odds ratio

3.

Performance evaluation of the Schistoscope 5.0 for (semi-) automated digital detection and quantification of *Schistosoma haematobium* eggs in urine: A field-based study in Nigeria

Brice Meulah, Prosper Oyibo, Michel Bengtson, Temitope Agbana, Romeo Lontchi, Akim Adegnika, Wellington Oyibo, Cornelis Hokke, Jan-Carel Diehl, and Lisette van Lieshout.

The American Journal of Tropical Medicine and Hygiene, 2022; *107*(5), p.1047.

Abstract

Conventional microscopy is the standard procedure for the diagnosis of schistosomiasis, despite its limited sensitivity, reliance on skilled personnel to read the prepared slides and the fact that it is error-prone. Hence, improved diagnostic methods including those based on (semi-) automated optical devices are in demand. Here, we report the performance of the innovative Schistoscope 5.0 for optical digital detection and quantification of *Schistosoma (S) haematobium* eggs in urine, using conventional microscopy as the reference standard. At baseline, 487 participants in a rural setting in Nigeria were assessed, of which 166 (34.1%) tested *S. haematobium* positive by conventional microscopy. In addition, 38 positive cases were retested 10 days post-praziquantel treatment to monitor the effect of drug therapy. Captured images from the Schistoscope 5.0 were analyzed manually (semi-automation) and by an artificial intelligence (AI) algorithm (full-automation). Semi- and fully-automated digital microscopy showed comparable sensitivities of 80.1% (95% confidence interval: 73.2-86.0) and 87.3% (95% CI: 81.3-92.0), but a significant difference in specificity of 95.3% (95% CI: 92.4-97.4) and 48.9% (95% CI: 43.3-55.0), respectively. Overall, estimated egg counts of the semi- and fully-automated digital microscopy correlated with the egg counts of conventional microscopy, although the fully-automated procedure generally underestimated the higher egg counts. Following drug treatment, conventional microscopy and semi-automated digital microscopy showed comparable diagnostic performance. In this first extensive field evaluation we found the Schistoscope 5.0 to be a promising tool for the detection and monitoring of *S. haematobium* infection, although further improvement of the AI algorithm for full-automation is required

Introduction

Schistosomiasis is a neglected tropical disease (NTD) affecting approximately 250 million people, and more than 700 million people are at risk of infection [1]. Sub-Saharan Africa shares the greatest burden of this disease [2], and pre-school and school-age children are the most affected. It is a parasitic worm infection of poverty that leads to chronic disease and significant disability-adjusted life years lost [3]. Several *Schistosoma* species are known to affect humans. Urogenital schistosomiasis is caused by *S. haematobium*, while *S. mansoni* is the major species causing intestinal disease. *S. haematobium* infections are most prevalent in Africa, affecting the urogenital system with hematuria, bladder- and kidney failure as the main complications, and genital schistosomiasis with presentations such as vaginal discharge and postcoital bleeding in women, and hematospermia in me [3, 4]. Chronic infections can lead to miscarriage and infertility, and may facilitate infection with sexually transmitted diseases, including HIV [4].

The prevailing strategy to control and eliminate this disease is a comprehensive integrated program of mass drug administration (MDA) with praziquantel, water sanitation and hygiene (WASH), snail vector control, and a multisectoral approach to diagnostic monitoring and evaluation [5]. The diagnosis of *S. haematobium* infection typically involves the detection of eggs in urine by conventional light microscopy. Counting the number of eggs seen per 10 mL of urine is commonly done in order to indicate the intensity of infection in a target population [3, 5], which is relevant for the purpose of monitoring and evaluation. However, the need for expert laboratory personnel, basic laboratory infrastructure, and a permanent power supply limits the use of conventional light microscopy in endemic resource-limited settings. In addition, in areas where laboratory infrastructure is inadequate, the ratio of trained personnel to sample analysis is often very low resulting in a very high workload per technician, and above threshold eye exposure to the microscopy light source causing visual health complications [6, 7]. Therefore, there is a need for innovative and preferably easy-to-use diagnostics that will suit endemic resource-limited settings to diagnose infections and complement control and elimination efforts.

During the last decade innovative optical diagnostic devices, with or without artificial intelligence (AI), have been developed for the detection of *S. haematobium* eggs [8-15]. While several of these devices scan through samples and save digitalized images for manual identification of *Schistosoma* spp [8-12], only a few have an integrated AI program for automated detection [13-15]. To our knowledge, only four of these devices have been field validated using samples from a *Schistosoma* exposed population [9-12], and only the Newton Nm1 microscope has been marketed commercially as a portable field microscope, though without a fully-automated AI application [12]. This limited validation highlights the technical challenges that are faced in order to transition working prototypes to commercialized and field applicable devices. Also, most studies have used only a small, often non-randomly selected, number of clinical samples to validate the diagnostic devices. Hence, there is a clear need for more extensive field-based studies.

The Schistoscope device (version 5.0) is a low-cost digital microscope (Figure 1A and 1B) that has gone through five design iterations in an ongoing process of co-creation including different potential stakeholders. In its current form it can function either as a semi-automated or AI integrated fully-automated digital microscope to detect and quantify *S. haematobium* eggs [16, 17]. In a recent proof-of-principle study, the device and its AI algorithms were trained successfully with phosphate buffer saline and urine samples that were spiked with *S. haematobium* eggs obtained from a laboratory maintained parasite life cycle, and a limited number of clinical samples [18]. This led to the conclusion that the Schistoscope was ready for further validation. The aim of the current study is to evaluate the performance of the Schistoscope 5.0 as a semi- and fully-automated digital microscope for the detection and quantification of *S. haematobium* eggs in a prospective study design under field conditions. For this purpose urine samples were collected in a rural area in Nigeria, filtered and each membrane filter was independently examined locally by conventional microscopy and the Schistoscope 5.0.

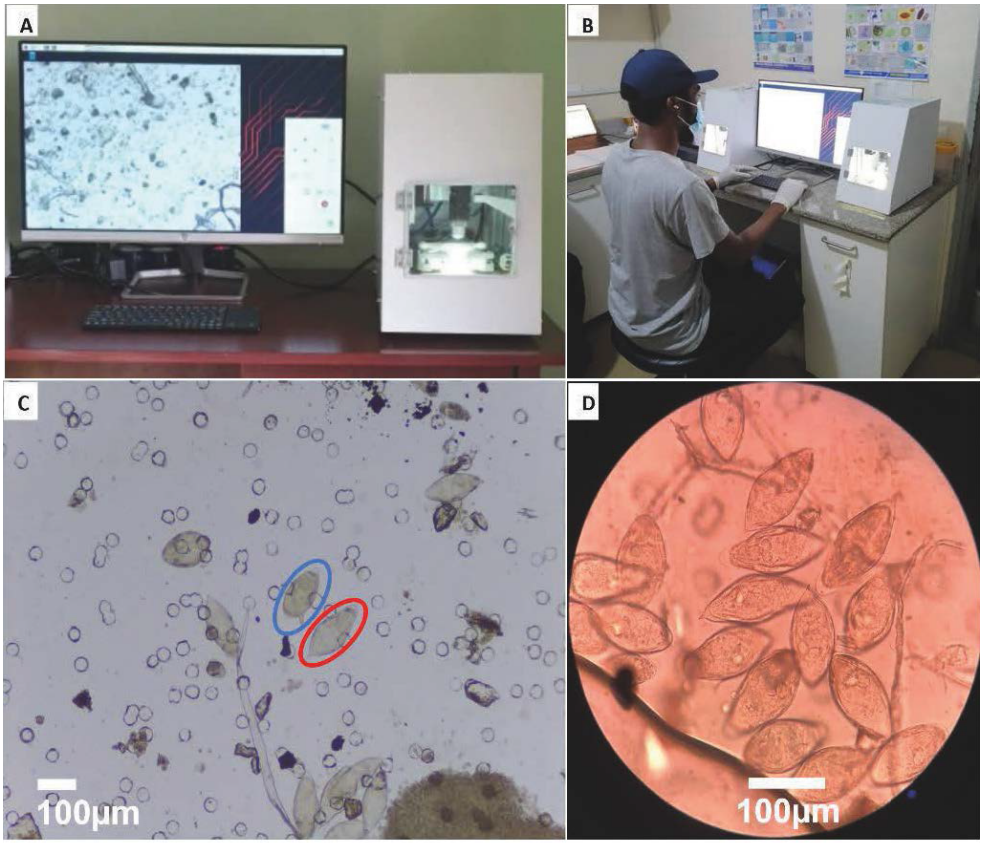

Figure 1. (A) Schistoscope 5.0 device (right) connected to a computer monitor (left), showing an image of a digitally screened sample; (B) Schistoscope 5.0 operated by a laboratory technician in the field; (C) Digital image of a urine filtered membrane showing several Schistosoma eggs captured with the Schistoscope 5.0 (4X objective). The red circle indicates a *S. haematobium* egg, the blue circle indicates a *S. mansoni* egg; (D) Image of a urine filtered membrane with several *S. haematobium* eggs captured by a camera attached to a conventional microscope (10x objective).

Materials And Methods

Ethical considerations

This study was done in collaboration with the Schistosomiasis Programme of the Neglected Tropical Diseases department, Federal Ministry of Health, Abuja and embedded in an ongoing, cross-sectional community-based survey in collaboration with the Public Health Department in charge of the MDA of praziquantel in the Federal Capital Territory (FCT), Nigeria. The ethical approval for this study was obtained from the FCT Health Research Ethics Committee (HREC) in Abuja, Nigeria (reference no. FHREC/2019/01/73/18-07-19). Written consent for adults, and for parents or legal guardians of children and teenagers was obtained prior to sample collection from persons willing to participate through their signatures or thumbprints. Confidentiality and anonymity of results were ensured by assigning unique codes to samples. According to the local standard operational procedures, all participants with detectable hematuria (see below) were considered *S. haematobium* positive and therefore treated with praziquantel (40mg/per Kg of body weight). The local health authorities have been informed of the outcome of the study and all participants have been offered (re)treatment where appropriate.

Study design and population

This cross-sectional and longitudinal study was carried out from August to September 2021 in two area councils in FCT, Abuja, Nigeria (Geographical coordinates: 9.0618° N latitude, 7.4221° E longitude and 8.950833° N latitude, 7.076737° E longitude). The FCT is the third highest endemic state for schistosomiasis in Nigeria [19]. In total, 14 communities from these two area councils were visited, where pre-school, school-age children and adults were allowed to participate. Strategic advocacy and engagement with community leaders in the study area preceded the sample collection at the communities studied.

Sample collection and processing

Figure 2 depicts the flowchart of sample collection. Briefly, a sterile 20 mL universal container with a unique identification code was given to those who consented to participate with the request to collect a urine sample between 11:00 am and 13:00 pm. Dipstick (Combur 10-Test M Roche Mannheim, Germany) urinalysis was performed on site according to the manufacturer's instructions. Of those who were confirmed as positive by conventional urine microscopy, 50 were randomly selected and asked to provide an additional sample 10 days after baseline screening. This small scale post-treatment evaluation was done to examine whether drug treatment could influence the performance of the Schistoscope 5.0, possibly via praziquantel induced changes in egg morphology [20, 21].

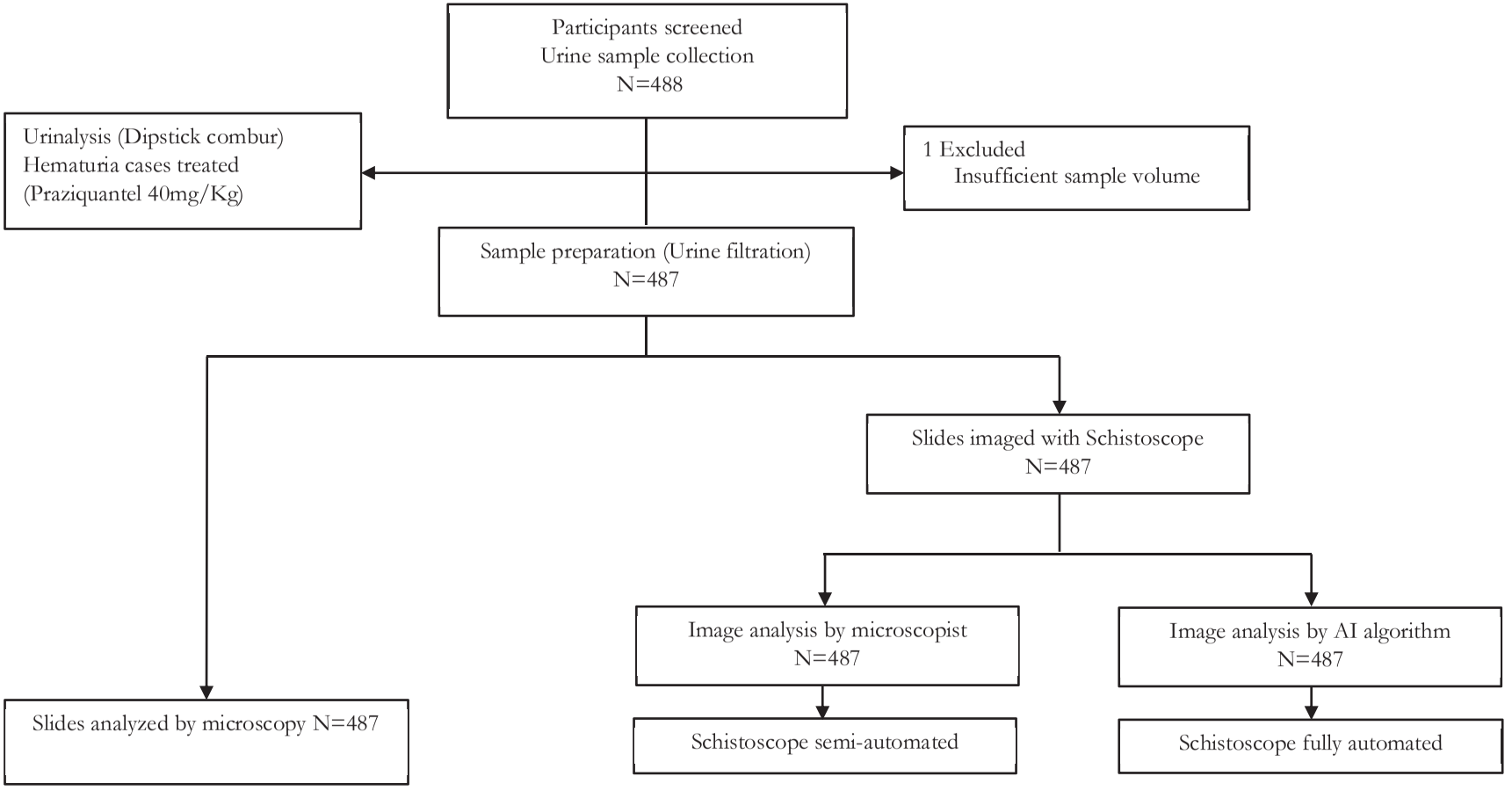

Figure 2. Flow-chart of urine sample collection and analysis, aiming to compare conventional microscopy with semi-automated and fully-automated digital microscopy.

All urine samples were transported to the laboratory of the Department of Public Health, Abuja, FTC, within two hours of sample collection and prepared for microscopy by urine filtration [22]. Urine samples were homogenized, and 10 mL urine was obtained with a syringe and pressed through a filter membrane (diameter 13 mm; pore size 30 μm; Whatmann International Ltd). The filter membrane was then placed on a standard microscope glass slide and a cover slip was placed over the membrane to keep the filter moist. Each slide was viewed under a standard microscope and the Schistoscope.

Description of the Schistoscope 5.0

The Schistoscope 5.0 (Figure 1) is a low-cost automated slide-scanner digital microscope that can be supported with AI algorithms for image processing [18]. The system is composed of custom-designed optical bright-field illumination, 3-axis movement (XYZ), and electronic and computing modules. The illumination module comprises a bright white light-emitting diode and condenser lenses to generate uniform illumination. The custom 3-axis motorized stage provides a step resolution of 2.5 μm on all three axes. A custom printed circuit board is used to control all three motors and the illumination. The on-board computer is a Raspberry Pi 4B connected to a Raspberry Pi HQ camera which has a pixel size of 1.55 μm and an image resolution of 2028 × 1520 pixels. The current study used a 4x microscope objective that provides an experimental resolution limit of 3.26 microns,18 which is sufficient to resolve *S. haematobium* eggs (Figure 1C). The device runs on mains electricity and does not have a built-in battery. Dedicated software with a graphical user interface was developed and installed on the device's onboard computer for easy user interaction and control of the device. The software comprises a simple autofocus procedure and an algorithm to scan the complete filter membrane and capture each field of view as an image. It takes 12 minutes to scan and capture 117 images of an entire 13 mm filter membrane. Additional analysis of the captured images, including counting the number of eggs, takes approximately 5 minutes on average per filter when done either manually or by AI. Captured images are stored in folders by their sample identification code, and semi-automated analysis can be done via a connected computer monitor or automated analysis can be done on an external computer. Further development is ongoing to enable automated processing and analysis on the device itself.

Detection of S. haematobium eggs by microscopy and the Schistoscope

Slides were examined immediately after preparation. The order of examination was randomized, resulting in approximately half of the slides being first analyzed by conventional microscopy and then imaged with the Schistoscope 5.0, while the other half were analyzed in the opposite sequence.

For conventional light microscopy, slides were analyzed using a 10x objective on an Olympus CX22RFS1 microscope (Olympus, Tokyo, Japan) (Figure 1D). Two microscopists independently examined each slide for the detection and quantification of *S. haematobium* eggs

with results blinded from each other. The average of egg counts from both microscopists was computed as the final result. Discrepancies of more than 20% between both microscopy readings were resolved by a third independent microscopy reading of which an average between two closest amongst the three readings was considered.

The imaging procedure of the Schistoscope included manual counting of the eggs seen on the images, which was done in the field by a fourth microscopist who was blinded from the results of the conventional light microscopy. The images were also uploaded to a cloud server (Google Colaboratory https://colab.research.google.com/) for remote access and AI analysis. For quality control of the manual analysis of the captured images, 10% of the images were randomly selected and re-examined by an independent senior microscopist, but as this showed no significant differences with the original manual readings, these data are not further discussed. Data from the two independent microscopists, the manual reading and the AI analysis were independently entered in an Excel spreadsheet and only shared with the results collation officer after finalizing.

Power calculations and statistical analysis

For the cross-sectional evaluation of the Schistoscope, the number of positive cases needed to achieve an assumed sensitivity and specificity of 80% and 90% using conventional microscopy as the reference, was calculated to be 107 [23]. The power of this calculation was set to 80% and a 5% degree of error was considered to be able to detect a difference of at most 10% from the assumed sensitivity and specificity. With a schistosomiasis prevalence of 25% in the FCT region [19], a total of 450 samples was needed to meet our target case number. Microscopy and Schistoscope data were merged and double-checked by the collation officer. Descriptive statistics for the data were obtained using IBM Statistical Package for Social Sciences version 25 (SPSS Inc., Chicago, United States of America). For the baseline sample subset, sensitivity, specificity, positive predictive value (PPV), and negative predictive value (NPV) of the semi- and fully-automated digital microscope were calculated for *S. haematobium* detection using conventional light microscopy as the reference standard. Qualitative agreement between the Schistoscope and conventional microscopy was assessed using the adjusted Cohen's Kappa, considering true positives and true negatives, as well as false positives and false negatives [24]. Egg counts were categorized as low-intensity infection (≤ 50 eggs/10 mL urine) or high-intensity infection (> 50 eggs/10 mL urine). Due to the non-gaussian nature and wide range of the egg count estimates by all three methods, the data set was log transformed before analysis was performed. The linear association in terms of egg counts (eggs/10 mL) between the different optical procedures was estimated using the Pearson's correlation coefficient (r), excluding the negative data points. Bland-Altman analysis was performed to quantitatively assess the agreement between semi- and fully-automated digital microscopy and conventional microscopy using GraphPad Prism version 9.0.1 for windows (GraphPad Software, San Diego, California USA, www.graphpad.com). Cure rate (CR), defined as the percentage of follow-up samples with no detectable eggs, and egg reduction rate (ERR), defined as the percentage reduction in the

geometric mean (GM; formula: GM (egg count +1) – 1) egg counts pre- and post-treatment, were estimated for each of the microscopy procedures.

Results

Performance evaluation of the Schistoscope and estimation of egg counts

In order to evaluate the capacity of the Schistoscope to detect and count *S. haematobium* eggs, each of the 487 prepared slides was examined by conventional microscopy, semi- and fully-automated digital microscopy. No differences were noticed resulting from the order in which the filters were examined (e.g. first by conventional microscopy, followed by image capturing by the Schistoscope or vice versa). The three detection methods, i.e. conventional microscopy, semi- and fully-automated digital microscopy, independently identified 166 (34.1%), 148 (30.4%) and 309 (63.4%) of the slides as positive for S. haematobium, respectively (Table 1). Egg count estimates per 10 mL of urine ranged from 1-4,386 eggs/10 mL for conventional microscopy, 1-2,059 eggs/10 mL for semi-automated digital microscopy, and 1-573 eggs/10 mL for fully-automated digital microscopy, with a median of 12, 12, and 2 eggs/10 mL, respectively. Compared to conventional microscopy, semi- and fully-automated digital microscopy showed an overall accuracy of 90.1% and 62.0%, respectively (Table 1).

Table 1. Cross tabulation of the detection of *S. haematobium* eggs by the Schistoscope 5.0 and conventional microscopy performed on 487 urines collected at baseline screening

		Conventional microscopy		
Schistoscope 5.0		Positive (N=166)	Negative (N=321)	Total (N=487)
Semi-automated digital microscope	Positive	133	15	148
	Negative	33	306	339
Fully-automated digital microscope	Positive	145	164	309
	Negative	21	157	178

Table 2 summarizes the sensitivity, specificity, PPV and NPV of the semi- and fully-automated digital microscopy. The sensitivities of the semi-and fully-automated digital microscope for the detection of *S. haematobium* eggs were comparable; 80.1% (95% confidence interval (CI) 73.2-86.0%) and 87.3% (95% CI 81.3-92.0%) respectively, but the fully-automated procedure showed a much lower specificity (48.9%; 95% CI 43.3-55.0%) than the semi-automated procedure (95.3%; 95% CI 92.4-97.4%). This resulted in a low PPV (46.9%) for the fully-automated digital microscope (Table 2). Conventional microscopy classified 129 (78%) as low-intensity infection and 37 (22%) as high-intensity infection, while semi- and fully-automated microscopy classified 111 (75%) and 294 (95%) as low-intensity infection and 37 (25%) and 15 (5%) as high-intensity infection, respectively. The sensitivities of semi- and fully-automated digital microscopy for low-intensity infections were 75.2% (95% CI 67.0-82.3%) and 83.7% (95% CI 76.1-90.0%) which increased for high-intensity infections (Table 2). The adjusted Cohen's Kappa demonstrated a fair (0.34) and a slight (0,2) qualitative agreement between conventional microscopy and semi- and fully-automated digital microscopy, respectively.

Table 2. Diagnostic performance of the Schistoscope 5.0 for the detection of *Schistosoma* eggs performed on 487 urines collected at baseline screening.

Conventional microscopy	Schistoscope 5.0							
	Semi-automated digital microscopy				Automated digital microscopy			
	Sensitivity (95% CI)	Specificity (95% CI)	PPV (95% CI)	NPP (95% CI)	Sensitivity (95% CI)	Specificity (95% CI)	PPV (95% CI)	NPV (95% CI)
All samples with *S. haematobium* infection (N=166)	80.1 (73.2-86.0)	95.3 (92.4-97.4)	89.8 (84.0-94.2)	90.3 (87.0-93.2)	87.3 (81.3-92.0)	48.9 (43.3-55.0)	46.9 (41.2-53.0)	88.2 (83.0-93.0)
Low-intensity infection (≤ 50 eggs/10mL urine, N=129)	75.2 (67.0-82.3)	—	—	—	83.7 (76.1-90.0)	—	—	—
High-intensity infection (> 50 eggs/10mL urine, N=37)	97.3 (86.0-100.0)	—	—	—	100	—	—	—

In terms of *S. haematobium* egg count estimates, conventional microscopy correlated strongly to semi-automated digital microscopy (N=133, r=0.90, P<0.001) and fully-automated digital microscopy (N=145, r=0.80, P<0.001) (Figure 3). To demonstrate reliability of conventional microscopy, Bland-Altman analysis showed a strong agreement between the first and second microscopy readings across the range of mean egg counts for both readings (bias=0.13, 95% limits of agreement from -0.66 to 0.94). Further Bland-Altman analysis demonstrated a strong agreement between conventional microscopy and semi-automated digital microscopy across the range of mean egg counts for both methods (bias=0.08, 95% limits of agreement from -0.69 to 0.85) (Figure 4). Conventional microscopy and fully-automated digital microscopy revealed a strong agreement at low mean egg counts of both methods. However, an underestimation of egg counts by fully-automated digital microscopy was observed at egg counts greater than 100 eggs/10 mL (bias=0.47, 95% limits of agreement from -0.69 to 1.63).

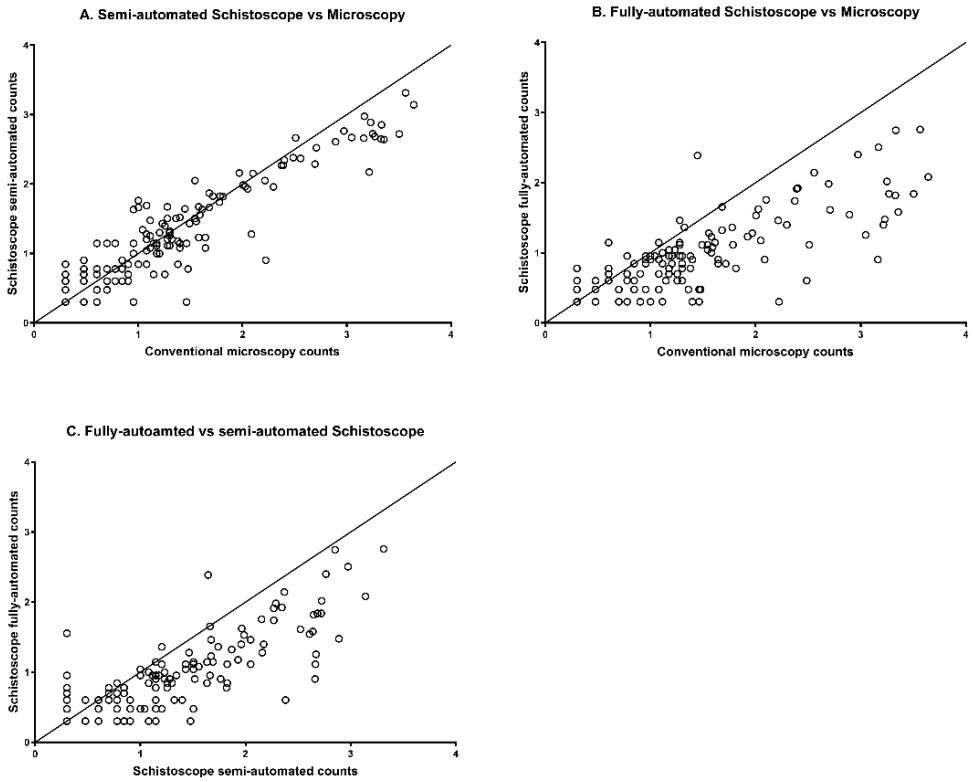

Figure 3. Correlation in *S. haematobium* egg counts per 10 mL of urine, on a Log10 scale on samples collected at baseline screening. Negative data points are excluded. A) Semi-automated digital microscopy versus conventional microscopy (N=133, r= 0.90, P<0.001); B) Fully-automated digital microscopy versus conventional microscopy (N=145, r=0.80, P<0.001); C) Semi-automated versus fully-automated digital microscopy (N=137, r=0.80, P<0.001). The depicted solid line indicates y=x.

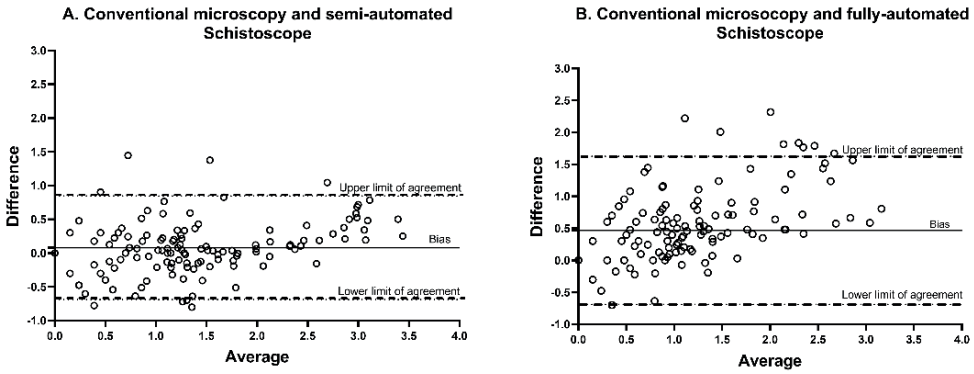

Figure 4: Bland-Altman plots showing the level of agreement between (A) conventional microscopy and semi-automated digital microscopy counts, (B) conventional microscopy and fully-automated digital microscopy counts.

Follow-up after praziquantel treatment

Conventional microscopy and the semi-automated Schistoscope procedure were also compared on 38 urine samples collected 10 days post-praziquantel treatment of participants with a confirmed infection at baseline. Thirty (79%) and 27 (71%) samples still had detectable *S. haematobium* eggs by conventional microscopy and semi-automated digital microscopy, resulting in a CR of 21% (95% CI: 10-37) and 29% (95% CI: 15-46), respectively. In four follow-up samples, eggs were only seen by conventional microscopy, and only one sample was positive by semi-automated digital microscopy. The ERR of conventional microscopy (80%; 95% CI: 64-90) and semi-automated digital microscopy (77%; 95% CI: 60-91) were similar.

Table 3. Monitoring the effect of treatment using the semi-automated digital microscopy and conventional microscopy

	Conventional microscopy	**Semi-automated digital microscopy**
Number of samples with *S. haematobium* eggs at base line (GM)	38 (43)	38 (32)
Range of *S. haematobium* eggs/10 mL (median) at base line	1-3,183 (36)	1-524 (31)
Number of samples with *S. haematobium* eggs at day 10 after treatment (GM)	30 (9)	27 (7)
Low-intensity infection (≤ 50 eggs/10mL urine) at day 10 after treatment	24	20
High-intensity infection (> 50 eggs/10mL urine) at day 10 after treatment	6	7
ERR (95% CI)	80.0% (64.0-90.0)	77.0% (60.0-91.0)
Cure rate (95% CI)	21% (9.5-37.3)	28.9% (15.4-45.9)

Discussion

In this study, the performance of the Schistoscope 5.0 was evaluated as a semi-automated digital microscope and as an AI-based fully-automated digital microscope for the detection and quantification of *S. haematobium* eggs in a field setting. The diagnostic parameters that were assessed include sensitivity, specificity, PPV, NPV and infection intensity. At baseline screening, the sensitivity of the semi-automated digital microscope (80.1%) was lower than that of the fully-automated digital microscope (87.3%), however, this difference was not statistically significant. As expected, the sensitivity of the Schistoscope increased with increasing egg excretion. On the other hand, the Schistoscope detected additional cases as positive, which might have been true cases missed by conventional microscopy. As conventional microscopy was used as the standard reference, this resulted in a reduced specificity of the Schistoscope. The specificity was significantly lower for the fully-automated digital microscope (48.9%) than for the semi-automated digital microscope (95.3%).

A probable reason for the low specificity recorded by the fully-automated digital microscope is the limited datasets used to train the AI algorithm to detect *S. haematobium* eggs. The AI algorithm was developed using two training datasets consisting of images obtained from egg-spiking experiments resulting in relatively clean samples, and a limited number of field samples that did not contain many egg-like artifacts (e.g. uric crystals). Therefore, the AI algorithm seemed not sufficiently trained to separate egg-like artifacts from *S. haematobium* eggs. Another reason could be limitations in the deep learning model used by the AI algorithm that was optimized for enhanced sensitivity at a trade-off of specificity. Additional iterations to enhance specificity are therefore needed and are currently in progress.

Several other studies have also field evaluated digital optical devices, with or without AI, for the detection and/or quantification of *S. haematobium* eggs [9, 11, 12]. The sensitivities and specificities obtained for the various devices in these studies, with conventional microscopy as a reference, range from 35.6 % to 81.1% and 91.0% to 100%, respectively. The sensitivities of the semi- and fully-automated digital microscope reported in the current study were generally higher compared to previous reports, except for results reported by Coulibaly et al. for the Newton Nm1 microscope which is considered to be comparable in sensitivity. However, the study by Coulibaly and colleagues had a slightly lower power compared to our study, with 266 samples examined, of which 90 were egg positive.

For egg count estimates, a strong correlation was observed between semi-automated digital microscopy and conventional microscopy, while for fully-automated digital microscopy a clear underestimation of the intensity of infection was observed for samples with more than 100 eggs/10 mL urine. A possible explanation is that overlapping eggs were recognized as a single egg by the deep learning model, leading to an underestimation of egg counts. In addition, hematuria might have also caused interference. Although not systematically recorded, our impression was that samples with more than 100 eggs/10 mL of urine were often strongly positive for hematuria with an abundance of blood cells compared to samples with lower egg

counts. This could have resulted in shading the eggs on the filter membrane and subsequently limiting the detection by the AI algorithm.

Although only performed in a small subset of cases and at one time point, no substantial differences were noticed before and after treatment when comparing the semi-automated digital microscope with the conventional microscopy, suggesting that the Schistoscope could also be used for monitoring treatment. More extensive post-treatment follow-up studies are needed to demonstrate how well the Schistoscope can differentiate viable *S. haematobium* eggs from dead eggs, which can be excreted up to many weeks after receiving praziquantel (personal observation).

The Schistoscope 5.0 captured high-resolution images that clearly show the specific features of *S. haematobium* and *S. mansoni* eggs, i.e. the terminal and lateral spines (Figure 1C). In terms of potential use-cases, this supports the application of the semi-automated microscope as a diagnostic tool to assist microscopists in field laboratory settings. The use of (semi-) automated digital microscopy could reduce visual health complications caused by high eye exposure to a conventional microscope light source. Upon further development to improve the AI, the fully-automated microscope would be useful for non-expert microscopists as well (e.g. community health workers and laboratory technicians). In both cases, task shifting could be gained as personnel could focus on other activities while the device analyzes samples. The added-value of task shifting could compensate for the current time difference between conventional microscopy that requires less than 10 minutes to scan a urine filter, and the Schistoscope 5.0 which can take on average 17 minutes to complete scanning and analysis.

Limitations of this study include the choice of conventional light microscopy on a single 10 mL urine sample as the reference test, which is known for its limited sensitivity, especially in cases with low-infection intensity. Further evaluation studies should be conducted to field validate the Schistoscope 5.0 for the detection of *S. haematobium* eggs in comparison to more sensitive reference tests such as the detection of adult worm-associated circulating anodic antigens (CAA) or the detection of parasite specific DNA [25]. The Schistoscope 5.0 currently does not meet the target product profile set by WHO for new diagnostics needed for monitoring and evaluating schistosomiasis control programs [26]. For example, it does not have an onboard display and is connected to a computer monitor for visual control of the device, thus making transportation impractical. Furthermore, the device lacks a backup power supply. Additional functionalities such as an onboard computer with a graphical processing unit for higher image processing capabilities and internet access would also be beneficial. These functionalities would create the capacity to generate results in real-time for patient management, store and share digital images with other experts, and facilitate mapping of schistosomiasis [27], thereby making (semi-) automated digital devices an attractive tool for future use in epidemiology and public health settings. Here we evaluated the Schistoscope 5.0 for the first time in a rural field setting, demonstrating its potential as a digital diagnostic tool for the detection and quantification of *S. haematobium* eggs, as well as for monitoring the effect of schistosomiasis treatment in settings with limited resources.

Acknowledgments

We acknowledge the staff of the FCT Public Health Department and Neglected Tropical Diseases (NTD) Department of the Federal Ministry of Health Abuja; The Area Council authorities/NTD coordinators and focal persons; the community leaders and community members in the FCT Area Councils that were assessed in the study.

References

1. WHO. Schistosomiasis and soil-transmitted helminthiases: treating millions of people, despite the pandemic 2021 [Available from: https://www.who.int/news/item/08-12-2021-schistosomiasis-and-soil-transmitted-helminthiases-treating-millions-of-people-despite-the-pandemic.
2. Aula OP, McManus DP, Jones MK, Gordon CA. Schistosomiasis with a Focus on Africa. Trop Med Infect Dis. 2021;6(3).
3. McManus DP, Dunne DW, Sacko M, Utzinger J, Vennervald BJ, Zhou XN. Schistosomiasis. Nat Rev Dis Primers. 2018;4(1):13.
4. Bustinduy AL, Randriansolo B, Sturt AS, Kayuni SA, Leustcher PDC, Webster BL, et al. An update on female and male genital schistosomiasis and a call to integrate efforts to escalate diagnosis, treatment and awareness in endemic and non-endemic settings: The time is now. Adv Parasitol. 2022;115:1-44.
5. WHO. Ending the neglect to attain the Sustainable Development Goals – A road map for neglected tropical diseases 2021–2030. Geneva: World Health Organization; 2020. Licence: CC BY-NC-SA 3.0 IGO. 2020.
6. Ngakhushi R, Kaiti R, Bhattarai S, Shrestha G. Prevalence of myopia and binocular vision dysfunctions in microscopists. International Eye Science. 2018;18.
7. Söderberg I, Calissendorff B, Elofsson S, Knave B, Nyman KG. Investigation of visual strain experienced by microscope operators at an electronics plant. Applied Ergonomics. 1983;14(4):297-305.
8. Koydemir HC, Coulibaly JT, Tseng D, Bogoch, II, Ozcan A. Design and validation of a wide-field mobile phone microscope for the diagnosis of schistosomiasis. Travel Med Infect Dis. 2019;30:128-9.
9. Bogoch, II, Coulibaly JT, Andrews JR, Speich B, Keiser J, Stothard JR, et al. Evaluation of portable microscopic devices for the diagnosis of Schistosoma and soil-transmitted helminth infection. Parasitology. 2014;141(14):1811-8.
10. Bogoch, II, Koydemir HC, Tseng D, Ephraim RKD, Duah E, Tee J, et al. Evaluation of a Mobile Phone-Based Microscope for Screening of Schistosoma haematobium Infection in Rural Ghana. Am J Trop Med Hyg. 2017;96(6):1468-71.
11. Ephraim RK, Duah E, Cybulski JS, Prakash M, D'Ambrosio MV, Fletcher DA, et al. Diagnosis of Schistosoma haematobium infection with a mobile phone-mounted Foldscope and a reversed-lens CellScope in Ghana. Am J Trop Med Hyg. 2015;92(6):1253-6.
12. Coulibaly JT, Ouattara M, D'Ambrosio MV, Fletcher DA, Keiser J, Utzinger J, et al. Accuracy of Mobile Phone and Handheld Light Microscopy for the Diagnosis of Schistosomiasis and Intestinal Protozoa Infections in Cote d'Ivoire. PLoS Negl Trop Dis. 2016;10(6):e0004768.
13. Holmstrom O, Linder N, Ngasala B, Martensson A, Linder E, Lundin M, et al. Point-of-care mobile digital microscopy and deep learning for the detection of soil-transmitted helminths and Schistosoma haematobium. Glob Health Action. 2017;10(sup3):1337325.
14. Agbana TE, Nijman P, Hoeber M, van Grootheest D, van Diepen A, van Lieshout L, et al. Detection of Schistosoma haematobium using lensless imaging and flow cytometry, a proof of principle study. Optical Diagnostics and Sensing XX: Toward Point-of-Care Diagnostics2020.
15. Linder E, Grote A, Varjo S, Linder N, Lebbad M, Lundin M, et al. On-Chip Imaging of Schistosoma haematobium Eggs in Urine for Diagnosis by Computer Vision. PLOS Neglected Tropical Diseases. 2013;7(12):e2547.
16. Agbana T, Oladepo O, Vdovin G, Oyibo W, Van GY, Diehl JC. Schistoscope: Towards a locally producible smart diagnostic device for Schistosomiasis in Nigeria. 2019 IEEE Global Humanitarian Technology Conference (GHTC)2019. p. 1-8.
17. Diehl JC, Oyibo P, Agbana T, Jujjavarapu S, Van GY, Vdovin G, et al. Schistoscope: Smartphone versus Raspberry Pi based low-cost diagnostic device for urinary Schistosomiasis. 2020 IEEE Global Humanitarian Technology Conference

(GHTC); 29 Oct.-1 Nov. 20202020. p. 1-8.
18. Oyibo P, Jujjavarapu S, Meulah B, Agbana T, Braakman I, van Diepen A, et al. Schistoscope: An Automated Microscope with Artificial Intelligence for Detection of Schistosoma haematobium Eggs in Resource-Limited Settings. Micromachines. 2022;13(5).
19. Gideon A, Nebe O, Nduka F, Njepuome N, Dakul D, Isiyaku S, et al. Schistosomiasis: Epidemiological Factors Enhancing Transmission In Nigeria. 2020:23-032.
20. Pinto-Almeida A, Mendes T, de Oliveira RN, Corrêa SdAP, Allegretti SM, Belo S, et al. Morphological Characteristics of Schistosoma mansoni PZQ-Resistant and -Susceptible Strains Are Different in Presence of Praziquantel. Frontiers in Microbiology. 2016;7.
21. Richards F, Jr., Sullivan J, Ruiz-Tiben E, Eberhard M, Bishop H. Effect of praziquantel on the eggs of Schistosoma mansoni, with a note on the implications for managing central nervous system schistosomiasis. Ann Trop Med Parasitol. 1989;83(5):465-72.
22. Kosinski KC, Bosompem KM, Stadecker MJ, Wagner AD, Plummer J, Durant JL, et al. Diagnostic accuracy of urine filtration and dipstick tests for Schistosoma haematobium infection in a lightly infected population of Ghanaian schoolchildren. Acta Trop. 2011;118(2):123-7.
23. Jones SR, Carley S, Harrison M. An introduction to power and sample size estimation. Emerg Med J. 2003;20(5):453-8.
24. McHugh ML. Interrater reliability: the kappa statistic. Biochem Med (Zagreb). 2012;22(3):276-82.
25. Hoekstra PT, van Dam GJ, van Lieshout L. Context-Specific Procedures for the Diagnosis of Human Schistosomiasis – A Mini Review. Frontiers in Tropical Diseases. 2021;2.
26. WHO. Public consultation: Target Product Profiles for diagnostic tests to meet Schistosomiasis and Soil-transmitted Helminth programme needs. 2021 [cited 2022 17/03]; Available from: https://wwwwhoint/news-room/articles-detail/public-consultation-target-product-profiles-for-diagnostic-tests-to-meet-schistosomiasis-and-soil-transmitted-helminth-programme-needs.
27. Bogoch, II, Lundin J, Lo NC, Andrews JR. Mobile phone and handheld microscopes for public health applications. Lancet Public Health. 2017;2(8):e355.

4.

Two-stage automated diagnosis framework for urogenital schistosomiasis in microscopy images from low-resource settings

Prosper Oyibo, Brice Meulah, Michel Bengtson, Lisette van Lieshout, Wellington Oyibo, Jan-Carel Diehl, Gleb Vdovine, Temitope E. Agbana

Journal of Medical Imaging 2023, Vol. 10, Issue 4, 044005

Abstract

Purpose

Automated diagnosis of urogenital schistosomiasis using digital microscopy images of urine slides is an essential step toward the elimination of schistosomiasis as a disease of public health concern in Sub-Saharan African countries. We create a robust image dataset of urine samples obtained from field settings and develop a two-stage diagnosis framework for urogenital schistosomiasis.

Approach

Urine samples obtained from field settings were captured using the Schistoscope device, and *S. haematobium* eggs present in the images were manually annotated by experts to create the SH dataset. Next, we develop a two-stage diagnosis framework, which consists of semantic segmentation of S. haematobium eggs using the DeepLabv3-MobileNetV3 deep convolutional neural network and a refined segmentation step using ellipse fitting approach to approximate the eggs with an automatically determined number of ellipses. We defined two linear inequality constraints as a function of the overlap coefficient and area of a fitted ellipses. False positive diagnosis resulting from over-segmentation was further minimized using these constraints. We evaluated the performance of our framework on 7605 images from 65 independent urine samples collected from field settings in Nigeria, by deploying our algorithm on an Edge AI system consisting of Raspberry Pi + Coral USB accelerator.

Result

The SH dataset contains 12,051 images from 103 independent urine samples and the developed urogenital schistosomiasis diagnosis framework achieved clinical sensitivity, specificity, and precision of 93.8%, 93.9%, and 93.8%, respectively, using results from an experienced microscopist as reference.

Conclusion

Our detection framework is a promising tool for the diagnosis of urogenital schistosomiasis as our results meet the World Health Organization target product profile requirements for monitoring and evaluation of schistosomiasis control programs.

Introduction

Schistosomiasis is endemic in 76 countries worldwide with approximately 252 million people infected and an estimated 779 million people at risk of infection [1]. Schistosomiasis is caused by blood flukes of the genus *Schistosoma* (S); both *S. mansoni* (intestinal schistosomiasis) and *S. haematobium* (urogenital schistosomiasis) are endemic in Africa [2]. Schistosomiasis presents a substantial public health and economic burden as it is a disease of poverty. In the drive to attain the World Health Organisation (WHO) control and elimination targets, diagnosis for adequate monitoring of interventions and surveillance is critical [2, 3]. Recently, the WHO published the diagnostic target product profiles (TPP) for monitoring, evaluation and surveillance of schistosomiasis control programmes [4] which identifies development of diagnostic tests for *S. haematobium* detection as a high-risk requirement due to lack of its readily availability. The TPP suggests a semi-quantitative analysis, capable of providing some degree of information regarding intensity of infection, as ideal for a diagnostic test for schistosomiasis to support monitoring and evaluation [4].

Currently, microscopy is the WHO reference standard for the diagnosis of schistosomiasis in resource-limited settings. For the detection of *S. haematobium* infection, urine samples, following filtration, sedimentation or centrifugation, are microscopically examined for the presence of eggs [3]. This method is operator dependent, costly, laborious and therefore time-consuming. Furthermore, it requires expertise, which means microscopy skills need to be gained and maintained, which can be an economic challenge, particularly in remote rural communities [3]. There is also the risk of visual health complications among microscopists resulting from excessive workload due to the low ratio of trained microscopists to samples for analysis in endemic regions [5]. Hence, a field adaptable, rapid and easy-to-use automated diagnosis is relevant for the prompt detection of cases, which will facilitate mapping and monitoring of interventions [4].

Recent advances in opto-mechanics and opto-electronics have rapidly transformed the field of biomedical optics. Optical imaging technologies, such as conventional light microscopes are being re-designed to integrate and miniaturise portable light microscopes for use at the point of care (POC) [6-9]. Although these technologies are available in high-income countries, unfortunately, nearly all schistosomiasis cases are seen in low-resource regions of low-income countries, significantly justifying the need for cost-effective and easy-to-use smart diagnostic technologies. In this work, we address these challenges by first increasing the size of the *S. haematobium* (SH) dataset in our previous work [10] from 5,198 to 12,051 images of clinical samples [11]. We carry-out detection and counting of *S. haematobium* eggs present in each image by proposing a two-stage framework consisting of a DeepLabv3 with MobilenetV3 backbone deep convolutional neural network [12] trained on the SH dataset using a transfer learning approach. The second stage of our proposed framework is a refined segmentation and egg counting procedure which adapts the Region-based Fitting of Overlapping Ellipses [13] to efficiently separate the boundaries of overlapping eggs in the image. Finally, the detected isolated eggs are screened for the presence of an egg which meets the defined boundary condition before the sample can be determined as positive/negative diagnosis. We further demonstrate the robustness and applicability of the proposed framework for field diagnoses of urogenital schistosomiasis by implementing our framework on an Edge AI system (Raspberry Pi + Coral

USB accelerator) and testing 65 clinical urine samples obtained in a field settings in Nigeria. The main contributions of this work can be summarised as follows:

1. A large-scale *S. haematobium* egg dataset of 12,051 images captured in field settings is created with respective manually annotated mask images. The dataset contains images with artifacts, such as crystals, glass debris, air bubbles, and fibres.

2. A *S. haematobium* egg detection framework consisting of the DeepLabv3 with MobileNetV3 backbone deep convolutional neural network, trained using transfer learning approach for semantic segmentation of the eggs. This effectively segments transparent eggs in noisy images taken in the field. The framework also separates overlapping eggs using a refined segmentation algorithm resulting in a more accurate egg count.

3. The implementation and testing of the *S. haematobium* egg on an Edge AI system to demonstrate its field applicability for the diagnosis of schistosomiasis in low-resource settings.

Related Work

A pioneering study on the identification and classification of human helminth eggs based on computer vision algorithms was carried out by Yang et al. [14]. However their focus was on helminth eggs found in microscopic faecal samples. Subsequent works [15-18] included the detection *S. haematobium* eggs found in urine but only in images pre-captured by professional clinical operators mostly with isolated and non-overlapping eggs in the field of view (FoV) images. Regarding the detection of *S. haematobium* eggs in microscopy images of urine from field settings, these images contain many artifacts with morphological and textural similarity to eggs such as crystals, glass debris, air bubbles, fabric fibres and human hair. This makes it difficult to achieve high accuracy using traditional artificial intelligence (AI) methods which detect objects in the images based on some threshold value or discontinuous local features of an image. The *S. haematobium* eggs are oval-shaped structures (110-170 μm long and 40-70 μm wide) with a thick transparent capsule and a sword-shaped protrusion known as the terminal spine located at the narrow end of the egg. Detecting an egg is challenging due to its similar appearance to its surroundings. Automated detection of an isolated *S. haematobium* egg by thresholding the cross-correlation coefficient of 2 sets of invariant moments for both a reference and sample image was performed by Hassan and AI-Hity [19]. However, this method had poor performance in noisy images and hence cannot be used for *S. haematobium* eggs detection in field settings.

Recently, Deep learning algorithms were used by Armstrong et al. [20] to solve the challenges of *S. haematobium* egg detection in images captured in field settings. Using transfer learning, they compared RetinaNet [21], MobileNet [22], and EfficientDet [23] architectures pre-trained on the COCO 2017 dataset [24]. They retained the feature extraction layers and fine-tuned the dense layers of these models to detect S. haematobium eggs as a single class. The RetinaNet architecture had improved egg detection performance with egg counts closely related to manual egg counts obtained by a trained user. It was also able to detect isolated eggs and reject other debris from a crowded FoV. However, air bubbles were incorrectly classified as eggs, and the automated detection of eggs aggregated in large clumps with other eggs or debris remained a challenge. In our previous work, we developed a low-cost automated digital microscope

(Schistoscope V5.0) with artificial intelligence for the detection S. haematobium eggs [10], and we reported the results from a field validation study in Nigeria [11]. A U-Net model [25] trained with the S. haematobium dataset consisting of 5,198 images captured from both clinical and spiked urine samples was used for automated egg detection. Although we achieved a high diagnostic sensitivity of 87.3%, the diagnostic specificity was low (48.9%). This was due to the high number of false positives by the U-Net architecture and the inability of the segmented pixel area-based linear model to filter out incorrectly segmented eggs while counting.

All these studies show that deep learning is a promising approach for the automated diagnosis of urogenital schistosomiasis. However, developing a model that is field applicable requires a robust dataset of images with varying degrees of urine artifacts from field settings. Also the separation of overlapping eggs for improved estimation of infection intensity has remained a challenge. This paper proposes a two-stage framework to solve these challenges.

Methods

To meet the WHO TPP requirements for a diagnostic test for schistosomiasis, the proposed urogenital schistosomiasis diagnostic framework consists of two stages (Figure 1). The first stage involves the semantic segmentation of candidate *S. haematobium* eggs in captured images. The segmentation results are further refined in the second stage by ellipse fitting and morphological filtering of the segmented regions. The two-stage framework minimizes false positive detection that enables a high diagnostic specificity, which is a requirement for diagnostic tools for monitoring and evaluation of schistosomiasis control programs and determining transmission interruption.

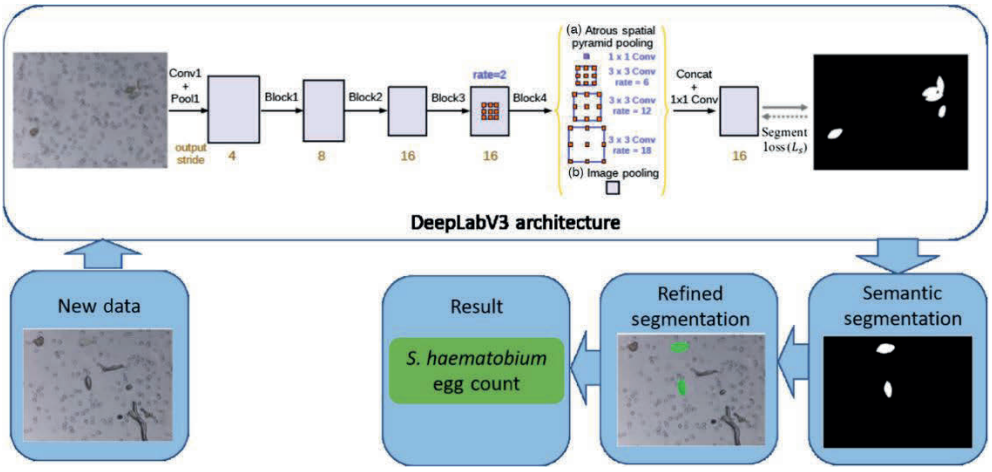

Figure 1. Schematics of the proposed two-stage diagnosis framework urogenital schistosomiasis with DeepLabV3-MobileNetV3 deep learning architecture for semantic segmentation of eggs and refined segmentation for overlapping eggs separation and count.

Sample Image Capture and S. haematobium Egg Annotation

The details of the Schistoscope's mechanical precision and optical quality are described in our previous work [10]. The Schistoscope optical system consists of a 4×4× magnification microscope objective and a Raspberry Pi High-Quality Camera Module V2.1 equipped with a Sony IMX477R camera sensor. The camera sensor has a pixel-pitch of 1.55μm1.55 μm and registers an image size of 2028×1520pixels2028×1520 pixels. The device consists of an autofocusing and an automated slide scanning system. For urine filtration, we made use of a 13 mm filter membrane, which results in 117 image grid segments per sample when scanned by the device. The *S. haematobium* eggs in the captured images used for training and development testing were manually annotated by an expert parasitologist using the coco annotator tool [26]. The annotation process is highlighted as follows.

1. Annotation of the exact boundary pixels of the *S. haematobium* eggs was not strictly enforced due to the limitation posed by the size of the eggs.
2. The pixel values of the filter membrane and artifacts in the ground-truth image were labeled as "0" (background) and the eggs as "1" (foreground).
3. There were few *S. mansoni* eggs found in the images of the clinical urine samples and their pixel values were labeled as "1" (foreground).
4. Pixels of partially cut eggs at the edges of the images were labeled as "1" (foreground).
5. The region of the eggs covered by artifacts was labeled as "0" (background).

Stage 1: Semantic Segmentation of S. haematobium Eggs

Transfer learning using DeepLabv3-MobileNetV3

In transfer learning, a model trained on one task is re-purposed to another related task, usually by some adaptation toward the new task. This approach is mainly useful for tasks where enough training samples are not available to train a model from scratch, such as medical image classification for neglected tropical diseases or emerging diseases [27]. To overcome the limited data sizes, transfer learning was used to re-train the DeepLabv3-MobileNetV3 [12] model for semantic segmentation of candidate *S. haematobium* eggs using the SH dataset. DeepLabv3 is a semantic segmentation architecture that was developed to handle the problem of segmenting objects at multiple scales. Modules are designed, which employ atrous convolution in cascade or in parallel to capture multi-scale context by adopting multiple atrous rates. We initialize the model with weights obtained from the pre-trained model on a subset of COCO train2017, on the 20 categories that are present in the Pascal VOC dataset [28]. Since our case consists of two output classes (background and foreground), we replace the 21-output channel convolutional layer with a single output-channel convolutional layer. The weights of all layers of the model are then updated during the training stage.

Loss function

The model was trained using the Dice similarity coefficient (DSC) loss function [29], which is widely used in medical image segmentation tasks to address the data imbalance problem between foreground and background:

$$L_{\mathrm{DSC}} = \frac{2\sum_{x,y}(S_{i,x,y} \times G_{i,x,y})}{\sum_{x,y} S_{i,x,y}^2 + \sum_{x,y} G_{i,x,y}^2}, \tag{1}$$

where $S_{i,x,y}$ and $G_{i,x,y}$ refer to the value of pixel (x,y) in the segmentation result S_i and ground truth G_i, respectively.

Stage 2: Refined Segmentation of S. haematobium Eggs

To solve the challenge of obtaining accurate egg counts in the occurrence of false positives or overlapping and clustered eggs, we adopted a refined segmentation procedure, which involves fitting ellipses over the region of interest in the binary output image of the semantic segmentation. The refined segmentation algorithm as shown in Algorithm 1 operates in a number of steps, which can be summarized as follows.

We assume a binary image I that represents the segmentation mask output of the DeepLabV3-MobileNetV3 deep neural network model. The binary image may contain one or more sliced binary region image R, which has the same size as the bounding box. This region image R represents a segmented isolated or overlapping eggs. A pixel p of R belongs to either the foreground FG ($R(p)$=1) or the background BG ($R(p)$=0). The area A_R of the segmented egg is given by

$$A_R = \sum_{p \in \mathrm{FG}} R(p). \tag{2}$$

We also assume a set E_R of N_R ellipses are fitted over the region image R. The binary image U_E is defined such that $U_E(p)$=1 at point p that is inside any of the ellipse $E_{R,i}$; otherwise $U_E(p)$=0. Also we define the coverage $\alpha(E_r)$ of the segmented eggs by the given set of ellipses E_R as

$$\alpha(E_r) = \frac{1}{A_R} \sum_{p \in \mathrm{FG}} R(p) U_E(p). \tag{3}$$

Essentially, $\alpha(E_r)$ is the percentage of the segmented eggs that are under some of the ellipse in E_R. Let the sum of the areas of all the ellipses be denoted by $|E_R| = \sum(i=1)|E_{R,i}|$ and let $C(E_R)$ denote the coverage area by all the ellipses:

$$C(E_R) = \sum_{p \in R} U_E(p). \tag{4}$$

Algorithm 1. The refined segmentation algorithm

Input: Binary segmentation mask image I

Output: Set of ellipse E_I^*, egg count N_I^*

$N_I^* = 0$

$E_I^* = \varnothing$

for each region image $R \in I$ **do**

  $N_R^* = 0$

  $E_R^* = \varnothing$

  $AIC_R^* = \infty$

  $N_{lb}, N_{ub} = ComputeBoundary(A_R)$

  $N_R = N_{lb}$

  repeat

    $E_R = FitEllipse(R, N_R)$

    $AIC_R = ComputeAIC(R, U_E)$

    if $AIC_R < AIC_R^*$ **then**

    $N_R^* = N_R$

    $AIC_R^* = AIC_R$

    $E_R^* = E_R$

    $N_R = N_R + 1$

  until $N_R = N_{ub}$

  $E_I^* = union(E_I^*, E_R^*)$

  $N_I^* = N_I^* + N_R^*$

end

return N_I^*, E_I^*

Legend

I: Binary segmentation mask image

E_I^*: Optimal set of ellipses for I

N_I^*: Optimal number of ellipses for I

R: Segmented egg region image

N_R^*: Optimal number of ellipses for R

E_R^*: Optimal set of ellipses for R

AIC_R^*: Optimal Akaike Information Criterion for R

N_{lb}: Lower boundary for N

N_{ub}: Upper boundary for N

Optimization problem formulation

It should be stressed that $C(E_R) < |E_R|$, with the equality holding in the case that all ellipses are pairwise disjoint. This is because in case of two overlapping ellipses, $|E_R|$ counts the area of their intersection two times, while $C(E_R)$ does not. Similar to the work of Panagiotakis and Argyros [13], we want to maximize the shape coverage $\alpha(E^*_R)$ with a set of ellipses E^*_R whose covered area by all ellipses $C(E^*_R)$ is as close as possible to A^*_R:

$$E_R^* = \arg\max_{E_R} \alpha(E_r) \quad \text{s.t. } C(E_R) = A_R. \tag{5}$$

We defined a model complexity measure the ratio of the area A_R of the segmented region to experimentally observed average area of segmented isolated egg A^*_R:

$$C = \frac{A_R}{A_R^*}. \tag{6}$$

To estimate the optimal number N^*_R of ellipses in a segmented egg region image R, a trade-off between the egg coverage $\alpha(E_r)$ and the model complexity C is optimized by employing the Akaike information criterion (AIC) [30]. The AIC-based model selection criterion amounts to the minimization of the quantity [13]:

$$\text{AIC}_R = C \ln(1 - \alpha(E_r)) + 2N_R. \tag{7}$$

This minimizes the error in egg count as intuitively the complexity is proportional to the area of the segmented eggs.

Extracting segmented egg regions

First, connected components in the binary segmentation mask image are extracted and binary region image R, which has the same size as bounding box of the connected component is created. If area A_R of the region image (i.e., the number of pixels in the segmented egg region) is less than the defined area threshold A_th, then the detected region is classified as noise; otherwise, we solve for the optimal number of ellipses as described in the next section.

Initializing ellipses solutions

For defined number N_R of ellipses in a segmented egg region image R, we initialize the ellipse hypotheses using k-means clustering this defines a set E_R of clusters, which are circular in shape with hard cut-off borders where each pixel is strictly allocated to one cluster. The cluster centers are the mean vector of the points belonging to the respective cluster, while the diameters are the maximum Euclidian distances of the cluster members from their respective cluster centers.

Optimizing ellipses solutions

To obtain a more complex, ellipsoid shapes with soft cut-off borders (i.e., overlapping ellipses) which closely describes the shape of *S. haematobium* eggs, the ellipse hypotheses is evolved using the Gaussian mixture model expectation maximization (GMM-EM) algorithm to finetune the parameters of the initialized set E_R of clusters with the best coverage $\alpha(E_r)$ of the given segmented egg region. This is achieved by expectation-step and the maximization-step iteratively of the GMM-EM algorithm. The log likelihood function is maximized until the GMM-EM algorithm converges. A detailed explanation of the GMM-EM algorithm can be found in the work of Bishop 2006 and Mitchell 1997 [31, 32].

Solving for the optimal number of ellipses

Different models (i.e., solutions involving different numbers N_R of ellipses) for a segmented egg image region are evaluated based on the AIC criterion [defined in Eq. (7)] that balances the trade-off between model complexity and approximation error. To minimize AIC$_R$, the refined segmentation algorithm increments the number of candidate ellipses N_R starting from a lower boundary, N_lb=0.6ceil (C), with a step size of 1. At each value of N_R, the set E_R of clusters is first initialized by k-means clustering (described in Sec. 3.3.3) and then evolved using the GMM-EM algorithm (described in Sec. 3.3.4). This process continues until N_R is equal to the upper boundary, N_ub=1.1ceil (C). In each iteration, the AIC$_R$ criterion is computed. The lower and upper boundaries of the number of ellipses are formulated using the complexity measure C, derived from prior knowledge about the average pixel area of the *S. haematobium* eggs. This helps to reduce the search space for the optimal number of ellipses. From all possible models (involving from N_lb to N_ub), the refined segmentation algorithm reports as the optimal solution as the set of ellipses E^*_R with the minimum AIC$_R$.

Morphological filtering of detected isolated eggs

To reduce these false positives diagnosis caused by pixels of artifacts, such as crystals wrongly segmented as isolated egg, we introduced two linear inequality constraints, which are functions of the area of the detected ellipse $|E_R|$ and overlap coefficient OC(R,U_E) defined by the following ratio:

$$\mathrm{OC}(R, U_E) = \frac{R \cap U_E}{\min(R, U_E)}. \tag{8}$$

These inequality constraints are derived experimentally and only applied to segmented regions with a single fitted ellipse for determination of diagnosis result. This improves the specificity of the algorithm by accepting only regions that fall within an experimentally defined boundary region as candidate *S. haematobium* eggs while discarding the others as a false positive prediction.

Dataset and Implementation Details

Dataset Description

A total of 103 captured urine samples were used for the creation of the SH dataset. The SH dataset was used for training and development testing of the DeepLabV3-MobileNetV3 deep neural network model, while a separate set of 65 captured urine samples referred to as diagnosis test dataset was used for testing the developed framework for urogenital schistosomiasis diagnosis. The images were captured from urine samples collected in a rural area in central Nigeria with the Schistoscope V5.0 [11]. The size of the captured images are 1520× 2028 pixels. The details of the sample collection and preparation process are described in our previous works [10, 11]. The procedure followed in capturing and annotation of the S. haematobium eggs in images is described in section 3. A summary of the SH image dataset is shown in Table 1. It consists of 12,051 images of clinical urine samples and their respective mask images. There are 17,799 annotated S. haematobium eggs in 2,997 captured FoV images. The dataset consists of images that are easy to identify eggs (Figure 2.) without the presence of artifacts in the background, as well as images that are difficult to analyse (Figure 3.) with backgrounds containing artifacts such as crystals, glass debris, air bubbles, fabric fibres and human hair which makes egg identification difficult. The SH dataset is split into 80% (9641 images) and 20% (2410 images) for training and development testing respectively. To our best knowledge, this SH dataset is the largest robust dataset focused on *S. haematobium* egg images captured in a field setting.

Table 1. Number of images per category in the SH dataset.

Split	Positive images	Negative images	Total
Training set (80%)	2420	7221	9641
Test set (20%)	577	1833	2410
Total	2997	9054	12,051

Implementation Details

The training of the DeepLabv3-MobileNetV3 model was performed using the Pytorch framework [33] on NVIDIA A100-SXM4-40GB GPU. All images were pre-processed by centring and normalizing the pixel density per channel. We fine-tuned the model for 100 epochs. The batch size is set to 8, and ADAM optimizer is used to optimize the Dice loss function, with an initial learning rate of 1×10^{-4}. We employ a "poly" learning rate policy [12], where the initial learning rate is multiplied by $(1-\text{iter}/(\max_i\text{ter}))^{\text{power}}$ with power=0.9. All images were down sampled to 6507×676 before being fed to the neural network.

To demonstrate the field applicability of the two-stage framework in low-resource settings, we performed the development testing and diagnosis testing on a Raspberry Pi 4 model B using a Coral USB accelerator. To perform semantic segmentation on the Edge AI system, we converted the DeepLabv3-MobileNetV3 model from Pytorch to TensorFlow lite [34]. This was

done by first exporting the Pytorch model in Open Neural Network Exchange (ONNX) format. The ONNX model is then converted to TensorFlow before the final conversion from TensorFlow to TensorFlow Lite. The refined segmentation algorithm was implemented on the Raspberry Pi.

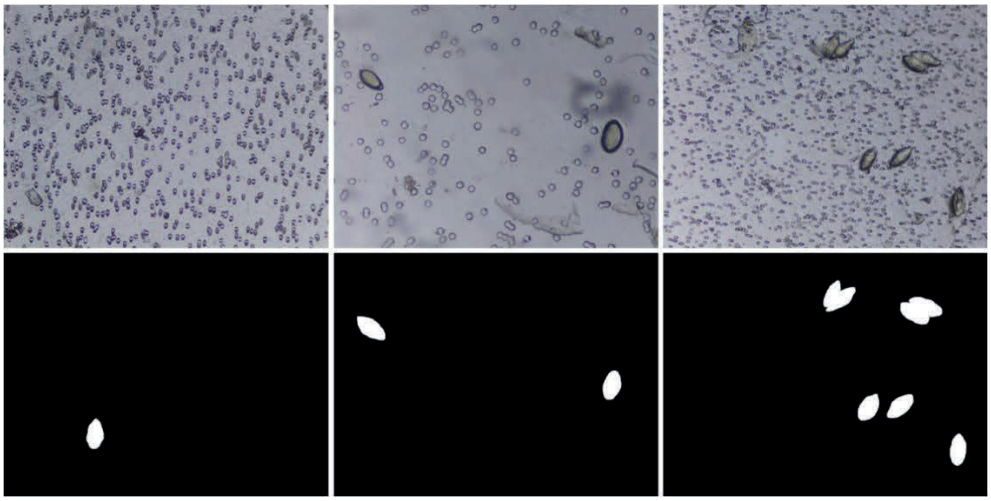

Figure 2. Example of sample images that are easy-to-identify eggs having glass slides and filter membranes as background and their respective ground truth images.

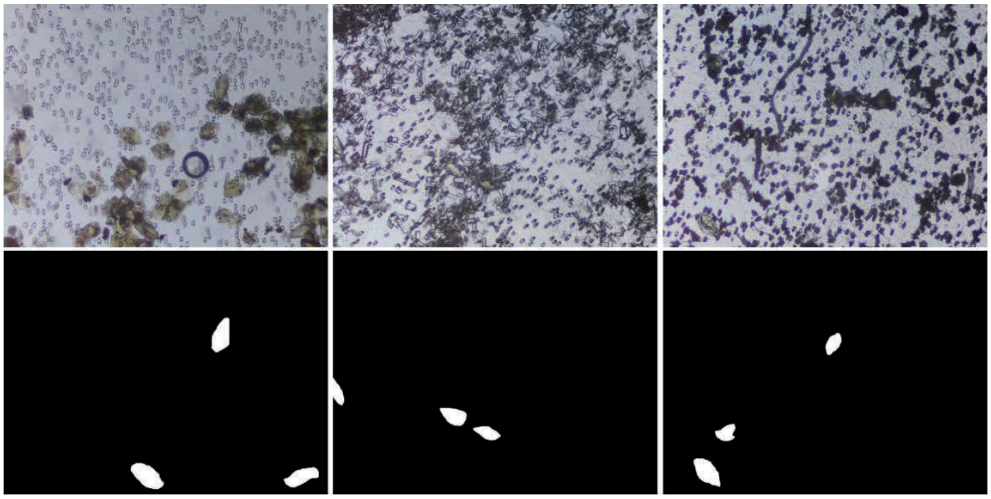

Figure 3. Example of sample images that are difficult-to-identify eggs with artifacts, such as crystals, glass debris, air bubbles, and fabric fibers in the background, and their respective ground truth images.

Evaluation Metrics

We evaluated the performance of semantic segmentation of *S. haematobium* egg by comparing the DeepLabV3-MobileNetV3 segmentation, which are the prediction results with a

ground truth (GT) that was manually annotated by a trained parasitologist using the pixel accuracy (PA):

$$\mathrm{PA} = \frac{1}{n}\sum_{i=0}^{n} 1_{(\mathrm{GT}_i = \mathrm{DS}_i)}. \tag{9}$$

We also compared the semantic segmentation performance using DSC and Jaccard similarity coefficient (JAC), which are widely used in evaluating medical segmentation algorithms:

$$\mathrm{DSC} = 2\frac{|\mathrm{GT} \cap \mathrm{DS}|}{|\mathrm{GT}| + |\mathrm{DS}|}, \tag{10}$$

$$\mathrm{JAC} = \frac{|\mathrm{GT} \cap \mathrm{DS}|}{|\mathrm{GT} \cup \mathrm{DS}|}. \tag{11}$$

Although the diagnostic performance of our two-stage diagnosis framework was evaluated by employing three metrics, precision, sensitivity, and specificity, which are commonly used for evaluating diagnostic devices:

$$\mathrm{precision} = \frac{\mathrm{TP}}{\mathrm{TP} + \mathrm{FP}}, \tag{12}$$

$$\mathrm{sensitivity} = \frac{\mathrm{TP}}{(\mathrm{TP} + \mathrm{FN})}, \tag{13}$$

$$\mathrm{specificity} = \frac{\mathrm{TN}}{(\mathrm{TN} + \mathrm{FP})}, \tag{14}$$

where TP, FP, TN, and FN are true positive, false positive, true negative, and false negative samples, respectively.

Experiments and Results

DeepLabV3-MobileNetV3 S. haematobium Egg Semantic Segmentation

To determine the applicability of the framework on the Edge AI system in low-resource settings with no internet connectivity, we implemented and evaluated its performance on a Raspberry Pi 4B with Coral USB accelerator. We evaluate the DeepLabV3-MobileNetV3 deep learning model for the semantic segmentation of *S. haematobium* eggs using the development test dataset. As shown in Table 2, the deep learning model achieved a segmentation accuracy of 99.69%. It is, however, important to note the existence of a very high imbalance between the foreground and background pixels in the images, which could hamper the segmentation accuracy. While using the Jaccard and dice coefficient as performance metric, the model obtained 85.30% and 87.20%, respectively. However, the average inference time per image was 7.13 s with a model size of 7.13 MB. We considered the inference time too high given the need to process 117 images per sample diagnosis. To reduce the processing time on the Edge AI system, we optimized the DeepLabV3-MobileNetV3 deep learning model using post-training quantization on TensorFlow. The optimized model was applied to the development test dataset. We observed

a significant reduction in inference time and model size (2× and 4×, respectively) with little effect (about 1% reduction) in the Jaccard and Dice coefficient metric. However, the segmentation accuracy remained the same. All further experiments in the work were carried out using the optimized model.

Table 2. Performance of DeepLabV3-MobileNetV3 for semantic segmentation of *S. haematobium* eggs.

	PA	JAC	DSC	Model size (MB)	Inference time (s)
Base model	99.69	85.30	87.20	42.1	7.13
Optimized model	99.69	84.64	86.55	11.1	4.39

The visual performance of the segmentation model is shown in Figure 4c. We observed that the model detected eggs in images heavily cluttered with artefacts, such as crystals and other particles (sample image 3). It also detected highly transparent *S. haematobium* eggs (sample image 1) present in the captured images. Partially cut eggs on the edge of the images and overlapping eggs were also detected as observed in sample image 2. However, the boundaries in the overlapping eggs are not clearly segmented.

Refined Segmentation and Egg Count

In the second stage of our framework, we applied a refined segmentation algorithm on the output segmentation mask image of the DeepLabV3-MobileNetV3 deep learning model as described in Sec. 3.2. From Figure 4d, we observed that the refined segmentation steps fills-in eggs pixels missed in the deep learning semantic segmentation stage. This improves the visual perceptibility of the eggs in the segmentation mask image especially in regions with overlapping eggs as seen in sample image 2. Figure 5 shows example regions with overlapping eggs in the deep learning segmentation mask image. We observed that the correct number of eggs in Figure 5a and 5c are equivalent to the optimal AIC criterion values in Figure 5b and 5d, respectively. The refined segmentation stage is able to separate overlapping eggs thus improving the accuracy of determining the infection intensity of the sample.

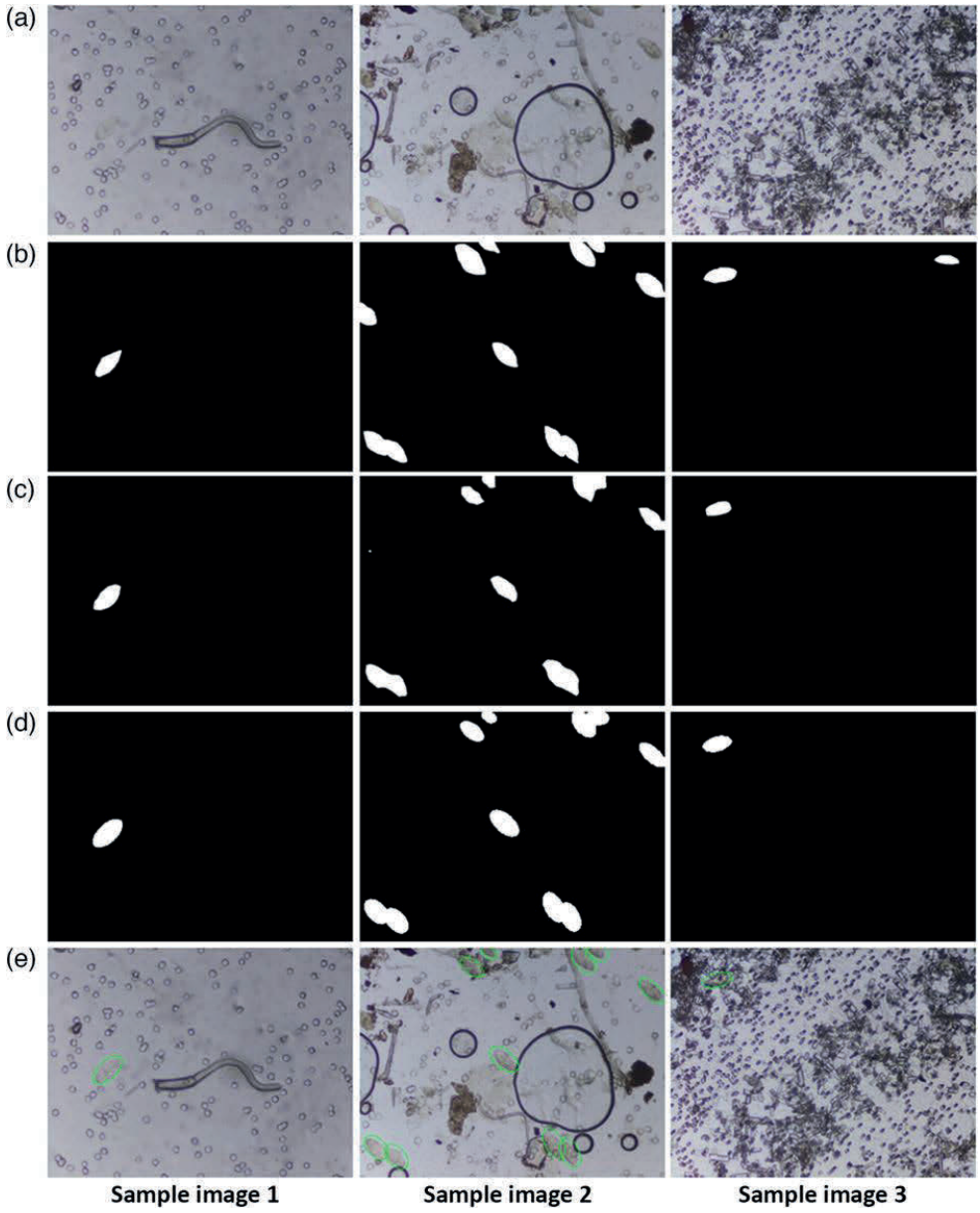

Figure 4. Visual performance of developed framework on sample images from the dataset. Schistoscope (a) captured and (b) ground truth images. The output mask images of (c) DeepLabV3-MobileNetV3 segmentation and (d) refined segmentation. (e) The result image with detected eggs.

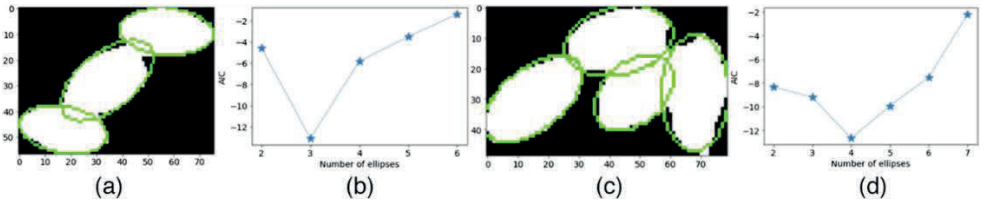

Figure 5. (b), (d) Estimated AIC criteria values for different number of ellipses fitted on the (a), (c) region images with optimal ellipses are highlighted in green.

Figure 6 shows the scatter log-scale plots of the automated egg counts versus the manual egg count (i.e., egg count by an experienced microscopist) of samples in the diagnosis test dataset. Although we observed that the predicted egg counts were mostly under the 1:1 line, this signifies underprediction especially in samples with high egg counts. However, the manual and automated egg counts are highly correlated in samples with both low and high egg counts, which indicate the applicability for the developed framework in determining infection intensity of a sample.

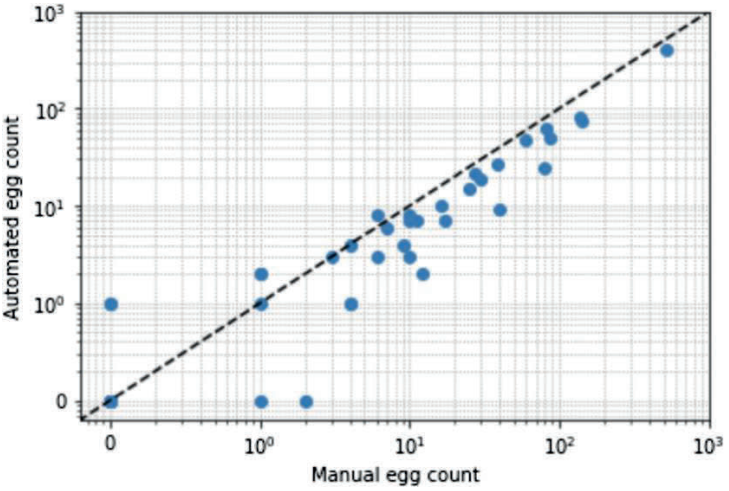

Figure 6. Logarithmic scale scatter plot of infection intensity per 10 mL urine sample. The manual egg count obtained by a microscopist manually counting the eggs in the diagnosis test image dataset is used as a reference, whereas the automated egg count is obtained using the developed framework.

Urogenital Schistosomiasis Diagnosis

A 10 mL urine sample consists of 117 FoV images when filtered with a 13 mm membrane and captured by the Schistoscope. For a sample to be determined as true negative diagnosis, the 117 FoV images must contain no false positives. We experimentally defined boundary conditions for the detected isolated eggs using inequality functions, defined by the overlap and area of the fitted ellipse as shown in Figure 7. The boundary conditions are defined by $OC \geq -4.75\times10^{-4}|E_R| + 1.15$ and $OC \leq 3.25\times10^{-4}|E_R| + 0.74$, where OC is the overlap and $|E_R|$ is the area of fitted ellipse. The experiment was carried out using images from the

development test dataset (Figure 7a), and boundaries were found to hold also in images from the diagnosis test dataset (Figure 7b). A sample was determined as positive diagnosis if an isolated egg is detected in the set of 117 FoV images, which satisfies the defined boundary conditions (an egg is detected in the green region of Figure 7). Otherwise, the sample is determined as negative diagnosis. We observed that most of the false negatives in Figure 7 (gray markers) were broken or partly captured eggs found at the edges of the image, whereas the false positives (yellow markers) are artefacts that are very similar in appearance to a *S. haematobium* egg.

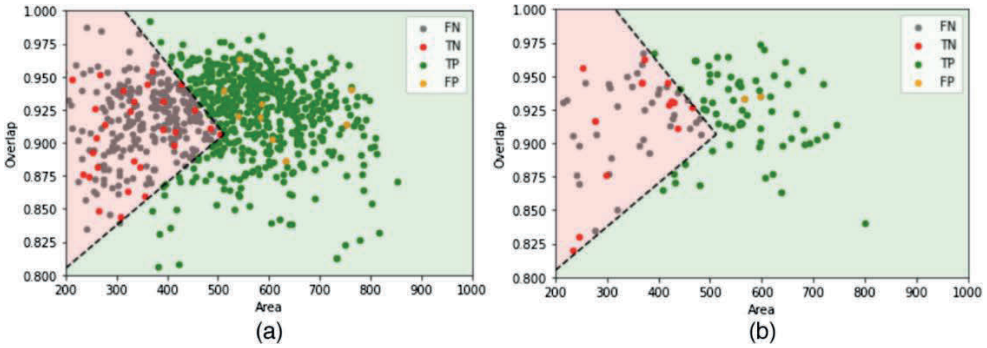

Figure 7. Boundary conditions to determine a sample as positive or negative diagnosis applied to images from (a) the development test dataset and (b) diagnosis test dataset. Samples are determined as positive if an egg in any of the 177 FoV images is detected in the green region.

The diagnostic performance of the developed framework is shown in Table 3. We observed a significant improvement in diagnosis specificity (from 72.73% to 93.94%) and precision (from 77.50% to 93.75%) when the boundary conditions are applied in determining the sample diagnosis. However, a reduction in the diagnosis sensitivity is observed. This is due to some samples with very low infection intensities (eggs per 10 mL of urine ≤2) not having any detected eggs, which meet the boundary constraint represented by the green region of Figure 7b. McNemar's test returned a p-value of 0.008, which indicates a statistically significant difference between both methods (p-value <0.05). Also we achieved a 7.39% and 92.11% performance improvement in diagnosis sensitivity and specificity, respectively, compared to our previously published work [11].

Table 3. Diagnostic performance of developed framework on the diagnosis test dataset.

	Sensitivity	Specificity	Precision
Without boundary conditions	96.88	72.73	77.50
With boundary conditions	93.75	93.94	93.75

Computational Time

To evaluate the computational performance of the developed framework, we measured the computational time of both stages of the proposed method as function of infection intensity. *S. haematobium* infection intensity has consistently been characterized by the number of schistosome eggs per 10 mL of urine with 1 to 49 eggs per 10 mL of urine defining a light infection and more than 50 eggs per 10 mL of urine indicating a heavy infection [35]. We

performed the running time experiments on a Raspberry PI 4B with Coral USB accelerator to study how the infection intensity affects the computational time. The algorithm was applied on images from the diagnosis test image dataset. Figure 8 shows the average computational time from the application of the first (DeeplabV3-MobileNetV3 semantic segmentation) and the second (refined segmentation and separation of overlapping eggs) stages of the developed framework to the diagnosis test image dataset as a function of the infection intensity. From this figure, it can be seen that there is little difference between the computational time of negative and light intensity samples (620 and 628 s, respectively). However, processing samples with heavy infection intensity is more time-consuming with an average computational time of 748 s.

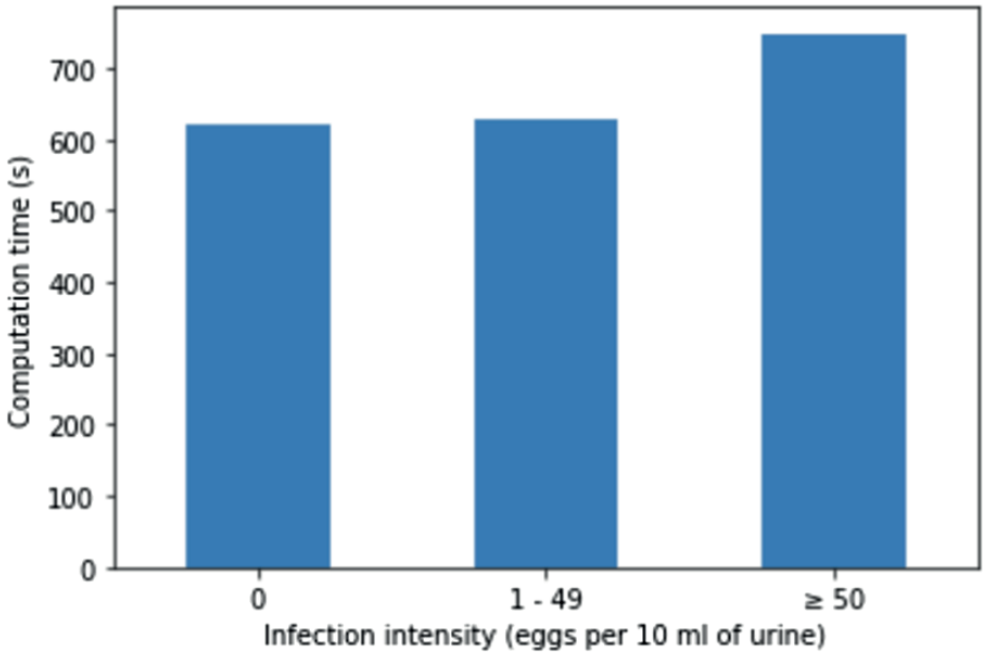

Figure 8. Average computational time in seconds from the application of framework on the diagnosis test image dataset.

Discussion

Impact on Schistosomiasis Control and Elimination

Schistosomiasis affects about 252 million people globally [2] with ~90% of infections and the vast majority of morbidity occurring in Sub-Saharan Africa. Chronic urogenital schistosomiasis infection can result in bladder fibrosis as well as female and male genital schistosomiasis, which is associated with greater risk of HIV transmission [36]. Also the bulk of the more than 1.6 million disability-adjusted life years [37] caused by schistosomiasis worldwide affect children, who have the highest prevalence and intensity of infections. Morbidity in children include anaemia, delays in physical and cognitive development, and reduced tolerance to exercise [38]. The main strategy for control of schistosomiasis focuses on mass drug administration (MDA) of praziquantel in priority to primary school-aged children because it is more cost-

effective to treat all school-aged children in a community above a certain prevalence threshold than to test and treat each individual [4]. On a population level, higher intensities of infection are associated with higher levels of morbidity, but these relationships are poorly defined, as most control programs monitor only prevalence of infection and not intensity [39]. Microscopic examination of urine samples is often a cheap and simple procedure recommended by WHO for the diagnosis of urogenital schistosomiasis. However, it has some critical shortcomings, which include access to microscopes and trained personnel as well as poor sensitivity and reproducibility, and an error-prone manual read-out [40]. This led to the recent formation of the WHO Diagnostic Technical Advisory Group with the mandate to identify and prioritize diagnostic needs and to subsequently develop TPPs for future diagnostics [4, 41, 42]. The TPP requires new diagnostic tools to have high specificity so as reliably measure when prevalence is above or below a cut-off of 10% in school-aged children. This informs decision on the frequency of the MDA. A diagnostic tool with high specificity is also needed to track changes of prevalence, ensuring that MDA is reducing overall prevalence, and to determine if transmission has been interrupted. In this work, we developed a two-stage diagnostic framework, which is a suitable candidate for estimating infection intensity and diagnostic prevalence in urogenital schistosomiasis monitoring and control.

Limitations

• *Image auto-focusing*. Some of the images in the dataset captured by the Schistoscope were blurry due to sub-optimal autofocusing. Although this had no effect on the diagnostic performance, it did have an effect on the automated egg counts of a few samples in the diagnosis test dataset. This problem has been solved by a more accurate auto-focusing algorithm in subsequent version of the Schistoscope.

• *Annotation problem*. Annotating the exact boundaries of the eggs was difficult due to their small sizes. This may contribute to the difficulty of the model to segment the exact egg boundaries, especially in overlapping eggs.

• *Diagnostic prevalence*. The determining diagnosis of a sample with eggs that are either broken or are at the edges of the images is mostly not considered by the developed framework as they do not meet the boundary requirements. This increases the chances of a false negative diagnosis especially in samples with very low egg counts.

• *Computational time*. On a Raspberry Pi with Coral USB accelerator, the developed framework processes 117 images of the 13 mm urine filter membrane in ~11 min. Therefore, an estimated processing time of 35 min required to process a 25 mm filter membrane with 372 captured FoV images. However, the processing time can halved by the use of 2 Coral USB accelerators for computation through multi-threading.

Conclusion

We created a robust dataset of manually annotated *S. haematobium* eggs in microscopy images of urine samples collected from an endemic population, captured by the Schistoscope V5.0 device. We then developed a two-stage diagnosis framework for urogenital schistosomiasis

using the SH dataset. The framework consists of two main stages, the first step involves the semantic segmentation of the eggs using the DeepLabV3 deep learning architecture with a MobileNetV3 backbone. The model effectively segmented the transparent eggs having low contrast with the background, and it also differentiated between eggs and other urine artifacts, such as crystals that have egg-like structures. In the next stage, a refined segmentation algorithm was applied to detect and count the eggs present. The refined segmentation algorithm separates overlapping eggs by fitting the region image with an optimal number of ellipses determined by optimising the AIC criterion. For improved diagnostic performance, we determine a sample as positive only if there is a detected egg present in the sample images that meet a defined boundary requirement, which is a function of the overlap and area of the fitted ellipse. We implemented the developed framework on an Edge AI system consisting of a Raspberry Pi 4B with Coral USB accelerator and applied it to a diagnosis test dataset of 65 samples using results obtained by an expert microscopist as reference. We obtained 93.75%, 93.94%, and 93.75% sensitivity, specificity, and precision, respectively. The automated egg count was also highly correlated with the manual count of the microscopist. The framework also provides causality for its estimated egg counts, which is relevant for diagnosis. From our results, it is evident that our automated framework for urogenital diagnosis combined with the Schistoscope device is a promising diagnostic tool for schistosomiasis. In a future study, the proposed multilayer framework, combined with the Schistoscope, will be validated for the diagnosis of urogenital schistosomiasis by comparing its performance with conventional microscopy as well as more accurate diagnostic methods, such as schistosome circulating antigen detection and DNA-based methods, such as polymerase chain reaction assays [43].

Acknowledgments

This work was funded under the INSPiRED (INclusive diagnoStics for Poverty REIated parasitic Diseases) Project (Grant No. W 07.30318.009) by WOTRO (the Science for Global Development department) of NWO (the Dutch Research Council). We would like to acknowledge the Neglected Tropical Disease Team from the Federal Ministry of Health Abuja and Federal Capital Territory Authority Public Health Laboratory, Abuja, Nigeria, and Delft University of Technology Global Initiative for their support toward this study. The study was conducted in accordance with the declaration of Helsinki and approved by the Federal Capital Territory Health Research Ethics Committee in Abuja, Nigeria (Reference No. FHREC/2019/01/73/18-07-19). Informed consent was obtained from all subjects involved in the study.

References

1. WHO. Schistosomiasis and soil-transmitted helminthiases: treating millions of people, despite the pandemic 2021 [Available from: https://www.who.int/news/item/08-12-2021-schistosomiasis-and-soil-transmitted-helminthiases-treating-millions-of-people-despite-the-pandemic.
2. Aula OP, McManus DP, Jones MK, Gordon CA. Schistosomiasis with a Focus on Africa. Trop Med Infect Dis. 2021;6(3).
3. Utzinger J, Becker S, Van Lieshout L, Van Dam G, Knopp S. New diagnostic tools in schistosomiasis. Clinical microbiology and infection. 2015;21(6):529-42.
4. Organization WH. Diagnostic target product profiles for monitoring, evaluation and surveillance of schistosomiasis control programmes. 2021.
5. Ngakhushi R, Kaiti R, Bhattarai S, Shrestha G. Prevalence of myopia and binocular vision dysfunctions in microscopists. Int Eye Sci. 2018;18(7):1180-3.
6. Rajchgot J, Coulibaly JT, Keiser J, Utzinger J, Lo NC, Mondry MK, et al. Mobile-phone and handheld microscopy for neglected tropical diseases. PLoS neglected tropical diseases. 2017;11(7):e0005550.
7. Saeed MA, Jabbar A. "Smart diagnosis" of parasitic diseases by use of smartphones. Journal of clinical microbiology. 2018;56(1):10.1128/jcm. 01469-17.
8. Vasiman A, Stothard JR, Bogoch II. Mobile phone devices and handheld microscopes as diagnostic platforms for malaria and neglected tropical diseases (NTDs) in low-resource settings: a systematic review, historical perspective and future outlook. Advances in Parasitology. 2019;103:151-73.
9. Zhu H, Isikman SO, Mudanyali O, Greenbaum A, Ozcan A. Optical imaging techniques for point-of-care diagnostics. Lab on a Chip. 2013;13(1):51-67.
10. Oyibo P, Jujjavarapu S, Meulah B, Agbana T, Braakman I, van Diepen A, et al. Schistoscope: An Automated Microscope with Artificial Intelligence for Detection of Schistosoma haematobium Eggs in Resource-Limited Settings. Micromachines. 2022;13(5).
11. Meulah B, Oyibo P, Bengtson M, Agbana T, Lontchi RAL, Adegnika AA, et al. Performance evaluation of the Schistoscope 5.0 for (semi-) automated digital detection and quantification of Schistosoma haematobium eggs in urine: A field-based study in Nigeria. Am J Trop Med Hyg. 2022;107(5):1047-54.
12. Chen L-C, Papandreou G, Schroff F, Adam H. Rethinking atrous convolution for semantic image segmentation. arXiv preprint arXiv:170605587. 2017.
13. Panagiotakis C, Argyros A. Region-based fitting of overlapping ellipses and its application to cells segmentation. Image and Vision Computing. 2020;93:103810.
14. Yang YS, Park DK, Kim HC, Choi M-H, Chai J-Y. Automatic identification of human helminth eggs on microscopic fecal specimens using digital image processing and an artificial neural network. IEEE Transactions on Biomedical Engineering. 2001;48(6):718-30.
15. Avci D, Varol A. An expert diagnosis system for classification of human parasite eggs based on multi-class SVM. Expert Systems with Applications. 2009;36(1):43-8.
16. Lee C-C, Huang P-J, Yeh Y-M, Li P-H, Chiu C-H, Cheng W-H, et al. Helminth egg analysis platform (HEAP): An opened platform for microscopic helminth egg identification and quantification based on the integration of deep learning architectures. Journal of Microbiology, Immunology and Infection. 2022;55(3):395-404.
17. Naing KM, Boonsang S, Chuwongin S, Kittichai V, Tongloy T, Prommongkol S, et al. Automatic recognition of parasitic products in stool examination using object detection approach. PeerJ Computer Science. 2022;8:e1065.
18. Şengül G. Classification of parasite egg cells using gray level cooccurence matrix and kNN. Biomedical research. 2016;27(3):829-34.
19. Hassan MOK, Al-Hity KM. Computer-aided diagnosis of schistosomiasis: automated schistosoma egg detection.

Journal of Clinical Engineering. 2012;37(1):29-34.
20. Armstrong M, Harris AR, D'Ambrosio MV, Coulibaly JT, Essien-Baidoo S, Ephraim RK, et al. Point-of-care sample preparation and automated quantitative detection of Schistosoma haematobium using mobile phone microscopy. The American Journal of Tropical Medicine and Hygiene. 2022;106(5):1442.
21. Lin T-Y, Goyal P, Girshick R, He K, Dollár P, editors. Focal loss for dense object detection. Proceedings of the IEEE international conference on computer vision; 2017.
22. Howard AG, Zhu M, Chen B, Kalenichenko D, Wang W, Weyand T, et al. Mobilenets: Efficient convolutional neural networks for mobile vision applications. arXiv preprint arXiv:170404861. 2017.
23. Tan M, Pang R, Le QV, editors. Efficientdet: Scalable and efficient object detection. Proceedings of the IEEE/CVF conference on computer vision and pattern recognition; 2020.
24. Lin T-Y, Maire M, Belongie S, Hays J, Perona P, Ramanan D, et al., editors. Microsoft coco: Common objects in context. Computer Vision–ECCV 2014: 13th European Conference, Zurich, Switzerland, September 6-12, 2014, Proceedings, Part V 13; 2014: Springer.
25. Ronneberger O, Fischer P, Brox T, editors. U-net: Convolutional networks for biomedical image segmentation. Medical image computing and computer-assisted intervention–MICCAI 2015: 18th international conference, Munich, Germany, October 5-9, 2015, proceedings, part III 18; 2015: Springer.
26. Brooks J. Features 2021 [Available from: https://github.com/jsbroks/coco-annotator.
27. Minaee S, Kafieh R, Sonka M, Yazdani S, Soufi GJ. Deep-COVID: Predicting COVID-19 from chest X-ray images using deep transfer learning. Medical image analysis. 2020;65:101794.
28. Everingham M, Van Gool L, Williams CK, Winn J, Zisserman A. The pascal visual object classes (voc) challenge. International journal of computer vision. 2010;88:303-38.
29. Xie E, Wang W, Wang W, Ding M, Shen C, Luo P, editors. Segmenting transparent objects in the wild. Computer Vision–ECCV 2020: 16th European Conference, Glasgow, UK, August 23–28, 2020, Proceedings, Part XIII 16; 2020: Springer.
30. Akaike H. A new look at the statistical model identification. IEEE transactions on automatic control. 1974;19(6):716-23.
31. Bishop C. Pattern Recognition and Machine Learning. 162006. p. 140-55.
32. Mitchell TM, Mitchell TM. Machine learning: McGraw-hill New York; 1997.
33. Paszke A, Gross S, Massa F, Lerer A, Bradbury J, Chanan G, et al. Pytorch: An imperative style, high-performance deep learning library. Advances in neural information processing systems. 2019;32.
34. Sithu3. TFLite Conversion 2022 [
35. Wiegand RE, Secor WE, Fleming FM, French MD, King CH, Deol AK, et al. Associations between infection intensity categories and morbidity prevalence in school-age children are much stronger for Schistosoma haematobium than for S. mansoni. PLoS neglected tropical diseases. 2021;15(5):e0009444.
36. HIV/AIDS JUNPo. No more neglect: female genital schistosomiasis and HIV: integrating sexual and reproductive health interventions to improve women's lives. 2019.
37. Organization WH. Global health estimates: leading causes of death; 2019. Retrieved from World Health Organization: https://www. who. int/data/gho …; 2021.
38. Colley DG, Bustinduy AL, Secor WE, King CH. Human schistosomiasis. The Lancet. 2014;383(9936):2253-64.
39. Wiegand RE, Secor WE, Fleming FM, French MD, King CH, Montgomery SP, et al., editors. Control and elimination of schistosomiasis as a public health problem: thresholds fail to differentiate schistosomiasis morbidity prevalence in children. Open Forum Infectious Diseases; 2021: Oxford University Press US.
40. Stuyver LJ, Levecke B. The role of diagnostic technologies to measure progress toward WHO 2030 targets for soil-transmitted helminth control programs. PLoS neglected tropical diseases. 2021;15(6):e0009422.
41. Organization WH. Report of the first meeting of the WHO Diagnostic Technical Advisory Group for Neglected

Tropical Diseases, Geneva, Switzerland, 30–31 October 2019: World Health Organization; 2020.

42. Souza AA, Ducker C, Argaw D, King JD, Solomon AW, Biamonte MA, et al. Diagnostics and the neglected tropical diseases roadmap: setting the agenda for 2030. Transactions of The Royal Society of Tropical Medicine and Hygiene. 2020;115(2):129-35.
43. Hoekstra PT, van Dam GJ, van Lieshout L. Context-Specific Procedures for the Diagnosis of Human Schistosomiasis – A Mini Review. Frontiers in Tropical Diseases. 2021;2.

5.

Validation of artificial intelligence-based digital microscopy for automated detection of *Schistosoma haematobium* eggs in urine in Gabon

Brice Meulah, Prosper Oyibo, Pytsje T. Hoekstra, Paul Alvyn Nguema Moure, Moustapha Nzamba Maloum, Romeo Aime Laclong-Lontchi, Yabo Josiane Honkpehedji, Michel Bengtson, Cornelis Hokke, Paul L.A.M. Corstjens, Temitope E. Agbana, Jan-Carel Diehl, Ayola Akim Adegnika, Lisette van Lieshout.

PLOS Neglected Tropical Diseases. (2024) 18(2): e0011967.

Abstract

Introduction

Schistosomiasis is a significant public health concern, especially in Sub-Saharan Africa. Conventional microscopy is the standard diagnostic method in resource-limited settings, but with limitations, such as the need for expert microscopists. An automated digital microscope with artificial intelligence (Schistoscope), offers a potential solution. This field study aimed to validate the diagnostic performance of the Schistoscope for detecting and quantifying *Schistosoma haematobium* eggs in urine compared to conventional microscopy and to a composite reference standard (CRS) consisting of real-time PCR and the up-converting particle (UCP) lateral flow (LF) test for the detection of schistosome circulating anodic antigen (CAA).

Methods

Based on a non-inferiority concept, the Schistoscope was evaluated in two parts: study A, consisting of 339 freshly collected urine samples and study B, consisting of 798 fresh urine samples that were also banked as slides for analysis with the Schistoscope. In both studies, the Schistoscope, conventional microscopy, real-time PCR and UCP-LF CAA were performed and samples with all the diagnostic test results were included in the analysis. All diagnostic procedures were performed in a laboratory located in a rural area of Gabon, endemic for *S. haematobium*.

Results

In study A and B, the Schistoscope demonstrated a sensitivity of 83.1% and 96.3% compared to conventional microscopy, and 62.9% and 78.0% compared to the CRS. The sensitivity of conventional microscopy in study A and B compared to the CRS was 61.9% and 75.2%, respectively, comparable to the Schistoscope. The specificity of the Schistoscope in study A (78.8%) was significantly lower than that of conventional microscopy (96.4%) based on the CRS but comparable in study B2 (90.9% and 98.0%, respectively).

Conclusion

Overall, the performance of the Schistoscope was non-inferior to conventional microscopy with a comparable sensitivity, although the specificity varied. The Schistoscope shows promising diagnostic accuracy, particularly for samples with moderate to higher infection intensities as well as for banked sample slides, highlighting the potential for retrospective analysis in resource-limited settings

.

Author summary

Assessment of schistosomiasis control programs is a crucial step to understanding the success rate of these control programs. The Schistoscope: an AI-powered automated digital microscope could overcome the limitations of conventional microscopy in endemic resource limited settings as well as in settings lacking microscopy experts. In this study, we carried out an extensive validation of the Schistoscope's diagnostic performance for diagnosis of urogenital schistosomiasis compared to conventional microscopy as well as more accurate diagnostic tests such as real-time PCR and the up-converting particle (UCP) lateral flow (LF) test for the detection of circulating anodic antigen (CAA) on freshly collected urines. We also assessed the performance of the Schistoscope for the diagnosis of schistosomiasis on banked sample slides, using a simple and sustainable storage method, for approximately two years. Having a tool that can prospectively and retrospectively analyse samples in an easy and sustainable way could facilitate schistosomiasis control programs in settings with little or no access to microscopists. Overall, we found the Schistoscope to be as good as conventional microscopy for the diagnosis of schistosomiasis, and given its downstream advantages of digital health, it would serve as a valuable diagnostic/screening tool in resource limited endemic settings.

Chapter 5

Introduction

Schistosomiasis is a tropical parasitic disease of significant public health concern, with an estimated 700 million individuals at risk of infection in areas known for transmission. Out of approximately 250 million people requiring preventive chemotherapy worldwide, Sub-Saharan Africa, including the centrally located country of Gabon, bears the highest proportion [1-3]. In order to control the disease morbidity and work towards its elimination as a public health problem, the World Health Organization (WHO) recommends annual preventive chemotherapy using a single dose of praziquantel for all individuals aged two years and above in communities where the prevalence of schistosomiasis is 10% or higher [4]. For communities with a prevalence below 10%, an optional test-and-treat strategy is recommended [4]. In both cases, reliable diagnostic tools are essential to support the monitoring and evaluation of these control strategies [5, 6].

Conventional microscopy is the standard diagnostic procedure for schistosomiasis. However, the need for expert microscopists limits its application in resource-limited settings. Real-time polymerase chain reaction (PCR) for amplification and detection of schistosome-specific nucleic acid sequences, as well as a lateral flow test (LF) for the detection of schistosome-specific circulating anodic antigen (CAA), offer higher sensitivity and specificity than conventional microscopy [7, 8]. Nevertheless, the requirement for specialized skills and advanced infrastructure currently limits their application in resource-limited settings.

Alternatively, automated digital microscopes have shown promising results in the diagnosis of schistosomiasis by detecting parasite eggs in stool or urine [9-12]. The application of artificial intelligence (AI) algorithms in the diagnosis and surveillance of infectious diseases has received significant attention [13-15]. Automated digital microscopes are designed to capture images of samples with simultaneous analysis by an AI algorithm trained to detect parasite components. Such innovative tools are relatively easy to use and can be customised for rural endemic settings. These tools also have propitious downstream applications including digital health [11, 16-18]. In particular for the detection of *S. haematobium* eggs in urine, multiple studies have validated the diagnostic accuracy of AI-based digital microscopes, demonstrating sensitivities ranging from 32% to 91% compared to conventional microscopy, as summarised in a recent review [11].

The Schistoscope is an automated digital microscope with an integrated AI algorithm to detect *S. haematobium* eggs in urine samples. It was developed for use at point-of-need and is relatively easy to operate requiring minimal training [19, 20]. The Schistoscope was first assessed in Nigeria for diagnosing urogenital schistosomiasis, revealing a high sensitivity but a rather low specificity compared to conventional microscopy [12]. Based on these results, the AI model was re-designed, retrained and embedded onboard the Schistoscope, and then validated using a set of field sample images, yielding better sensitivity and specificity [21]. A limitation of the previous studies has been the small size of validation sample dataset and the lack of an accurate reference standard. To perform more in-depth validation of the diagnostic accuracy of the Schistoscope in detecting *S. haematobium* eggs, urine samples were collected and analysed in a laboratory setting in Lambaréné, Gabon. The diagnostic performance of the Schistoscope was compared to

conventional microscopy as well as to a composite reference standard (CRS), consisting of real-time PCR and UCP-LF CAA.

Methods

Study design

The validation study was conducted in Lambaréné and surrounding areas, located in the Moyen-Ogooué province in Gabon, a region known to be endemic for *S. haematobium* with a prevalence of about 30% [22]. It was carried out in two parts: study A and study B (Figure 1). Study A was an independent cross-sectional study focusing on school-age children and adults from whom urine samples were collected and analysed by the Schistoscope, conventional microscopy, real-time PCR and UCP-LF CAA (see details below). Study B was partly embedded in several ongoing studies at Centre de Recherches Médicales de Lambaréné (CERMEL) in Gabon, where urine samples were collected from different populations (school-age children, adults and pregnant women) and analysed with a range of diagnostic methods including conventional microscopy, real-time PCR and UCP-LF CAA (see details below). Microscopy slides were subsequently biobanked at 4 °C for retrospective analysis with the Schistoscope (~2 years later). All diagnostic procedures were conducted at CERMEL.

Ethical considerationsEthical approval for the study was obtained from the Comité d'Éthique Institutionnel (CEI) du Centre de Recherches Médicales de Lambaréné in Lambaréné, Gabon (reference no. CEI-CERMEL 005/2020). Prior to sample collection, written consent was obtained from adults and from parents or legal guardians of children and teenagers who wished to participate, indicated by their signatures. To ensure confidentiality and anonymity of the results, unique codes were assigned to the samples. Participants with detectable *S. haematobium* eggs/10 mL of urine based on microscopy were treated with praziquantel (40 mg/Kg of body weight) following local guidelines. The study was registered at ClinicalTrials.gov (NCT04505046).

Sample size calculations

The Schistoscope was assumed to have a sensitivity and specificity non-inferior to conventional microscopy, which were realistically assumed to be 80% and 90%, respectively based on field expert estimates using real-time PCR and UCP-LF CAA. The sample size for both study A and B were determined based on a 30% prevalence of schistosomiasis in Lambaréné and its surrounding areas using a two-sample matched paired design, resulting in a required sample size of 350 urine samples [23]. A power of 80% and a 5% degree of error was considered for the calculations.

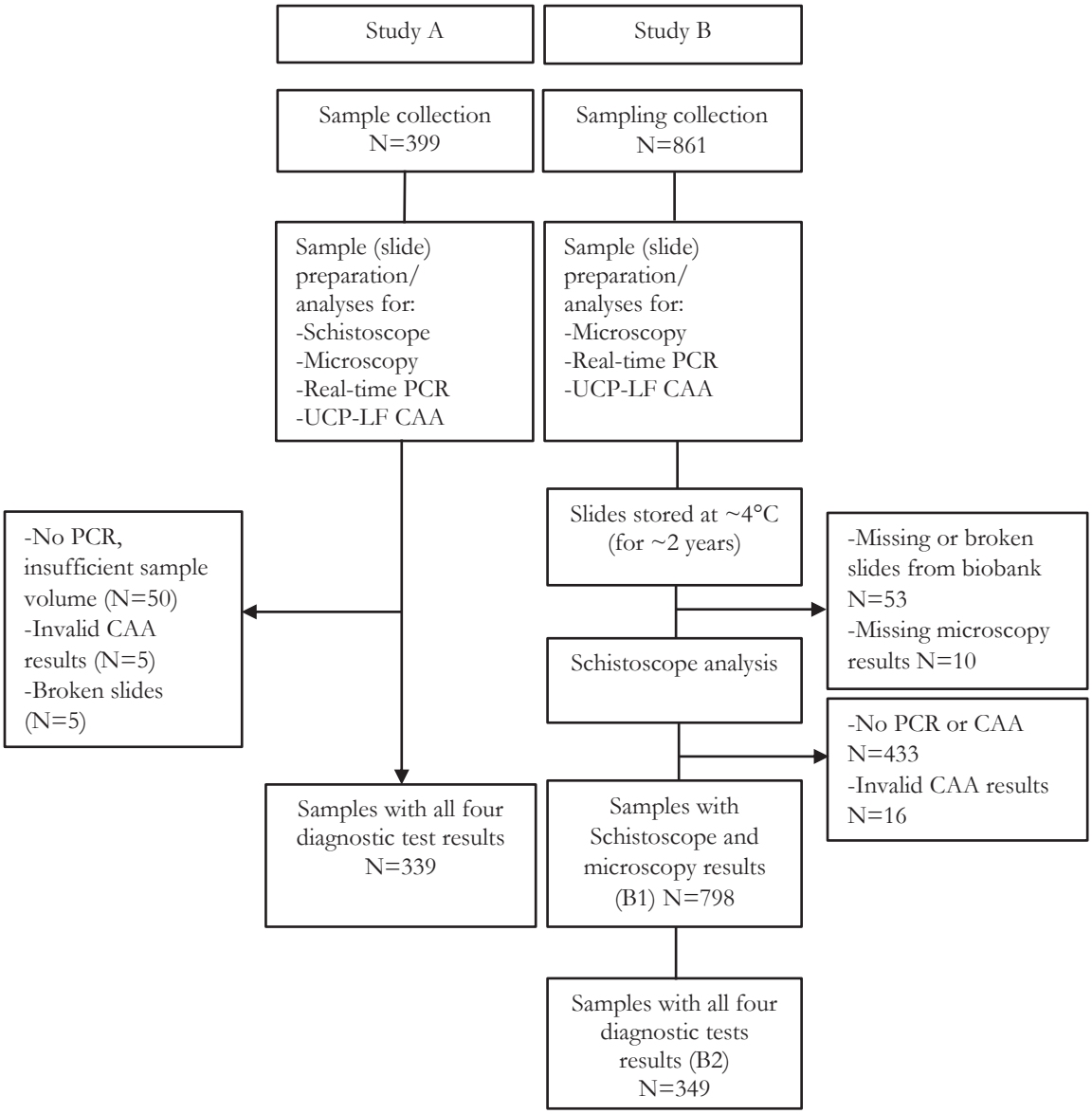

Figure 1: Comprehensive flow chart detailing the methodical sequence of urine sample collection, processing by the Schistoscope, conventional microscopy, real-time PCR and UCP-LF CAA and data analysis.

Sample collection and processing

Collection of urine samples in study A was carried out starting in 2023 while the urine sample biobanking (study B) was initiated in 2020. Study participants were provided with sterile containers labelled with unique identifiers and instructed to provide urine samples between 11 am and 2 pm. The samples were transported to CERMEL within 2 hours of collection for analysis. Microscopy slides were prepared by pressing 10 mL of homogenised urine through a 25mm membrane (pore size 30 μm; Whatmann International Ltd) with the use of a syringe and a filter holder and transferred onto a glass slide. For study A, the slides were examined on the same day using conventional microscopy and the Schistoscope. For study B, the slides were examined using conventional microscopy and stored at 4°C for about 2 years awaiting analysis with the Schistoscope. For both studies, 1 mL of urine from each sample was used for UCP-LF CAA analysis and 10 mL of homogenised urine was centrifuged and the resulting 1mL pellet was used for DNA extraction and amplification before biobanking the sample slides for retrospective analysis with the Schistoscope.

Diagnostic methods

The Schistoscope

Five Schistoscopes were used in this study (Figure 2a, Supplementary video S1). Analysis was done following the standard operating procedure (Supplementary material S1) of the Schistoscope. Briefly, the slide was placed on the slide holder of the Schistoscope such that its microscope objective aligned with the filter membrane of the slide. The device's autofocus algorithm positioned the microscope objective in the optimal focal plane. High resolution images of the sample were registered and analysed simultaneously by the integrated AI algorithm. The number of detected eggs (expressed in eggs/10~ml of urine) is displayed on a pop-up result window which also indicated the end of the sample analysis. Detected eggs are marked as shown in Fig. 2b & c. The results from the Schistoscope were exported as an Excel-compatible file.

Conventional microscopy

Slides from both studies were analysed immediately after urine filtration under 10x objective of a Leica microscope (model: DM1000 LED, Microsystems CMS GmbH Ernt-Leitz-Str.17-37 Wetzlar, Germany). Each slide was examined by two independent microscopists and the mean egg count was calculated. In case of a >20% discrepancy in egg count, an additional reading by a third independent microscopist was required and the final egg count was determined by calculating the mean of the two closest egg counts obtained from the three readings. All egg counts were expressed as eggs/10 mL of urine. In addition, the storage conditions (4 °C) and quality of the biobanked slides were monitored using conventional microscopy once every four months during the storage period. This was done by monitoring daily temperature of the fridge as well as by determining the egg counts of three known slides. Additionally, during the Schistoscope analysis the integrity of the biobank was quality controlled by re-examining a random selection of 10% of the slides by conventional microscopy and comparing the results to the outcomes before storage.

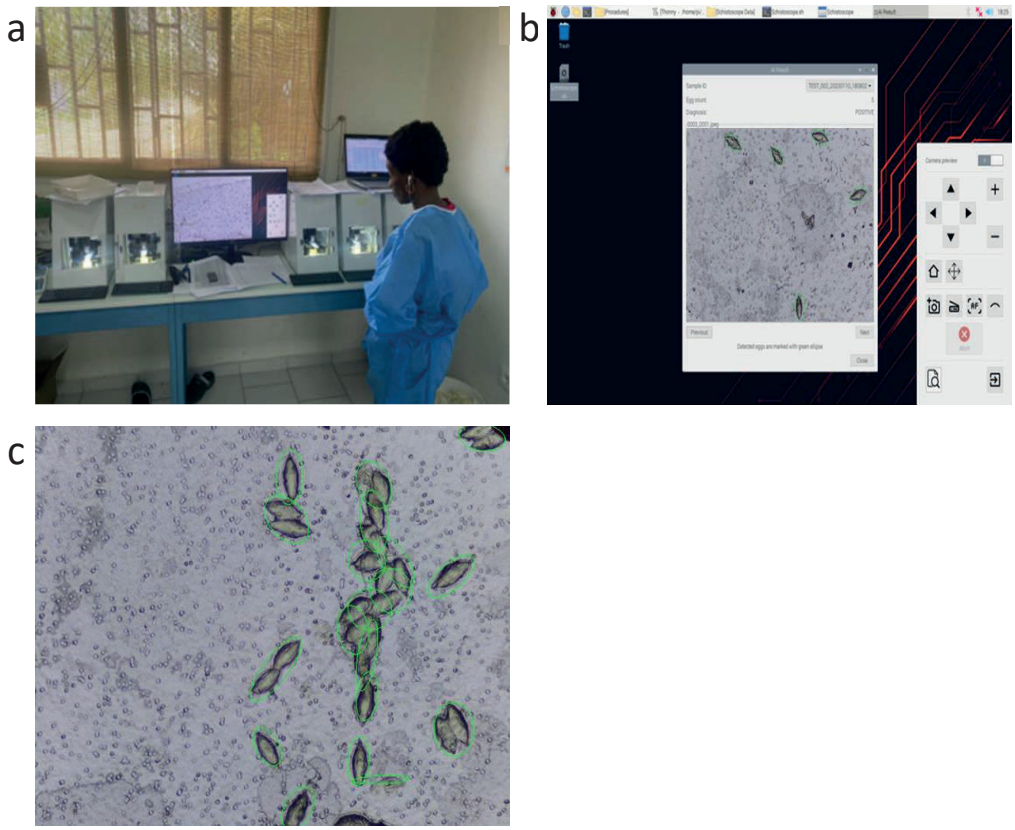

Figure 2: (a) Five Schistoscopes connected to a single display and in use for slide analysis by a laboratory technician. (b) Schistoscope display of result window after slide analysis is completed. (c) Schistoscope image showing some of the overlapping eggs counted as a single egg by the AI algorithm.

Nucleic acid extraction and real-time PCR

Genomic DNA extraction was carried out using the QIAamp Mini kit (cat: 51306; Qiagen) according to the manufacturer's instructions. Briefly, 195µL of each centrifuged urine pellet was mixed with 5µL of internal control DNA commercially available as a DNA Extraction Control (DEC) 670 kit (Cat: BIO-35028; Bioline). The DEC 670 kit is supplied as a vial of internal control DNA sequence (with no known homology to sequences of any organism) and a vial of control mix containing primers and probes complementary to the internal control DNA sequence. The final mixture was then processed as previously described [8].

Real-time PCR was performed as previously described [8, 24] using a set of primers (Ssp48F and Ssp124R) and probe (Ssp78T) complementary to the 77-bp internal transcribed spacer-2 (ITS2) sequence, with minor modifications on the internal control (see above) as well as on the reaction mixture and conditions used (see below).

Amplification reactions were performed in a 15µL reaction mixture containing 1x No-ROX master mix (Cat: BIO-86005; Bioline), 4.5pmol of each *Schistosoma*-specific primer, 1.5pmol Schistosoma-specific probe, 0.4µL of control mix, 1.2µL of nuclease free water and 2.5µL DNA extract. The PCR runs consisted of an initial step of 5 min at 95 °C followed by 40 successive cycles of 10 sec at 95 °C and 60 sec at 60 °C. The reaction was run on a Light cycler 480 II real-time PCR system (Roche Diagnostics). *Schistosoma* DNA detection was expressed in threshold (Ct) cycles. For every run, a non-template control and a positive control (*S. haematobium* DNA, Ct-value 23-25) was included. A test was considered positive when the threshold was attained within 40 PCR cycles (Ct-value ≤ 40). Each sample was run in duplicate and was considered positive when at least one of the duplicates was positive. Amplification of the internal control at the expected Ct-value showed success of nucleic acid extraction and no evidence of PCR inhibitors.

UCP-LF CAA

Urine CAA concentration was determined by the UCP-LF CAA assay using the UCAA*hT*417 format as previously described [7]. Briefly, 500µL of each urine sample was mixed with 100µL of 12% trichloroacetic acid, incubated and centrifuged. The clear supernatant obtained was concentrated to 20µL using an Amicon Ultra-4 concentration column (Millipore, Merck Chemicals B.V., Amsterdam, The Netherlands) and subsequently mixed with 50µL run buffer and added to 50 µL UCP solution. The resulting mixture was then used for the lateral flow assay. A set of CAA standards was used to validate the cut-off (2 pg/ml) as well as to reliably quantify the amount of CAA per sample up to 1000 pg/ml [7].

Statistical analyses

In study A, only samples with all four diagnostic test results available were included in the final analysis. For study B, samples with both the Schistoscope and conventional microscopy test results only were first analysed (B1). Additionally, a subset of samples (B2) which had outcomes of all four diagnostic tests was analysed separately (Figure 1). The percentage positive samples for a *Schistosoma* infection was determined for each diagnostic test. The sensitivity and specificity of the Schistoscope were assessed using conventional microscopy as the reference (study A, B1 and B2). Sensitivity and specificity of the Schistoscope and conventional microscopy were further evaluated using a combination of real-time PCR and/or UCP-LF CAA as a CRS (study A and B2). A sample was deemed positive by the CRS if it showed the presence of *Schistosoma* spp DNA and/or CAA. Conversely, a sample was considered negative if both diagnostic tests showed a negative outcome. A ≤10% difference in sensitivity and specificity between the Schistoscope and conventional microscopy based on the CRS was considered non-inferior. To determine the performance of the Schistoscope at different infection intensities, egg counts based on conventional microscopy were categorised into very low intensity infection (1-9 eggs/10 mL), low-intensity infection (10-49 eggs/10 mL) and high-intensity infection (≥50 eggs/10 mL) [25, 26]. Cohen's Kappa (k) statistics was computed to assess the qualitative agreement between the Schistoscope and conventional microscopy, and the CRS. Spearman's correlation (r) was used to assess the strength of association between the Schistoscope and conventional microscopy, real-time PCR and UCP-LF CAA. Bland-Altman analysis was further

used to assess the quantitative agreement between the Schistoscope and conventional microscopy. Wilcoxon sign rank test was used to compare the microscopy egg count of the randomly selected banked slides before and after storage. Statistical analysis was performed using IBM Statistical Package for Social Sciences version 25 (SPSS Inc., Chicago, United States of America) and GraphPad Prism version 9.0.1 for Windows (GraphPad Software, San Diego, California USA, www.graphpad.com).

Results

Study A: Diagnostic performance of the Schistoscope on freshly prepared samples

A total of 339 samples had outcomes available for all four diagnostic tests and were included in the analysis. Table 1 shows the proportion of positive results per diagnostic test. Real-time PCR found the highest proportion of positives (51.0%) followed by the UCP-LF CAA assay (46.6%). The proportion of positives detected by the Schistoscope (46.0%) was higher than that of conventional microscopy (38.3%). The median egg count of the Schistoscope (17 eggs/10ml) was lower than that of microscopy (31 eggs/10ml). The proportion of positives with egg count ≥50 eggs/10 mL by the Schistoscope and microscopy were comparable, 47 (30.1%) and 49 (37.7%), respectively (Supplementary Figure S1a).

Qualitatively, a moderate agreement between the Schistoscope and conventional microscopy was observed (K=0.579, P<0.001). However, the agreement was only fair when compared to the CRS (K=0.396, P<0.001) whereas a moderate agreement was observed between conventional microscopy and the CRS (K=0.537, P<0.001) (Table 2). The sensitivity and specificity of the Schistoscope were 83.1% and 77.0%, respectively, when conventional microscopy was used as reference. In addition, when the Schistoscope and conventional microscopy were evaluated using the CRS, the sensitivity of the Schistoscope was 62.9% comparable to that of conventional microscopy, 61.9%. However, the specificity of the Schistoscope was significantly lower compared to the specificity of conventional microscopy. All samples with an egg count of ≥50 eggs/10mL defined by conventional microscopy were detected by the Schistoscope (Supplementary Figure S1a). Of the microscopy positive samples with 1-9 eggs/10mL and 10-49 eggs/10mL, the Schistoscope detected 52.6% and 90.7% respectively. Conversely, the Schistoscope found 48 additional cases (of which 40 had <50 eggs/10mL) which were not detected by conventional microscopy. Of these additional cases, 35.4% and 27.1% were confirmed by real-time PCR and the UCP-LF CAA assay, respectively.

A strong correlation was observed between egg counts estimated by the Schistoscope and conventional microscopy (r=0.71, P<0.0001) (Figure 3a). A moderate correlation was observed between the Schistoscope egg counts and real-time PCR Ct-value (r=-0.58, P<0.0001), and CAA concentration (r=0.58, P<0.0001) (Figure 3b and 3c, respectively). Bland-Altman analysis revealed that the Schistoscope tended to underscore egg counts compared to conventional microscopy, but approximately 95% of the difference in the egg count estimates between both methods fell within the limit of agreement (Figure 4a).

Study B: Diagnostic performance of the Schistoscope on banked samples

A total of 798 samples, for which both Schistoscope and conventional microscopy results were available, were included in the analysis (Study B1). Quality control of the biobank revealed no significant difference in microscopy egg count before and after storage which confirmed the integrity of the biobank. The percentage of positive cases detected by the Schistoscope (46.9%) was higher than by conventional microscopy (38.5%). The proportion of positives with an egg count of ≥50 eggs/10 mL was substantially lower by the Schistoscope (32.6%) than by conventional microscopy (59.3%) (Supplementary Figure S1b & c).

A subset of 349 samples had test results available from all four diagnostic tests and were further analysed (Study B2). Based on real-time PCR and UCP-LF CAA a high percentage positive was observed, 62.2% and 64.5%, respectively. The percentage of positive cases detected by the Schistoscope and conventional microscopy were similar, 58.5% and 54.4% respectively, with a significantly different median egg count (Table 1). All samples with high infection intensity were detected by the Schistoscope (Supplementary Figure S1c). In addition, the Schistoscope detected 76.5% and 93.0% of samples with microscopy egg count 1-9 eggs/10mL and 10-49 eggs/10mL respectively. On the contrary, the Schistoscope found 21 additional cases with low infection intensity not detected by conventional microscopy. Of the 21 cases, 57.6% and 38.1% were confirmed by real-time PCR and UCP-LF CAA assay respectively.

A substantial to almost perfect qualitative agreement between the Schistoscope and conventional microscopy was observed in study B1 and B2 respectively (Table 2). The agreement between the Schistoscope and the CRS was similar to the agreement between conventional microscopy and the CRS. The sensitivities and specificities of the Schistoscope in study B1 and B2 when conventional microscopy was used as a reference were comparable. Furthermore, a comparable sensitivity and specificity between the Schistoscope and conventional microscopy was observed when evaluating both methods against the CRS.

A very strong correlation between the egg counts of the Schistoscope and conventional microscopy was observed in study B1 ($r=0.87$; $P<0.0001$, Figure 3d) and study B2 ($r=0.93$, $P<0.0001$, Figure 3e). In study B2, a lower though significant correlation was observed between the Schistoscope egg counts and PCR Ct-values ($r=-0.82$, $P<0.0001$) and CAA concentration ($r=0.78$, $P<0.0001$) (Figure 3f and Figure 3g). Bland-Altman analysis further demonstrated a strong quantitative agreement between the Schistoscope and conventional microscopy in both study B1 and B2 (Figure 4b and 4c) with a trend in the Schistoscope underestimating egg count.

Table 1: Diagnostic outcomes of the Schistoscope in comparison to conventional microscopy, real-time PCR and UCP-LF CAA in study A and B

	Study A (N=339)				Study B1 (N=798)		Study B2 (N=349)			
Diagnostic test	**Schistoscope**	**Microscopy**	**Real-time PCR**	**UCP-LF CAA**	**Schistoscope**	**Microscopy**	**Schistoscope**	**Microscopy**	**Real-time PCR**	**UCP-LF CAA**
Positive (%)	156 (46.0%)	130 (38.3%)	173 (51.0%)	158 (46.6%)	374 (46.9%)	307 (38.5%)	204 (58.5%)	190 (54.4%)	217 (62.2%)	225 (64.5%)
Range	1-1623 eggs/10mL	1-2516 eggs/10mL	20.2-37.0 Ct	2.6-1000.0 pg/mL	1-2879 eggs /10mL	1-9350 eggs/10 mL	1-1943 eggs/10mL	1-9350 eggs/10mL	19.1-38.7 Ct	2.1-1000.0 pg/mL
Median of the positives	17 eggs/10mL	31 eggs/10mL	29.0 Ct	65.0 pg/mL	17 eggs/10mL	105 eggs/10mL	32 eggs/10mL	209 eggs/10mL	26.6 Ct	189.6 pg/mL
Mean of the positives	78 eggs/10mL	119 eggs/10mL	29.7 Ct	134.0 pg/mL	136 eggs/10mL	464 eggs/10mL	160 eggs/10mL	565 eggs/10mL	27.8 Ct	310.5 pg/mL

Table 2: Diagnostic performance and pairwise level of agreement by Cohen's Kappa statistics between the Schistoscope and conventional microscopy and the composite reference for the detection of *S. haematobium* infection in study A and B

Sample set	Diagnostic test	Reference test		Diagnostic test Sensitivity % (95% CI)	Diagnostic test Specificity % (95% CI)	Kappa	P value	Interpretation*
Study A (N=339)		**Microscopy**						
	Schistoscope	Positive	Negative	83.1 (75.5-89.1)	77.0 (70.7-82.5)	0.579	<0.001	Moderate
	Positive	108	48					
	Negative	22	161					
		Composite reference						
	Schistoscope	Positive	Negative	62.9 (55.8-69.6)	78.8 (71.0-85.3)	0.396	<0.001	Fair
	Positive	127	29					
	Negative	75	108					
		Composite reference						
	Microscopy	Positive	Negative	61.9 (54.8-68.6)	96.4 (91.7-98.8)	0.537	<0.001	Moderate
	Positive	125	5					
	Negative	77	132					
Study B1 (N=798)		**Microscopy**						
	Schistoscope	Positive	Negative	93.2 (89.7-95.7)	82.1 (78.4-85.4)	0,723	<0.001	Substantial
	Positive	286	88					
	Negative	21	403					
Study B2 (N=349)		**Microscopy**						
	Schistoscope	Positive	Negative	96.3 (92.6-98.5)	86.8 (80.5-91.6)	0.837	<0.001	Almost perfect
	Positive	183	21					
	Negative	7	138					
		Composite reference						
	Schistoscope	Positive	Negative	78.0 (72.3-83.0)	90.9 (83.4-95.8)	0.604	<0.001	Moderate
	Positive	195	9					
	Negative	55	90					
		Composite reference						
	Microscopy	Positive	Negative	75.2 (69.4-80.4)	98.0 (93.0-99.8)	0.619	<0.001	Substantial
	Positive	188	2					
	Negative	62	97					

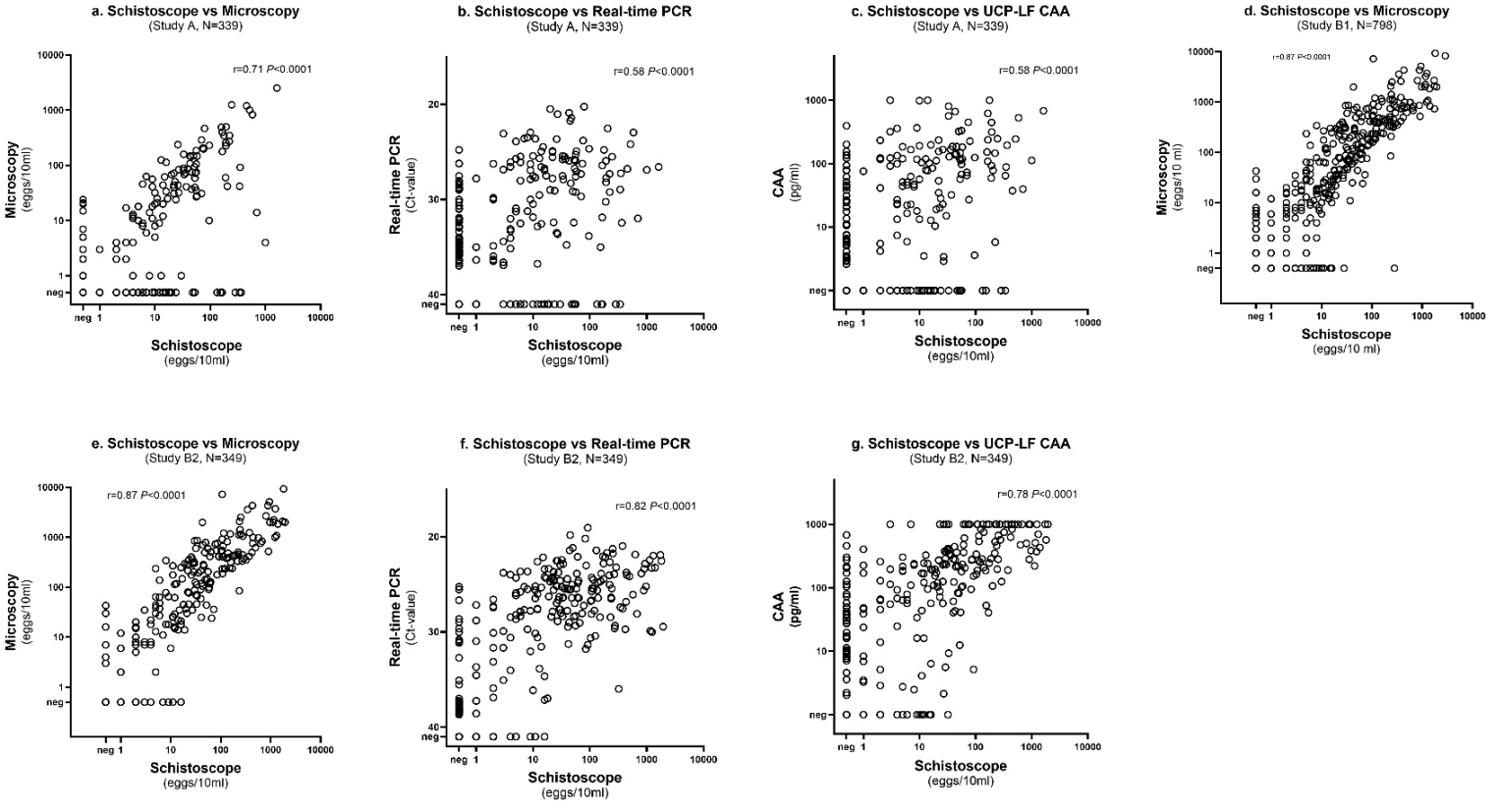

Figure 3: Correlation between *S. haematobium* egg counts measured by the Schistoscope and *S. haematobium* egg counts measured by conventional microscopy (a, d, e), Ct-values determined by real-time PCR (b, f) and urine CAA concentration measured by UCP-LF CAA (c, g) in study A and B.

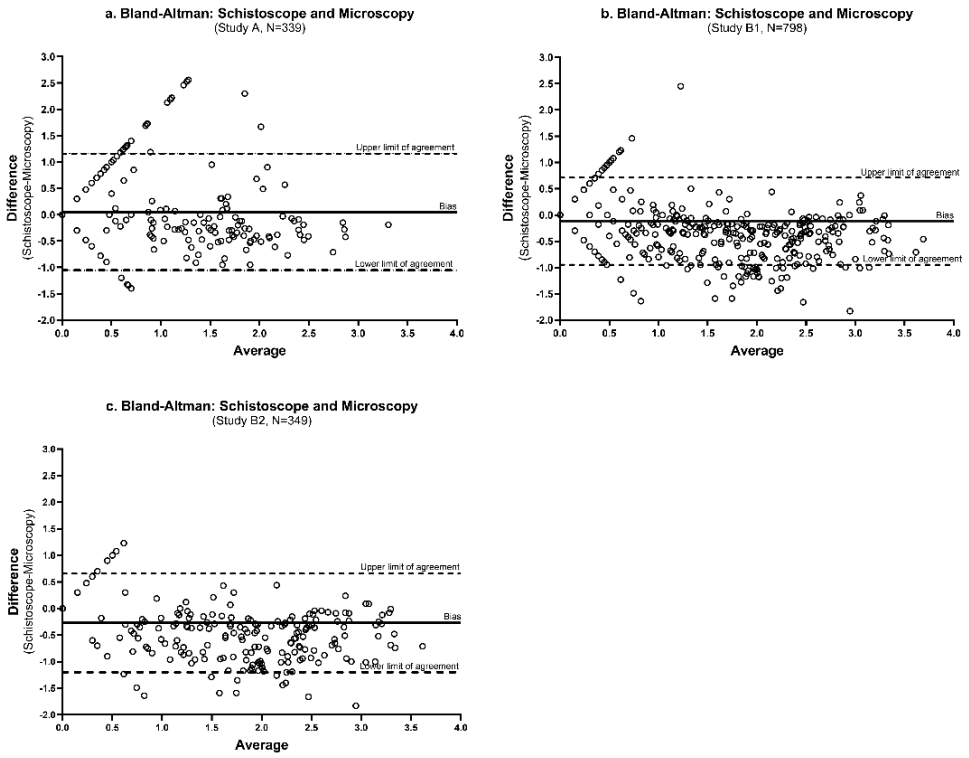

Figure 4: Bland-Altman analysis demonstrating the quantitative agreement between the Schistoscope and conventional microscopy in study A (a) and B (b, c).

Discussion

For the first time, we demonstrate the sensitivity and specificity of the Schistoscope with an onboard integrated AI on fresh (study A) and stored (study B) sample sets in comparison to conventional microscopy as well as to a more sensitive CRS consisting of real-time PCR and UCP-LF CAA. Five Schistoscopes were successfully transported and implemented in the parasitology laboratory of CERMEL, a reference laboratory setting within a rural part of Gabon, which is a region endemic for *S. haematobium*. All other diagnostic tests were also performed at CERMEL. Overall, the performance of the Schistoscope was non-inferior to conventional microscopy with a comparable sensitivity and a slightly lower specificity. The Schistoscope is a promising tool for urogenital schistosomiasis screening in endemic settings and offers the advantage of data connectivity and the possibility of task shifting [27-29].

Qualitatively, a moderate to almost perfect agreement between the Schistoscope and conventional microscopy was found while a fair to moderate agreement was observed when compared to the CRS. This lower agreement can mainly be attributed to the fact that the two additional diagnostic tests included in the CRS (PCR and CAA) are more accurate, especially at low infection intensities, and these tend to be missed by the Schistoscope and/or conventional microscopy. The sensitivity of the Schistoscope was found to be non-inferior to conventional

microscopy in both study A and B2. The specificity of the Schistoscope was however inferior to conventional microscopy in study A, but comparable in study B2. This is thought to be a consequence of the presence of relatively more artifacts in the freshly prepared slides (study A) compared to stored slides (study B), which the AI algorithm could not differentiate from eggs. Secondly, although samples in study A and B were obtained from the same geographical area in Gabon (Lambaréné and its surrounding villages), they were collected at different time points (~2 years apart) as well as from different populations, i.e. community-based in study A versus specific populations including pregnant women in study B. Differences in urine composition due to differential seasonal concomitant bacterial infections was assumed to explain increase in egg-like crystals formation in urine that interfered with AI detection. Manual re-analysis of the images of a selection of samples that were positive by the Schistoscope but negative by conventional microscopy, revealed that indeed crystals were present in these slides, which the AI incorrectly identified as eggs (Supplementary Figure S3).

Although the sensitivity of the Schistoscope in study A (83.1%) was comparable to previously reported results from a field setting in Nigeria (87.3%) [12], the observed specificity was significantly higher (77.0% compared to 48.9% in Nigeria) as well as the correlation between egg counts by the Schistoscope and conventional microscopy, indicating the successful re-designing and re-training of the AI algorithm [21]. The slightly lower correlation observed between the Schistoscope egg count and real-time PCR Ct-values or CAA concentration could be because of the differences in diagnostic target; eggs, egg-DNA and circulating antigen, respectively. The correlation between conventional microscopy and real-time PCR or UCP-LF CAA resulted in a similar observation (Supplementary Figure S2). The correlation observed between egg counts by conventional microscopy and Ct-values is comparable to previous findings [30]. Furthermore, although a better correlation would be expected between egg counts and Ct-values (egg-DNA), considering that they are both egg-based detection methods, it is important to note that, an egg does not have a fixed target DNA copy number. This variation is influenced by the egg developmental stage, which could account for the broad spectrum of Ct-values observed across varying infection intensities or egg count [31].

In study B overall, over 50% of the samples had only results for microscopy and the Schistoscope and rather than discarding this number of samples from our data set, it was analysed separately as B1. For both studies, all cases with high infection intensity based on conventional microscopy, known to correlate strongly with morbidity of the disease [32], were detected by the Schistoscope. Following Bland-Altman's analysis, a constant but clinically fair bias (absolute error) between Schistoscope and conventional microscopy egg counts was observed in both the fresh and stored sample sets, suggesting that the Schistoscope is slightly underestimating egg counts at a constant rate. This could be explained by the fact that with increasing infection intensity, eggs tend to overlap which could not be accurately counted by the AI algorithm (Figure 2c), as also observed previously [12]. Furthermore, the AI algorithm was designed and optimised for specificity at the expense of sensitivity, i.e. it was programmed to refrain from detecting truncated eggs located on boundaries of images so as to reduce the chances of detecting artifacts as well as eggs with lower morphological attributes. Such errors can be corrected by further optimisation of the AI algorithm in order to quantify the number

of eggs more accurately. Also, in both the fresh and stored sample set, the majority of missed cases by the Schistoscope had a very low intensity of infection based on conventional microscopy (≤ 5 eggs/10mL), highlighting another area of focus for the next generation of the Schistoscope.

Our results indicated a better sensitivity of the Schistoscope on banked sample slides compared to fresh samples. This could be due to the difference in the infection intensity observed in the two studies. The median egg count, based on conventional microscopy, was lower in the fresh samples compared to the banked samples, which implies that the Schistoscope performs better on samples with a higher infection intensity, as also previously reported [12, 21]. Nevertheless, our results demonstrate a good performance of the Schistoscope on banked sample slides, indicating the possibility for retrospective analysis of banked sample slides in settings lacking direct access to microscopists.

In study A, the sensitivity of conventional microscopy estimated based on the CRS (62%) was lower than the sensitivity (80%) assumed for power calculations, in contrast to study B where the sensitivity (75.2%) observed was comparable. Retrospectively, the sample size calculation was limited in that it did not take into account the proportion of high-intensity infections but only incorporated prevalence, which could have had a significant impact on the sensitivity of conventional microscopy as it is known that the sensitivity of microscopy is limited in case of low intensity infections [33]. Overall, the proportion of high-intensity infections in study A was significantly lower compared to study B, resulting in a lower sensitivity of conventional microscopy as observed in study A. Despite the difference between the assumed and obtained sensitivity of conventional microscopy, we still believe our study had sufficient power to accurately determine the performance of the Schistoscope. So far, the performance of the Schistoscope has been evaluated in two endemic settings in urine samples producing promising outcomes. There is need for more performance evaluation in diverse schistosomiasis endemic settings (in urine and stool) with different climatic conditions, such as the northern part of Sahel region. Also, a cost effective analysis should be performed to support the integration of such a tool in large scale control programmes.

Limitations of this study include the time it took to analyse a slide by the Schistoscope, which on average was ~25 mins. for samples with egg counts ≥200egg/10mL even more time was needed. Furthermore, in this study a filter membrane of diameter 25mm was used (following the standard protocol of CERMEL), which also increased the time of analysis by 3-fold compared to the use of a 13mm filter membrane [12]. If a smaller filter membrane is used and the Schistoscope is programmed to stop counting when reaching 50 eggs/10mL – as this is classified as a high infection intensity and in such cases a detailed egg count is often not required [34] – the total reading time could be reduced to less than 10 mins. A tool as such would complement the existing POC-CCA urine test, which has been recommended by the WHO for S. mansoni infections, in settings co-endemic for *S. haematobium*. Although the Schistoscope has been fully automated, the aesthetics are currently unsatisfactory [20]. Furthermore, there is need to make the Schistoscope field-friendly and compatible to very rural settings, including the addition of a power source, improving the user interface and making it more compact and portable.

To conclude, in this study a follow-up assessment of the Schistoscope was conducted in a rural laboratory setting in Gabon, further validating its potential as a digital diagnostic tool for the identification and quantification of *S. haematobium* eggs in freshly collected as well as banked urine sample slides. Although the specificity of the Schistoscope could still be improved, its overall performance was non-inferior to conventional microscopy hence, a promising tool for urogenital schistosomiasis screening in endemic settings.

Acknowledgements

We extend our appreciation to Mermoz Ndong-Essone Ondong, Danny Carrel Manfoumbi Mabicka, Moutsinga Dalia Coralline ep Lehoumbou, Elsy Myrna N'noh Dansou, Marguerite Nzame Ngome, and the coordination team, along with all the members of Immuno-Epi research group of CERMEL. We thank Bertrand Lell for IT support in the field. Our gratitude also goes to Jean-Aimé Massande Ndzokou's and the CERMEL field team for their valuable contributions to the advancement of this project.

References

1. Adenowo AF, Oyinloye BE, Ogunyinka BI, Kappo AP. Impact of human schistosomiasis in sub-Saharan Africa. Braz J Infect Dis. 2015;19(2):196-205.
2. World Health Organisation. Schistosomiasis and soil-transmitted helminthiases: treating millions of people, despite the pandemic.: World Health Organisation. ; 2021 [Available from: https://www.who.int/news/item/08-12-2021-schistosomiasis-and-soil-transmitted-helminthiases-treating-millions-of-people-despite-the-pandemic.
3. World Health Organisation. Schistosomiasis: World Health Organisation. https://www.who.int/news-room/fact-sheets/detail/schistosomiasis. Access 01/24; 2024 [Available from: https://www.who.int/news-room/fact-sheets/detail/schistosomiasis.
4. World Health Organisation. New guideline for the control and elimination of human schistosomiasis.: World Health Organisation. https://www.who.int/publications/i/item/9789240041608; 2022 [Available from: https://www.who.int/publications/i/item/9789240041608.
5. World Health Organisation. Strengthening diagnostic capacity: World Health Organisation. https://www.eliminateschisto.org/news-events/news/world-health-assembly-resolution-on-strengthening-diagnostics-capacity. Access 07/2023; 2023 [Available from: https://www.eliminateschisto.org/news-events/news/world-health-assembly-resolution-on-strengthening-diagnostics-capacity.
6. World Health Organisation. Public consultation: Target Product Profiles for diagnostic tests to meet Schistosomiasis and soil-transmitted Helminth programme needs 2021 [Available from: https://www.who.int/news-room/articles-detail/public-consultation-target-product-profiles-for-diagnostic-tests-to-meet-schistosomiasis-and-soil-transmitted-helminth-programme-needs.
7. Corstjens PL, de Dood CJ, Knopp S, Clements MN, Ortu G, Umulisa I, et al. Circulating Anodic Antigen (CAA): a highly sensitive diagnostic biomarker to detect active Schistosoma infections—improvement and use during SCORE. The American journal of tropical medicine and hygiene. 2020;103(1 Suppl):50.
8. Obeng BB, Aryeetey YA, de Dood CJ, Amoah AS, Larbi IA, Deelder AM, et al. Application of a circulating-cathodic-antigen (CCA) strip test and real-time PCR, in comparison with microscopy, for

the detection of Schistosoma haematobium in urine samples from Ghana. Ann Trop Med Parasitol. 2008;102(7):625-33.
9. Ward P, Dahlberg P, Lagatie O, Larsson J, Tynong A, Vlaminck J, et al. Affordable artificial intelligence-based digital pathology for neglected tropical diseases: A proof-of-concept for the detection of soil-transmitted helminths and Schistosoma mansoni eggs in Kato-Katz stool thick smears. PLoS Negl Trop Dis. 2022;16(6):e0010500.
10. Coulibaly JT, Silue KD, Armstrong M, de León Derby MD, D'Ambrosio MV, Fletcher DA, et al. High Sensitivity of Mobile Phone Microscopy Screening for Schistosoma haematobium in Azaguié, Côte d'Ivoire. The American journal of tropical medicine and hygiene. 2023;108(1):41.
11. Meulah B, Bengtson M, Van Lieshout L, Hokke CH, Kreidenweiss A, Diehl J-C, et al. A review on innovative optical devices for the diagnosis of human soil-transmitted helminthiasis and schistosomiasis: From research and development to commercialisation. Parasitology. 2022:1-41.
12. Meulah B, Oyibo P, Bengtson M, Agbana T, Lontchi RAL, Adegnika AA, et al. Performance evaluation of the Schistoscope 5.0 for (semi-) automated digital detection and quantification of Schistosoma haematobium eggs in urine: A field-based study in Nigeria. Am J Trop Med Hyg. 2022;107(5):1047-54.
13. Agrebi S, Larbi A. Use of artificial intelligence in infectious diseases. Artificial intelligence in precision health: Elsevier; 2020. p. 415-38.
14. Brownstein JS, Rader B, Astley CM, Tian H. Advances in Artificial Intelligence for infectious-disease surveillance. New England Journal of Medicine. 2023;388(17):1597-607.
15. Shenoy S, Rajan AK, Rashid M, Chandran VP, Poojari PG, Kunhikatta V, et al. Artificial intelligence in differentiating tropical infections: A step ahead. PLoS Neglected Tropical Diseases. 2022;16(6):e0010455.
16. Prieto-Egido I, González-Escalada A, García-Giganto V, Martínez-Fernández A. Design of New Procedures for Diagnosing Prevalent Diseases Using a Low-Cost Telemicroscopy System. Telemed J E Health. 2016;22(11):952-9.
17. Dacal E, Bermejo-Peláez D, Lin L, Álamo E, Cuadrado D, Martínez Á, et al. Mobile microscopy and telemedicine platform assisted by deep learning for the quantification of Trichuris trichiura infection. PLoS Negl Trop Dis. 2021;15(9):e0009677.
18. Onasanya A, Bengtson M, de Goeje L, Van Engelen J, Diehl JC, van Lieshout L. Developing inclusive digital health diagnostic for schistosomiasis: a need for guidance via target product profiles. Frontiers in Parasitology. 2023;2.
19. Oyibo P, Jujjavarapu S, Meulah B, Agbana T, Braakman I, van Diepen A, et al. Schistoscope: An Automated Microscope with Artificial Intelligence for Detection of Schistosoma haematobium Eggs in Resource-Limited Settings. Micromachines (Basel). 2022;13(5).
20. Bengtson M, Onasanya A, Oyibo P, Meulah B, Samenjo KT, Braakman I, et al., editors. A usability study of an innovative optical device for the diagnosis of schistosomiasis in Nigeria. 2022 IEEE Global Humanitarian Technology Conference (GHTC); 2022: IEEE.
21. Oyibo P, Meulah B, Bengtson M, Lisette van L, Oyibo W, Diehle J-C, et al. Two-stage automated diagnosis framework for urogenital schistosomiasis in microscopy images from low-resource settings. Journal of Medical Imaging. 2023;10(4):044005.
22. Dejon-Agobé JC, Honkpehedji YJ, Zinsou JF, Edoa JR, Adégbitè BR, Mangaboula A, et al. Epidemiology of schistosomiasis and soil-transmitted helminth coinfections among schoolchildren living in Lambaréné, Gabon. The American Journal of Tropical Medicine and Hygiene. 2020;103(1):325.
23. Machin D, Campbell MJ, Tan SB, Tan SH. Sample size tables for clinical studies: John Wiley & Sons; 2011.
24. Kenguele HM, Adegnika AA, Nkoma AM, Ateba-Ngoa U, Mbong M, Zinsou J, et al. Impact of short-time urine freezing on the sensitivity of an established Schistosoma real-time PCR assay. Am J Trop Med Hyg. 2014;90(6):1153-5.
25. Wiegand RE, Secor WE, Fleming FM, French MD, King CH, Deol AK, et al. Associations between infection intensity categories and morbidity prevalence in

school-age children are much stronger for Schistosoma haematobium than for S. mansoni. PLoS Negl Trop Dis. 2021;15(5):e0009444.
26. Organization WH. Prevention and control of schistosomiasis and soil-transmitted helminthiasis: report of a WHO expert committee: World Health Organization; 2002.
27. Tilahun B, Gashu KD, Mekonnen ZA, Endehabtu BF, Angaw DA. Mapping the role of digital health technologies in the case detection, management, and treatment outcomes of neglected tropical diseases: a scoping review. Tropical medicine and health. 2021;49:1-10.
28. Mustafa U-k, Kreppel KS, Brinkel J, Sauli E. Digital Technologies to Enhance Infectious Disease Surveillance in Tanzania: A Scoping Review. Healthcare. 2023;11(4):470.
29. Onasanya A, Bengtson M, Agbana T, Oladunni O, van Engelen J, Oladepo O, et al. Towards Inclusive Diagnostics for Neglected Tropical Diseases: User Experience of a New Digital Diagnostic Device in Low-Income Settings. Tropical Medicine and Infectious Disease. 2023;8(3):176.
30. Vinkeles Melchers NV, van Dam GJ, Shaproski D, Kahama AI, Brienen EA, Vennervald BJ, et al. Diagnostic performance of Schistosoma real-time PCR in urine samples from Kenyan children infected with Schistosoma haematobium: day-to-day variation and follow-up after praziquantel treatment. PLoS Negl Trop Dis. 2014;8(4):e2807.
31. Keller D, Rothen J, Dangy JP, Saner C, Daubenberger C, Allan F, et al. Performance of a real-time PCR approach for diagnosing Schistosoma haematobium infections of different intensity in urine samples from Zanzibar. Infect Dis Poverty. 2020;9(1):128.
32. Kura K, Hardwick RJ, Truscott JE, Toor J, Hollingsworth TD, Anderson RM. The impact of mass drug administration on Schistosoma haematobium infection: what is required to achieve morbidity control and elimination? Parasites & Vectors. 2020;13(1):1-10.
33. Hoekstra PT, van Dam GJ, van Lieshout L. Context-Specific Procedures for the Diagnosis of Human Schistosomiasis – A Mini Review. Frontiers in Tropical Diseases. 2021;2.
34. World Health Organization. Prevention and control of schistosomiasis and soil-transmitted helminthiasis: report of a WHO expert committee 2002 [Available from: https://apps.who.int/iris/handle/10665/42588

.

Supporting information

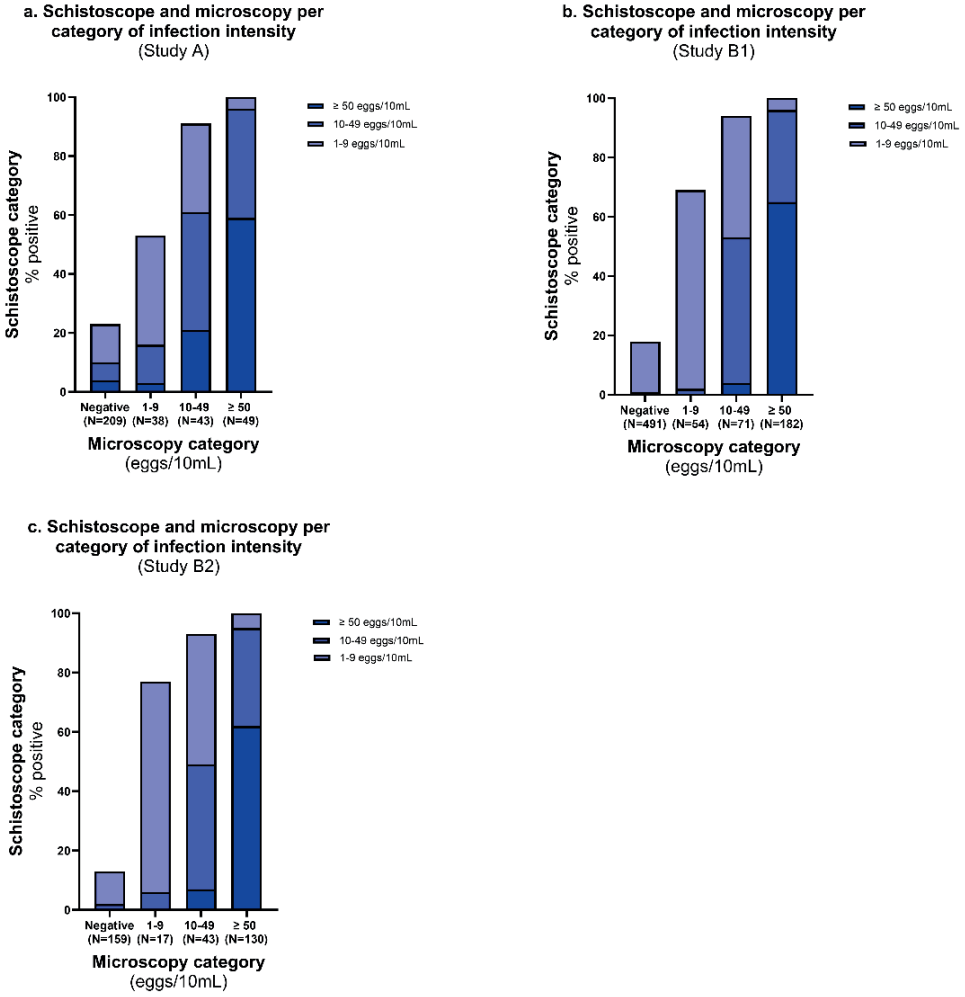

S1 Figure: Agreement between the Schistoscope and microscopy per category of infection intensity in study A and B.

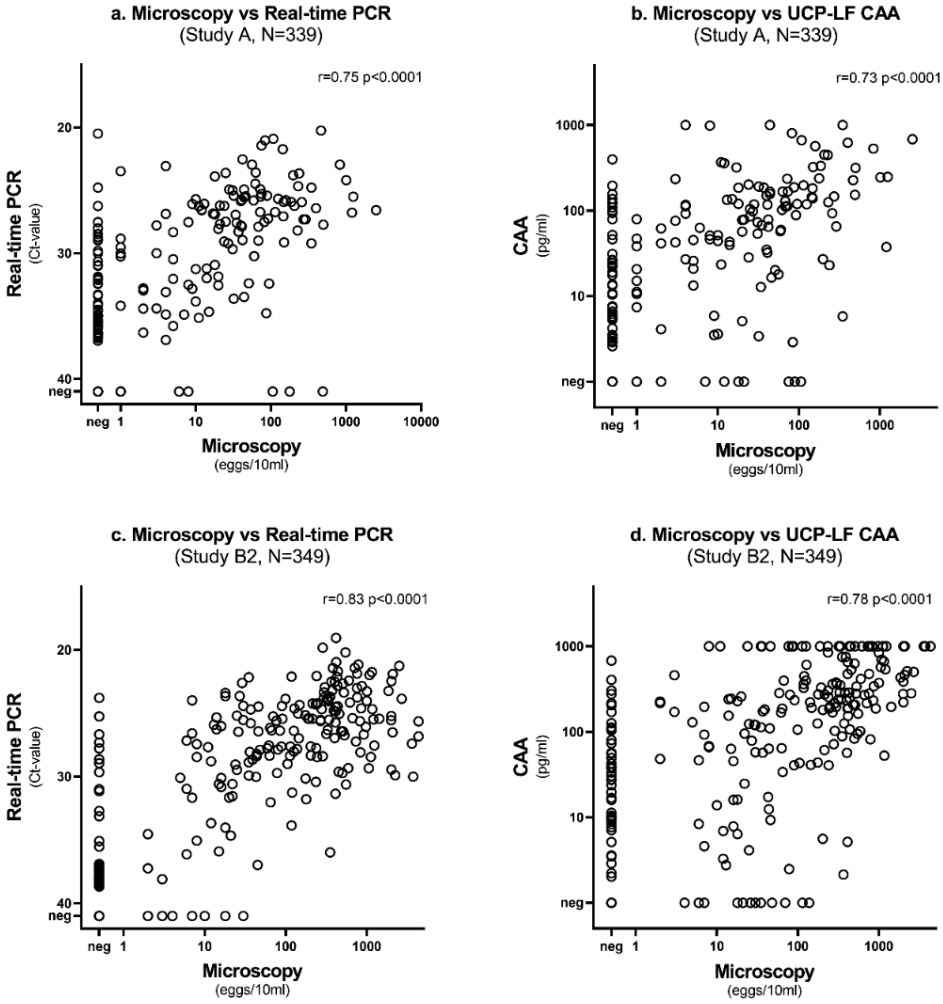

S2 Figure: Correlation between *S. haematobium* egg counts measured by the conventional microscopy and Ct-values determined by by real-time PCR (a, c) and urine CAA concentration.

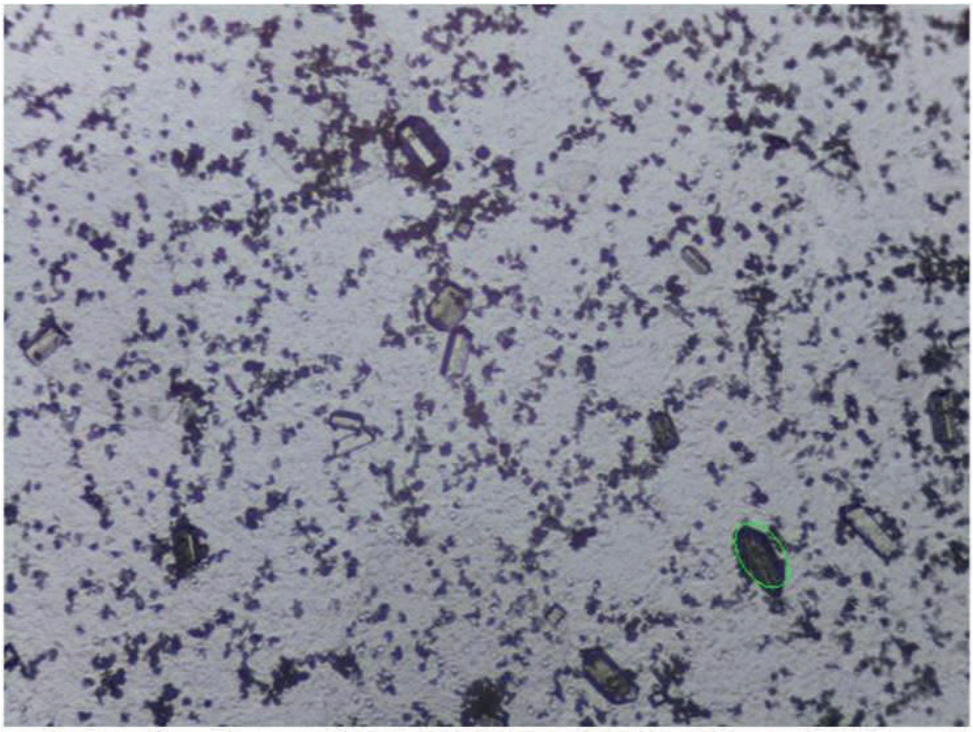

S3 Figure: Image showing crystal incorrectly detected as an egg by the Schistoscope.

S1 Manual: Schistoscope user manual (https://doi.org/10.1371/journal.pntd.0011967.s005)

S1 video: Video showing the Schistoscopes running in the laboratory (https://doi.org/10.1371/journal.pntd.0011967.s006).

S1 Checklist: STARD-2015-Checklist (https://doi.org/10.1371/journal.pntd.0011967.s001).

S1 Raw dataset: Overall raw dataset containing data for Schistoscope validation on fresh urine samples (study A), Banked slides (study B) and quality control of banked slides (https://doi.org/10.1371/journal.pntd.0011967.s007).

6.

Validation of AiDx Assist device for automated detection of *Schistosoma* eggs in stool and urine samples in Nigeria

Brice Meulah, Pytsje T. Hoekstra, Samuel Popoola, Satyajith Jujjavarapu, Moses Aderogba , Joseph O. Fadare, John A. Omotayo, David Bell, Cornelis Hokke, Lisette van Lieshout , Gleb Vdovine, Jan Carel Diehl, Temitope Agbana, Louise Makau-Barasa, Jacob Solomon.

Under review (2024): Frontiers in Parasitology, section Parasite Diagnostics

Abstract

Schistosomiasis is a public health concern and there is need for reliable, field compatible diagnostic methods in endemic settings. The AiDx Assist, an artificial intelligence (AI)-based automated microscope, has shown promising results for the detection of *Schistosoma haematobium* eggs in urine. It has been further developed for the detection of *Schistosoma mansoni* eggs in stool. In this study, we evaluated the performance of the AiDx Assist for the detection of *S. mansoni* eggs in stool as well as further validating the performance of the AiDx Assist for the detection of *S. haematobium* eggs in urine. Additionally, the potential of AiDx Assist for the detection of other helminths in stool was explored.

In total, 405 participants from an area endemic for both *S. mansoni* and *S. haematobium* provided stool and urine samples which were subjected to AiDx Assist (semi- and fully-automated), while conventional microscopy was used as the diagnostic reference. Only samples with complete test results were included in the final analysis, resulting in 375 stool and 398 urine, of which 38.4% and 65.3% showed *Schistosoma* eggs by conventional microscopy. The collected images of stool samples were retrospectively examined for other helminth eggs via manual analysis.

For the detection of *S. mansoni* eggs, the sensitivity of the semi-automated AiDx Assist (86.8%) was significantly higher compared to the fully-automated AiDx Assist (56.9%) while the specificity was comparable, being 81.4% and 86.8%, respectively. Retrospectively, eggs of *Ascaris lumbricoides* and *Trichuris trichiura* were visualized. For the examination of urine samples, a comparable sensitivity in the detection of *S. haematobium* eggs was seen between the semi- and the fully automated mode of the AiDx Assist, showing 94.6% and 91.9%, respectively. Also the specificity was comparable, with 90.6% and 91.3% respectively.

The AiDx Assist meets the World Health Organization Target Product Profile criteria in terms of diagnostic accuracy for the detection of *S. haematobium* eggs in urine, while performing modestly for the detection of *S. mansoni* eggs in stool. With some further improvements, it has the potential to become a valuable diagnostic tool for screening multiple helminth parasites in stool and urine.

Introduction

Schistosomiasis is a neglected tropical disease and a public health concern in endemic settings [1]. Conventional microscopy is the reference method for the diagnosis of schistosomiasis. It involves the detection and quantification of *Schistosoma* eggs in stool or urine [WHO 2]. The need for trained experts to perform this method limits its wide application in resource limited settings. Furthermore, the high demands for microscopy expertise not met by the number of trained microscopists in endemic settings highlights the need for high throughput methods [3, 4]. Automating microscopy method such that the dependency on trained experts is reduced could be a matching solution.

Several automated microscopes with embedded artificial intelligence (AI) algorithms have been developed for detecting *S. mansoni* or *S. haematobium* eggs [5-10]. To the best of our knowledge, none of these microscopes have been validated as a single system for the detection and quantification of both *S. mansoni* and *S. haematobium* eggs in stool and urine respectively, within a field setting.

The AiDx Assist is a low-cost and compact automated microscope with integrated AI. It is relatively easy to use without the need for high-level training compared to conventional microscopy [11] and has been validated for the diagnosis of *S. haematobium* infection in rural endemic settings in two modes: semi-automated and fully-automated mode [5]. In the semi-automated mode, the AI algorithm is disabled, and parasite count is detected and counted by an expert based on visual examination of images registered by the device. Operations in the fully-automated mode however, include automated parasite detection and counting by the integrated AI algorithm. The design of the AiDx Assist makes it possible to develop and customize for the detection of different parasites in the same or different sample types.

The AiDx Assist has been shown to be a promising diagnostic tool for urogenital schistosomiasis [5] and could also have great potential for future and timely diagnosis of intestinal schistosomiasis. Since the first evaluation for the detection of *S. haematobium* eggs in Nigeria, the device has been further developed for the detection of *S. mansoni* eggs on Kato-Katz (KK) slides and now requires validation in an endemic setting. In the current study, we carried out a validation of the AiDx Assist demonstrating its performance in detecting *S. mansoni* and *S. haematobium* eggs in stool and urine samples collected in Nigeria in a setting endemic for both *Schistosoma* species. We also explored the potential of the AiDx Assist to detect other helminth parasites in stool samples.

Methods

Study design

This cross-sectional study was conducted in local communities of the Federal Capital Territory, Abuja, Nigeria with known endemicity for *S. mansoni* and *S. haematobium* infections. The number of egg positive samples needed to achieve an assumed sensitivity and specificity of 90% using conventional microscopy as the reference was calculated to be approximately 130 [12]. A school-based approach was employed for sampling participants across 5 communities

based on the schistosomiasis prevalence data (approximately 40%) obtained from the database of the Neglected Tropical Disease Division of the Federal Ministry of Health. To attain 130 positive samples, sampling of 325 participants was aimed. Participants age 5 or older were eligible to take part in the study.

Ethics statement

Ethical approval for this study was obtained from the Federal Capital Territory (FCT, Nigeria), Health Research Ethics Committee (FCT, HREC). Before collecting samples, a written consent was obtained from adults and from the parents or legal guardians of children who wanted to take part, which was confirmed by their signatures. To safeguard the confidentiality and anonymity of the results, distinct codes were assigned to each of the samples. Following sample collection, mass treatment with praziquantel was administered to all communities according to local guidelines by the NTD unit of the public health department.

Sample processing

Each participant was given two sterile containers to provide a stool and urine sample at designated collection sites. These samples were then transported in appropriate boxes within two hours of collection to the laboratory. From the stool sample, KK slides were prepared [13]: 41.7mg of sieved stool was transferred to a microscopy slide using a template and then covered with cellophane, which has been dipped in malachite green overnight. Some light pressure was applied to the slide, in order to spread out the smear, and examination started after 10 minutes. For the urine sample, microscopy slides were prepared by urine filtration (UF). Briefly, 10 ml of homogenised urine was pressed through a 13 mm membrane (pore size 30 μm; Whatmann International Ltd) using a syringe and a filter holder and transferred onto a glass slide. The slides were examined using the semi- and fully-automated mode of the AiDx Assist and conventional microscopy (Figure 1).

Slide examination by the AiDx Assist and conventional microscopy

Each KK and UF slide was analysed with the AiDx Assist (Figure 2) in the semi-automated and the fully-automated mode, as previously described [5]. In the semi-automated mode, the images registered by the AiDx Assist were visually examined by an expert for the presence of *Schistosoma* eggs and counted. In the fully-automated mode, the artificial intelligence algorithm was enabled to automatically detect and count *Schistosoma* eggs in the images. The output of the AI algorithm was displayed and confirmed by the operator of the device at the end of each sample analysis. Results from the AiDx Assist was exported in an Excel compatible format. The same slides were subsequently analysed by conventional microscopy (10/40(×) objective on a Leica microsystems DM 300 microscope). Two independent microscopy readings were done and recorded. The average of the eggs counted between the two readings was considered for each sample. Quality control was performed retrospectively on images captured with the AiDx assist as well as for the presence of other stool parasites on KK slides on a selected sample with high infection intensity based on conventional microscopy.

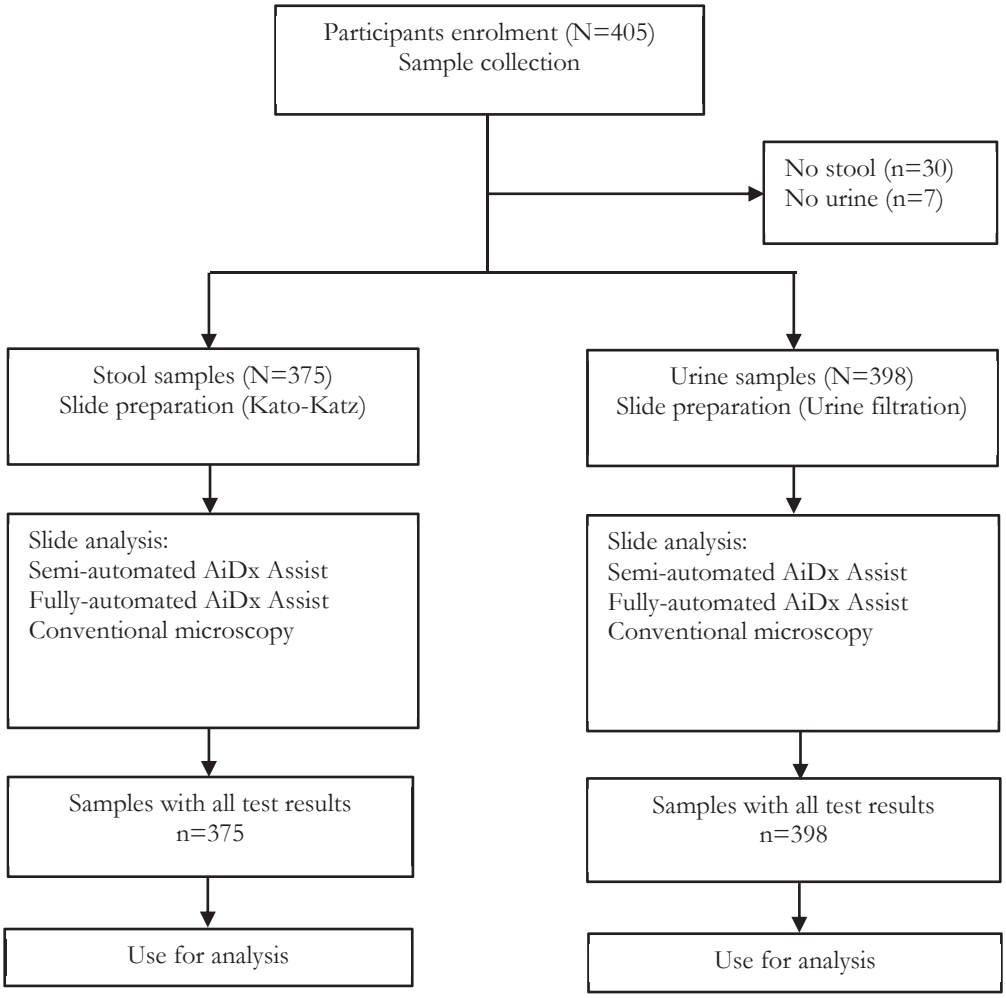

Figure 1. Flow chart of stool and urine sample collection, processing and analyses by the AiDx Assist and conventional microscopy.

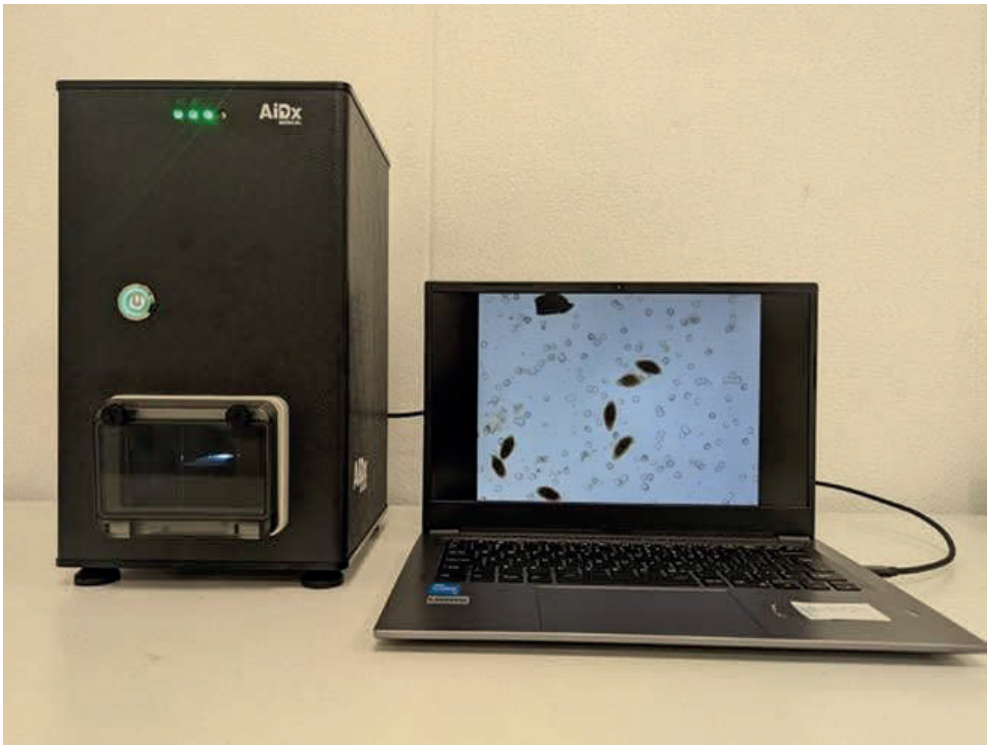

Figure 2. AiDx Assist digital microscope (104).

Statistical analysis

The number of eggs counted for all methods from the KK and UF slides were expressed in eggs per gram (EPG) of stool and eggs per 10 ml of urine, respectively. The percentage positive by AiDx Assist (semi- and fully-automated mode) and conventional microscopy was determined. The sensitivity and specificity of the AiDx Assist (semi- and fully-automated) was assessed using conventional microscopy as a reference. Cohen's Kappa (k) statistics was computed to assess the qualitative agreement between methods. Spearman's correlation (r) was used to assess the pairwise strength of association between eggs counted by the different methods. All statistical analyses were performed with IBM Statistical Package for Social Sciences version 25 (SPSS Inc., Chicago, United States of America) and graphs were generated using GraphPad Prism version 9.0.1 for Windows (GraphPad Software, San Diego, California USA).

Results

AiDx Assist performance for detection of S. mansoni eggs on Kato-Katz slides

A total of 375 stool samples had results for all diagnostic methods and were therefore included in the final analysis (Figure 1). Table 1 shows the proportion of positive per method for *S. mansoni* infection. The semi-automated AiDx Assist found the highest proportion of positive (44.8%) followed by conventional microscopy (38.4%) and then the fully-automated AiDx Assist (25.9%). Different median egg counts were observed for semi-automated (96 EPG),

fully-automated AiDx Assist (48 EPG) and conventional microscopy (72 EPG). In addition to *S. mansoni*, *Ascaris lumbricoides* and *Trichuris trichiura* eggs were manually detected on digital images captured with the AiDx Assist following retrospective image analysis (Figure 3a, b & c respectively).

Table 1. Characteristic outcomes of the semi-automated and fully-automated AiDx Assist in comparison to conventional microscopy for *Schistosoma* egg detection

	***S. mansoni* (N=375)**			***S. haematobium* (N=398)**		
Tests	**Semi-automated AiDx-assist**	**Fully automated AiDx-assist**	**Conventional microscopy**	**Semi-automated AiDx-assist**	**Fully automated AiDx-assist**	**Conventional microscopy**
Positive samples (%)	168 (44.8%)	97 (25.9%)	144 (38.4%)	259 (65.1%)	251 (63.1%)	260 (65.3%)
Low intensity	85 (50.6%)	74 (76.3%)	99 (68.8%)	170 (65.6%)	173 (68.9%)	179 (68.8%)
Moderate intensity	46 (27.4%)	20 (20.6%)	39 (27.0%)	-	-	-
High intensity	37 (22.0%)	3 (3.1%)	6 (4.2%)	89 (34.4%)	78 (31.1%)	81 (31.2%)
Range	24-2304 EPG	24-792 EPG	24- 576 EPG	1-1483 eggs/10ml	1-1169 eggs/10ml	1-181 eggs/10ml
Median	96 EPG	48 EPG	72 EPG	18 eggs/10ml	19 eggs/10ml	16 eggs/10ml

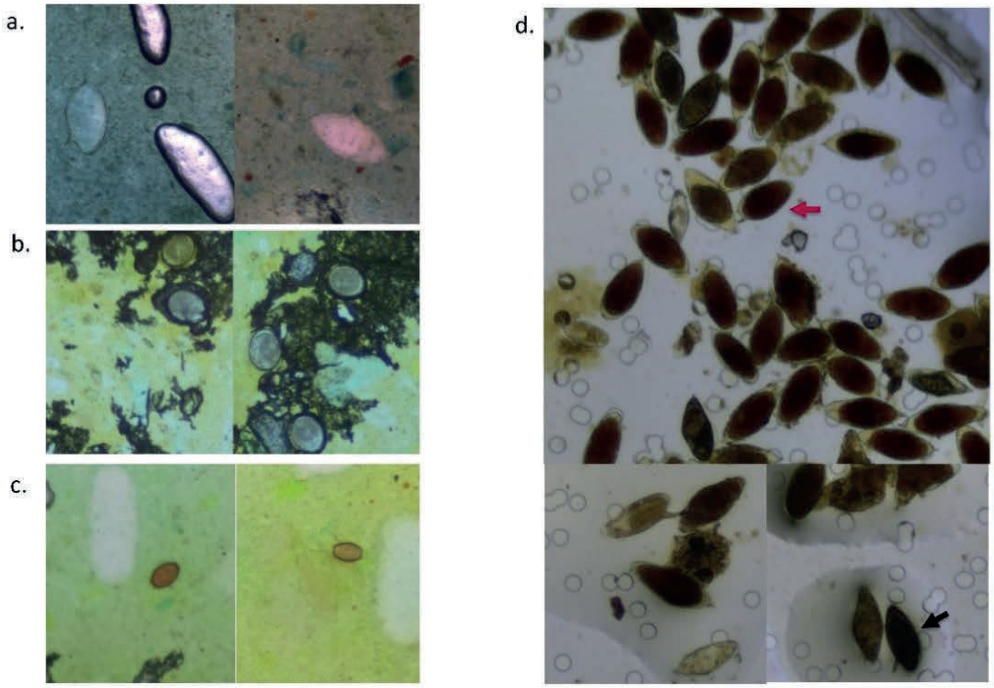

Figure 3. Digital image of Kato-Katz smear (a, b & c) and urine filtration slide (d) captured with the AiDx Assist showing *S. mansoni* eggs (a), *A. lumbricoides* eggs b) *T. trichiura* eggs (c) and several *S. haematobium* eggs (indicated with a red arrow) and *S. mansoni* eggs (indicated with a black arrow) (d).

Qualitatively, the agreement between the AiDx Assist (semi- and fully-automated) and conventional microscopy was moderate to substantial for the detection of *S. mansoni* eggs (K=0.538 and K=661, P<0.05 respectively). Figure 4a illustrates the diagnostic agreement between conventional microscopy and the semi- and fully-automated mode of the AiDx Assist. Based on conventional microscopy, the sensitivity of the semi-automated AiDx Assist (86.8%) for the detection *S. mansoni* egg was significantly higher than the fully-automated AiDx Assist (56.9%) although their specificities were comparable (81.4% and 86.8%, respectively).

Table 2. Diagnostic performance of the semi-automated and fully-automated AiDx Assist for the detection of *Schistosoma* eggs performed on urine and stool.

	S. mansoni		***S. haematobium***	
Index test	**Sensitivity % (95% CI)**	**Specificity % (95% CI)**	**Sensitivity % (95% CI)**	**Specificity % (95% CI)**
Semi-automated AiDx Assist	86.8 (80.2-91.9)	81.4 (75.8-86.2)	94.6 (91.1-97.0)	90.6 (84.4-94.9)
Fully automated AiDx Assist	56.9 (48.4-65.2)	86.8 (80.2-91.9)	91.9 (87.9-94.9)	91.3 (85.3- 95.4)

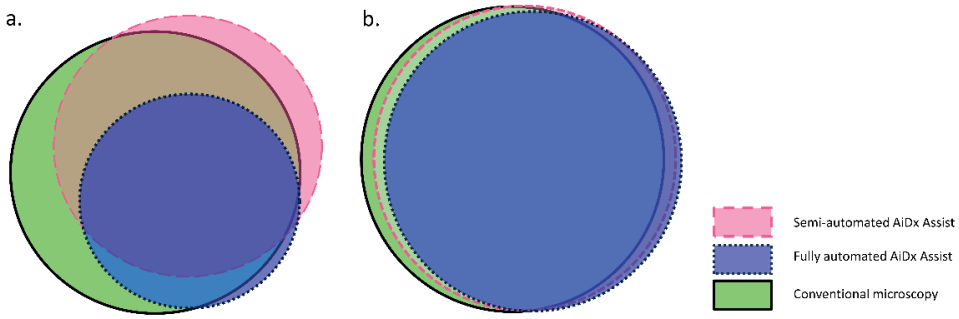

Figure 4. Proportional Venn diagram demonstrating agreement of percentage positive by semi-automated AiDx Assist, fully-automated AiDx Assist and conventional microscopy for the detection *S. mansoni* and *S. haematobium* egg on a) stool and b) urine respectively.

A moderate correlation was observed between the semi- and fully-automated mode of the AiDx Assist and conventional microscopy for quantification of *S. mansoni* eggs (r = 0.64 P<0.05, r = 0.78, P<0.05 respectively) (Figure 5a & b).

AiDx Assist performance for detection of S. haematobium eggs on urine slides

A total of 398 urine samples had results for all three diagnostic methods (Figure 1). The proportion of *S. haematobium* infection was comparable among the semi- and fully-automated AiDx Assist and conventional microscopy (65.1%, 63.1% and 65.3% respectively) (Table 1). The median egg count for *S. haematobium* by all three methods; semi-automated, fully-automated

AiDx Assist and conventional microscopy were comparable (18 eggs/10ml, 19 eggs/10ml, 16 eggs/10ml respectively). Figure 3d shows digital images of urine slides where *S. haematobium* and *S. mansoni* eggs are visualized.

An almost perfect agreement was observed between the semi-automated AiDx Assist and conventional microscopy (K=0.820, P<0.05) as well as between the fully-automated AiDx Assist and conventional microscopy (K=0.851, P<0.05) for the detection of *S. haematobium* eggs (Figure 3b). Using conventional microscopy as the reference, the sensitivity and specificity of the semi-automated (94.6% and 90.6% respectively) and fully-automated AiDx Assist (91.9% and 91.3% respectively) for the detection of *S. haematobium* eggs were comparable (Table 2).

Also, a very strong correlation was observed between egg counts of the semi- and fully-automated AiDx Assist and conventional microscopy (r = 0.93 P<0.05, r = 0.95 P<0.05, respectively) (Figure 5c & d).

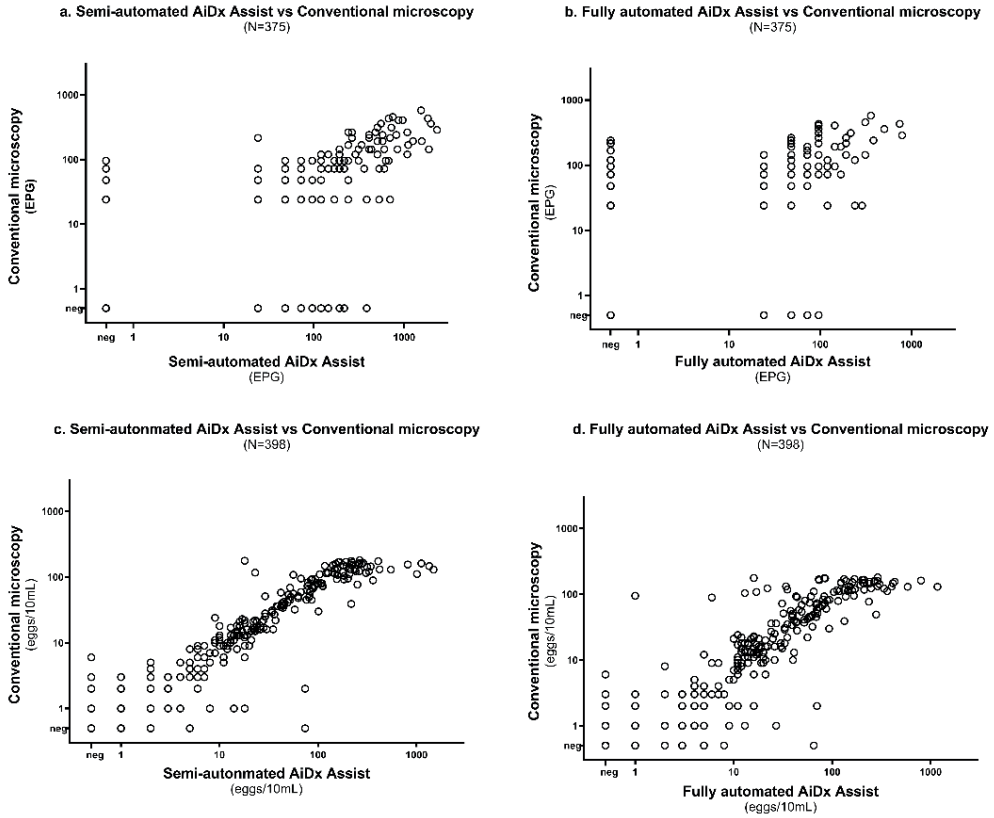

Figure 5. Correlation plot on a log scale between semi-automated AiDx Assist, fully-automated AiDx Assist and conventional microscopy for a & b) *S. mansoni* egg count c & d) *S. haematobium egg* count.

Discussion

For the first time we report the performance of the semi- and fully-automated AiDx Assist, as a single device in a field setting for detecting and quantifying *S. mansoni* and *S. haematobium* eggs in stool and urine samples, respectively, using conventional microscopy as the reference. Overall, the performance of semi-automated and the fully-automated AiDx Assist was found to be modest for the detection of *S. mansoni* eggs and requires optimization to improve the performance. Furthermore, the performance of the semi-automated AiDx Assist and the fully-automated AiDx Assist for the detection of *S. haematobium* eggs in urine samples was consistent with Makau-Barasa et al [5]. We also demonstrated that the AiDx Assist has a multi-diagnostic potential as other helminth eggs were visualized in digital images of some of the stool samples.

The significantly higher sensitivity of the semi-automated AiDx Assist (86.8 %) over the fully-automated AiDx Assist (56.9 %) for the detection of *S. mansoni* eggs on KK slides could be due to the fact that stool samples often contain dirt (artifacts) which interferes with the AI detection algorithm, while a trained expert would be able to ignore this and only detect *S. mansoni* eggs a phenomenon also observed in Dacal et al [14]. Another reason could be the difference in stool properties such as colour, texture and consistency as well as variation in stain preparation leading to variable KK smears (as observed in Figure 3a-c). The AiDx Assist AI algorithm for the detection of *S. mansoni* eggs in stool samples requires optimization, and such factors need to be taken into consideration. That is, a high quality and diverse data set covering as many different KK smear variations as possible, is required to further train the AI algorithm. Also, validation of the AiDx Assist using alternative stool preparation methods, e.g. the floatation preparation methods which results in relatively clean slides, could be a solution to the challenges with dirt or artifacts. However, such methods are not very field compatible [15, 16].

Additional analysis revealed that majority of the stool samples (68.8 %) based on conventional microscopy had low infection intensity (1-99 EPG, Table 1) of which more than half were missed by the AI algorithm. Therefore, further optimizing the AI algorithm for accurately detecting light infections would significantly improve the overall performance of the fully-automated AiDx Assist. The comparable specificity of the semi-automated AiDx Assist (81.4 %) to the fully-automated AiDx Assist (86.8 %) is due to the additional validation step by the operator during the fully-automated AiDx Assist as the positive cases detected by the AI are further checked and ruled out if false positive.

The sensitivity and specificity between the semi-automated AiDx Assist and fully-automated AiDx Assist for the detection *S. haematobium* eggs based on conventional microscopy were comparable (Table 2) and was consistent with previously reported findings [5]. Despite differences in the positive rates and similarities in the infection intensity observed between studies the consistent outcome provides more evidence on the reliability and robustness of the AiDx Assist for the detection of *S. haematobium* infection in urine. It also provides more evidence that, the AiDx Assist meets the required WHO diagnostic Target Product Profile (TPP) (WHO76) for sensitivity and specificity of *S. haematobium.*

Although a strong to moderate correlation was observed between the semi-automated AiDx Assist, fully-automated AiDx Assist and conventional microscopy for *S. mansoni* and *S. haematobium* egg quantification, at high infection intensities microscopy tended to underestimate egg count. This observation is in contrary to that of Meulah et al. [6] where for ≥100 eggs/10ml of urine the AI-algorithm integrated in the Schistoscope underestimated egg counts due to egg overlap. This contradicting observation could be partly due the differences in AI architecture used as well as the level of experience of the microscopists between studies. Images of samples with high egg counts (≥100 eggs/10ml for *S. haematobium* and ≥1000 EPG for *S. mansoni*) based on the semi-automated AiDx Asist were re-analyzed manually by an independent experienced microscopist which confirmed that conventional microscopy underestimated egg counts for samples with high infection intensity. This could be due to less experience by the microscopist in estimating egg count for sample with high infection intensity. Moreover, a better correlation scatter between the semi- and fully-automated AiDx Assist was observed across all infection intensities for both *S. mansoni* and *S. haematobium* egg quantification (Supplementary Figure 1).

Through retrospectively analysing digital images of KK slides prepared from various samples, it was possible to visualize other stool helminth parasites. The design of the AiDx Assist optical system theoretically enables the visualization of parasite features within a size range of approximately 15-400µm. This implies that, parasites and/or their eggs within this size range can be manually detected as also demonstrated by other studies [4, 10, 14, 18, 19]. However, the current AI-powered prototype of the AiDx Assist has been specifically developed for detecting eggs of *S. mansoni* and *S. haematobium*. While visualizing other helminth eggs on digital images captured with the AiDx Assist demonstrates its potential for detecting additional parasites, further development and optimization are necessary for these parasites. This process would involve generating datasets for different stool helminth parasites to train an AI algorithm to recognize these eggs, followed by validation. The digital images generated in this study could serve this purpose. Also, with the different variations in the digital image data set collected within this study, it could be used to optimise the diagnostic performance of the fully-automated AiDx Assist for detecting *S. mansoni* eggs and to develop the device for other helminth parasites in stool.

The limitation of this study is the fact that during conventional microscopy, the technicians were only asked to mark the number of *Schistosoma* eggs. Consequently, when exploring the AiDx Assist's capability to identify other stool helminths through digital images, no comparison could be made to conventional microscopy. This missed opportunity could have provided further evidence regarding the device's potential to detect other stool parasites.

In conclusion, the overall diagnostic performance of the semi- and fully-automated AiDx Assist for the detection of *S. mansoni* infection was found to be modest and requires improvement to meet the WHO TPP in terms of diagnostic accuracy. The consistent finding on *S. haematobium* detection and the additional observation of *A. lumbricoides* and *T. trichiura* revealed its potential for screening multiple diseases in endemic settings.

Author contributions

BM: Writing – original draft, Writing – review & editing, Data curation, Formal Analysis, Conceptualization, Methodology, Software, Validation, Visualization. PTH: Writing – review & editing, Methodology, Validation, Visualization. SP: Conceptualization, Validation, Data curation, Writing – review & editing. SJ: Data curation, Software, Validation. MA: Conceptualization, Writing – review & editing. JOF: Methodology, Writing – review & editing. JAO: Methodology, Writing – review & editing. DB: Conceptualization, Writing – review & editing. CH: review & editing. LvL: Conceptualization, Methodology, Writing – review & editing. GV: Conceptualization, Writing – review & editing. JC: Conceptualization, Writing – review & editing. TA: Conceptualization, Data curation, Writing – review & editing. JCD: Writing – review & editing, Conceptualization. LMB: Conceptualization, Writing – review & editing. JS: Conceptualization, Methodology, Writing – review & editing.

References

1. Wiegand RE, Secor WE, Fleming FM, French MD, King CH, Montgomery SP, et al. Control and Elimination of Schistosomiasis as a Public Health Problem: Thresholds Fail to Differentiate Schistosomiasis Morbidity Prevalence in Children. Open Forum Infectious Diseases. 2021;8(7).
2. World Health Organization. Prevention and control of schistosomiasis and soil-transmitted helminthiasis: report of a WHO expert committee 2002 [Available from: https://apps.who.int/iris/handle/10665/42588.
3. Chala B. Advances in Diagnosis of Schistosomiasis: Focus on Challenges and Future Approaches. Int J Gen Med. 2023;16:983-95.
4. Boonyong S, Hunnangkul S, Vijit S, Wattano S, Tantayapirak P, Loymek S, et al. High-throughput detection of parasites and ova in stool using the fully automatic digital feces analyzer, orienter model fa280. Parasites & Vectors. 2024;17(1):13.
5. Makau-Barasa L, Assefa L, Aderogba M, Bell D, Solomon J, Urude RO, et al. Performance evaluation of the AiDx multi-diagnostic automated microscope for the detection of schistosomiasis in Abuja, Nigeria. Sci Rep. 2023;13(1):14833.
6. Meulah B, Oyibo P, Bengtson M, Agbana T, Lontchi RAL, Adegnika AA, et al. Performance evaluation of the Schistoscope 5.0 for (semi-) automated digital detection and quantification of Schistosoma haematobium eggs in urine: A field-based study in Nigeria. Am J Trop Med Hyg. 2022;107(5):1047-54.
7. Meulah B, Oyibo P, Pytsje T. Hoekstra PANM, Moustapha Nzamba Maloum, Romeo Aime Laclong-Lontchi, Yabo Josiane Honkpehedji, Michel Bengtson, Cornelis Hokke, Paul L.A.M. Corstjens, Temitope Agbana, Jan Carel Diehl, Ayola Akim Adegnika, Lisette van Lieshout. Validation of artificial intelligence-based digital microscopy for automated detection of Schistosoma haematobium eggs in urine in Gabon. PLOS Neglected Tropical Diseases. 2023.
8. Oyibo P, Jujjavarapu S, Meulah B, Agbana T, Braakman I, van Diepen A, et al. Schistoscope: An Automated Microscope with Artificial Intelligence for Detection of Schistosoma haematobium Eggs in Resource-Limited Settings. Micromachines (Basel). 2022;13(5).
9. Sangameswaran R. MAIScope: A low-cost portable microscope with built-in vision AI to automate microscopic diagnosis of diseases in remote rural settings. arXiv preprint arXiv:220806114. 2022.
10. Ward P, Dahlberg P, Lagatie O, Larsson J, Tynong A, Vlaminck J, et al. Affordable artificial intelligence-based digital pathology for neglected tropical diseases: A proof-of-concept for the detection of soil-transmitted helminths and Schistosoma mansoni eggs in Kato-Katz stool thick smears. PLoS Neglected Tropical Diseases. 2022;16(6):e0010500.
11. Onasanya A, Bengtson M, Agbana T, Oladunni O, van Engelen J, Oladepo O, et al. Towards Inclusive Diagnostics for Neglected Tropical Diseases: User Experience of a New Digital Diagnostic Device in Low-Income Settings. Tropical Medicine and Infectious Disease. 2023;8(3):176.
12. Jones SR, Carley S, Harrison M. An introduction to power and sample size estimation. Emerg Med J. 2003;20(5):453-8.
13. Katz N, Chaves A, Pellegrino J. A simple, device for quantita tive stool thick-smear technique in schistosomiasis mansoni. Revista do instituto de medicina tropical de São Paulo. 1972;14(6):397-400.
14. Dacal E, Bermejo-Peláez D, Lin L, Álamo E, Cuadrado D, Martínez Á, et al. Mobile microscopy and telemedicine platform assisted by deep learning for the quantification of Trichuris trichiura infection. PLoS Negl Trop Dis. 2021;15(9):e0009677.
15. Khurana S, Singh S, Mewara A. Diagnostic Techniques for Soil-Transmitted Helminths - Recent Advances. Res Rep Trop Med. 2021;12:181-96.
16. Meurs L, Polderman AM, Vinkeles Melchers NV, Brienen EA, Verweij JJ, Groosjohan B, et al. Diagnosing Polyparasitism in a High-Prevalence Setting in Beira, Mozambique: Detection of Intestinal Parasites in Fecal Samples by Microscopy and Real-Time PCR. PLoS Negl Trop Dis. 2017;11(1):e0005310.

17. World Health Organisation. Public consultation: Target Product Profiles for diagnostic tests to meet Schistosomiasis and soil-transmitted Helminth programme needs 2021 [Available from: https://www.who.int/news-room/articles-detail/public-consultation-target-product-profiles-for-diagnostic-tests-to-meet-schistosomiasis-and-soil-transmitted-helminth-programme-needs.
18. Yang A, Bakhtari N, Langdon-Embry L, Redwood E, Grandjean Lapierre S, Rakotomanga P, et al. Kankanet: An artificial neural network-based object detection smartphone application and mobile microscope as a point-of-care diagnostic aid for soil-transmitted helminthiases. PLoS Negl Trop Dis. 2019;13(8):e0007577.
19. Lundin J, Suutala A, Holmström O, Henriksson S, Valkamo S, Kaingu H, et al. Diagnosis of soil-transmitted helminth infections with digital mobile microscopy and artificial intelligence in a resource-limited setting. PLOS Neglected Tropical Diseases. 2024;18(4):e0012041.

Supplementary information

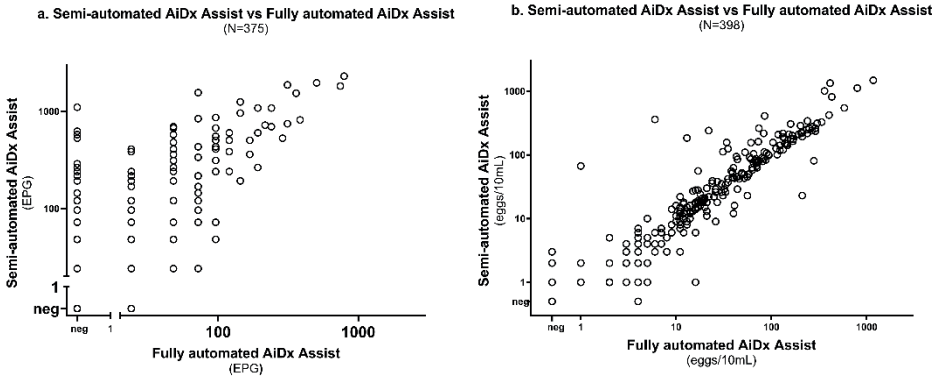

S1 Figure. Correlation plot on a log scale between semi-automated AiDx Assist and fully-automated AiDx Assist for the for a) *S. mansoni* egg count b) *S. haematobium egg* count.

7.

General discussion

Adapted and extended from: A review on innovative optical devices for the diagnosis of human soil-transmitted helminthiasis and schistosomiasis: From research and development to commercialisation

Brice Meulah, Michel Bengtson, Lisette Van Lieshout, Cornelis Hendrik Hokke, Andrea Kreidenweiss, Jan-Carel Diehl, Ayola Akim Adegnika, and Temitope Ebenezer Agbana.

Parasitology. 2023;150(2):137-149.

Simple, inexpensive, portable, robust and reliable diagnostics are urgently needed for individual case management, as well as for the assessment of the progress of control strategies for NTDs in endemic settings. This is particularly so for schistosomiasis, soil-transmitted helminths (STHs) and other helminthiases such as filariasis. For these diseases conventional microscopy is still the most commonly used method, despite the fact that there are alternatives available. In the case of schistosomiasis, the haematuria dipstick and the antigen detecting lateral flow tests POC-CCA are the most broadly accepted alternatives for the detection of *S. haematobium* and *S. mansoni*, respectively. For infections with the filaria species: *Wuchereria bancrofti*, the filariasis test strip (FTS) for the detection of circulating antigens in blood can be used to diagnose lymphatic filariasis [1]. However, as the saying goes "no-one-size fits all", each of these tests have their own diagnostic characteristics, which cater to specific contextual needs. For example, the reagent strip test for detecting microhaematuria is only indicative for *S. haematobium* infection and is not parasite-specific [2]. The POC-CCA tests have been validated extensively in settings endemic for *S. mansoni* infection [3-8], while showing variable outcomes in *S. haematobium* endemic setting [9-11]. The more advanced diagnostic alternatives such as the UCP LF-CAA test and PCR are known to be highly accurate, but they are not field friendly and require a relatively high level of training and laboratory infrastructure, especially for PCR. In the case of lymphatic filariasis, the FTS is useful in endemic settings to support ivermectin MDA control programs. However, in settings with unknown co-endemicity with *Loa loa* an additional test is required to guide the treatment due to contraindication of ivermectin for persons with *Loa loa* infection [12]. Conventional microscopy which remains the most commonly used method in endemic settings for schistosomiasis, STH and filariasis is laborious, requires well-trained personnel and infrastructure which are often lacking. Eye defects resulting from long term exposure of the eyes to light of microscopes while in use over a long period of time have been reported [13-15]. Low-cost AI powered digital optical diagnostic device (DODD) platforms have the potential to revolutionise the health systems in LMICs. These devices are relatively easy to use [16] and in combination with digital health applications could be an acceptable alternative to conventional microscopy in field settings, if the diagnostic performance is proven to be equally as good. In this thesis, we carried out validation of the diagnostic performance of DODDs, the Schistoscope and AiDx Assist digital microscope, at different iterations during their development for the diagnosis of schistosomiasis and other helminthiases.

We began by demonstrating the need for microscopy methods in specific field settings (chapter 2). With the limitations of conventional microscopy acknowledged, we validated DODDs which are innovations of microscopes (Schistoscope and AiDx Assist) through research and development to detect and quantify eggs of *Schistosoma* and STHs against a range of diagnostic reference tests in different settings (chapter 3-6). These devices are designed by integrating AI software programs to digital optical hardware systems to automate diagnosis. In Nigeria, a high sensitivity but low specificity as well as low count accuracy (≥100 egg/10mL of urine) of the Schistoscope for the detection of *S. haematobium* eggs compared to conventional microscopy was obtained. This was due to limitations in the Schistoscope's AI framework (chapter 3). The AI framework was further improved for specificity and count accuracy for *S. haematobium* egg detection and validated on a set of microscopy images from the field (chapter

4). A high diagnostic sensitivity and specificity of the Schistoscope was obtained through validation on a large set of clinical samples, consisting of fresh urine and banked filters for *S. haematobium* egg detection using conventional microscopy, real-time PCR and UCP-LF CAA as reference standards in Gabon (chapter 5). A modest performance of the AiDx Assist for the detection and quantification of *S. mansoni* eggs in stool (Kato-Katz (KK) slides) was obtained with high accuracy for detection of *S. haematobium* eggs in urine. The potential of the AiDx Assist to detect STHs was explored. The STHs eggs could be manually identified on images captured with the AiDx Assist (chapter 6). In contrast to the Schistoscope, the AiDx Assist over-estimated *S. haematobium* egg count compared to conventional microscopy. These differential observations are further discussed within this chapter.

Diagnostic sensitivity and specificity of Schistoscope and AiDx Assist for schistosomiasis and soil-transmitted helminths in endemic settings

From the validation studies, the diagnostic performance of the Schistoscope and AiDx Assist at different iterations of their development was reported. With the use of urine samples collected from different endemic settings, the sensitivity and specificity of the Schistoscope for the detection of *S. haematobium* eggs varied depending on the reference test used (chapter 3, 4 and 5 or Table 2). For example, the first field validation of the Schistoscope in Nigeria showed a high sensitivity (85.0 %) but low specificity (48.9%) compared to conventional microscopy for detecting *S. haematobium* eggs in urine. This study importantly revealed that the quality and coverage of the dataset generated and used to train the AI algorithm for the detection of *S. haematobium* eggs was limited in terms of variation of the type of artifacts that could be present in field samples. Overcoming this limitation significantly improved the specificity (77.0 %) of the Schistoscope when validated in Gabon while maintaining a sensitivity (83.1 %) comparable to conventional microscopy (Chapter 4). However, when compared to a more accurate composite reference consisting of UCP-LF CAA and real-time PCR, the sensitivity dropped to 62.9%. This decrease in sensitivity was primarily due to the Schistoscope, similar as conventional microscopy, missing very low infection intensities which were detected by the more sensitive diagnostic procedures such as PCR and CAA detection. This clearly highlights the limitation of microscopy methods in settings approaching elimination of this disease and calls for more sensitive, field compatible tests [17, 18]. Examination of larger urine volumes for negative samples could potentially improve the diagnostic sensitivity. This method normally results in increased work load as well as analysis cost rendering it impractical in resource-limited-settings relying on conventional microscopy. However, with the Schistoscope this approach could be more feasible, given that its design permits the analysis of an unlimited number of slides daily. This implies there is still room to improve the performance of the Schistoscope to match that of conventional microscopy.

Furthermore, the sensitivity (91.9%) and specificity (91.3%) of the AiDx Assist for the detection of *S. haematobium* eggs in urine was comparable to conventional microscopy and was consistent with previous findings [19]. However, for the detection of S. mansoni eggs on Kato-Katz (KK) slides, the sensitivity was modest (56.9 %) with a high specificity (86.8 %). The low

sensitivity is attributed to the fact that majority of the samples missed had light infections (1-99 EPG) and the few eggs available might have been covered by stool components, making detection by AI algorithm challenging (Chapter 6 or Table 2). For the detection *S. haematobium* eggs, the overall sensitivity of the Schistoscope is comparable to that of the AiDx Assist (AI powered mode). However, the specificity is significantly lower. The difference in specificity is due to the fact that the AiDx Assist is designed such that the output of the AI algorithm (positive images) is displayed and confirmed by the operator of the device at the end of each sample analysis. This subsequently improves the specificity of the AiDx Assist as any false positive detection by the AI algorithm is ruled out by the operator. An approach similar to this has been used and reported by Lin et al., for filaria detection [20]. The difference in Lin et al., is that, confirmation of AI detection is done in real time by the user during image capture to improve sensitivity only. And when artifacts are detected by their algorithm, no correction is made by the operator.

Additionally, the Schistoscope performance was validated by analysing banked samples, recording promising results mostly attributed to the high infection intensity and relatively low level of artifacts in the samples used (chapter 5). Regardless, this finding opens up solutions to practical challenges in field settings including access to microscopists for real time analysis of samples for control program evaluation. The option of sampling and storage provides a lot of flexibility for organisation and execution of surveillance program in field settings.

Accuracy and relevance of egg count determination of Schistosoma and soil-transmitted helminths

Egg load serves as a proxy for disease morbidity and so far has been an essential marker in assessing the efficacy of control programs in endemic regions [21-24]. However, there is a debate regarding the relevance of precise egg quantification when dealing with high infection intensities (e.g. ≥50 egg/10mL or ≥400 EPG) as outlined by World Health Organisation (WHO) [25]. The field validation of the fully-automated Schistoscope in Nigeria revealed lower accuracy in quantifying *S. haematobium* eggs in urine samples with ≥100 eggs/10mL compared to conventional microscopy (chapter 3). Subsequent field validation of the improved Schistoscope in Gabon demonstrated better egg count accuracy, although still inferior to conventional microscopy (chapter 5). On the contrary, the fully automated AiDx Assist showed superior accuracy in quantifying *S. haematobium* and *S. mansoni* eggs compared to conventional microscopy based on the semi-automated AiDx Assist counts confirmed by an external quality control performed on digital images. This observation was made particularly for urine and stool samples with high egg counts (≥100 egg/10mL or ≥1000 EPG respectively). The discrepancy in egg count accuracy between the Schistoscope and AiDx Assist observed in the different studies stems from the level of expertise of the microscopist and the AI framework integrated in both devices.

Following the WHO categorization for infection intensity, accurate quantification of eggs for samples with the high infection intensity threshold is less of importance. As a result, these

devices could be programmed to stop counting upon reaching the high infection intensity threshold making the egg differences observed at very high count less of a problem. While this would also reduce the sample analysis time, the data obtained would still be valuable for surveillance in control programs. Despite egg count being considered as a proxy to infection intensity, in clinical settings, detection (positive or negative) of schistosomiasis and STH infections remains the primary interest to physicians in order to decide on whether to treat or not [26-28]. Also, since the treatment of schistosomiasis and STH infections with e.g. praziquantel and albendazole respectively, is independent of infection intensities [26, 27], egg quantification is often unnecessary. In such a case detection of an egg is enough to make decisions about treatment. For such a use case, these devices can as well be programmed to detect and count to a required threshold. This also highlights the importance of stakeholder engagement for the development of such tools [29].

Multiplex diagnosis with the Schistoscope and AiDx Assist

The exploratory potential of DODDs lies in is its ability to be adapted for different parasitic infections. For example, multiple studies have demonstrated or validated DODDs for visualisation or detection of different stool parasites [30-35]. Also, the optical systems of the Schistoscope and AiDx Assist coupled with their computing unit, enables customization for detecting various parasites across different sample types. This makes it possible to develop, train and install new AI algorithm on these devices to detect different disease of interest. These optical systems possess sufficient resolution to effectively resolve parasite signatures e.g. eggs, ranging in size of approximately 20-400 μm in cross-sectional diameter. We demonstrated as a proof-of-concept for use on stool samples, the manual visualisation of Schistosoma and STHs eggs in images of KK slides captured with the Schistoscope [36]. Furthermore, the Schistoscope has been tested for the manual visualisation of hookworm and *S. stercoralis* larvae in stool culture (data unpublished). The AiDx Assist has been validated for the detection of *S. haematobium* and *S. mansoni* eggs in urine and stool respectively in field settings (chapter 6 and Table 2). In addition, during the research period of this thesis we also have tested AiDx Assist for the detection of L. loa microfilaria on Giemsa stained thick blood smear (data unpublished).

In this side study, the AiDx Assist (Semi- and fully-automated mode as described in chapter 6) was validated on 514 thick blood smears for the detection and quantification of microfilaria using conventional microscopy as the reference standard (Table 2). Blood samples were collected from individuals residing in a Lambaréné in Gabon endemic for *Loa loa* and *Mansonella* spp. The positivity rate based on conventional microscopy was found to be 6.2% (Table 1). Table 2 shows the diagnostic performance of the AiDx Assist. Each thick smear was prepared using 5μl of blood, spread over an area of 2x4cm. Although comparable diagnostics performance between the AiDx Assist and conventional microscopy was observed, the sample size in terms of positive cases was limited. Figure 1. shows an image registered with the AiDx Assist showing *Loa loa* microfilaria. A strong correlation was observed between AiDx assist and conventional microscopy for microfilaria quantification ($r=0.37$, 0.92 $P<0.05$). In endemic settings, MDA of ivermectin serves as the primary control measure for onchocerciasis and/or

lymphatic filariasis. However, the deleterious effects observed in individuals co-infected with *Loa loa* during treatment with ivermectin underscore the importance of detecting and quantifying *Loa loa* microfilariae before initiating treatment [37]. Although the AiDx Assist could be beneficial in these MDA programs, practical challenges related to sample collection, processing, and turnaround time limits its real-time application for test-and-treat strategies during community MDA campaigns. In previous studies a digital microscope called the LoaScope was developed and validated for the detection of *Loa loa* microfilaria [12, 38]. This device is designed to detect microfilaria movement directly on fresh blood smears (no staining required) obtained via finger prick, enabling real-time analysis and subsequent treatment decision-making regarding ivermectin administration. Conversely, the AiDx Assist sample preparation approach as well as the approach used by Lin et al, [20] are better suited for use in reference or local laboratory settings where slide fixing and staining are required.

Table 1. Characteristic outcome of the semi-automated, fully-automated AiDx Assist and conventional microscopy for the detection of microfilaria performed on 514 Giemsa thick blood smears.

	Semi-automated AiDx Assist	**Fully-automated AiDx Assist**	**Convectional microscopy**
Positive sample (%)	33 (6.4)	143 (27.8)	32 (6.2)
Median (microfilaria count/5uL)	4	11	8
Range (microfilaria count/5uL)	1-134	1-100	1-147

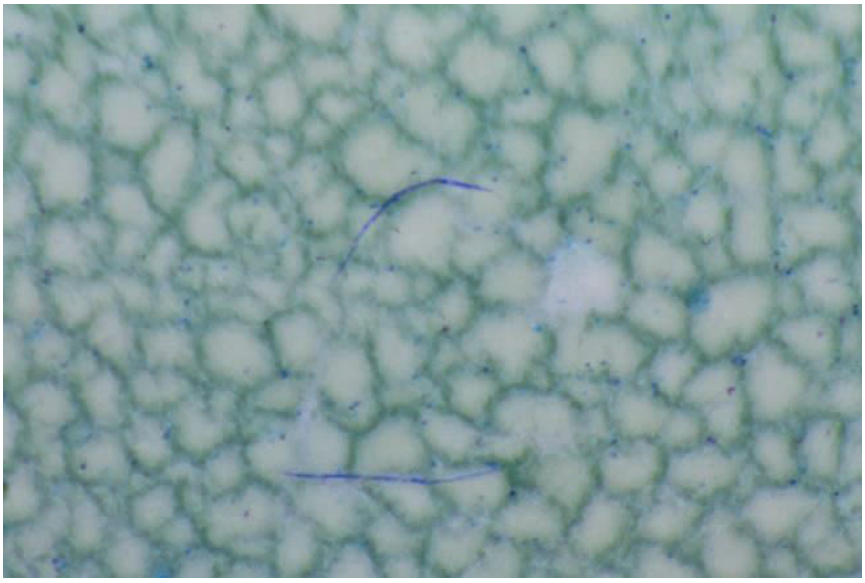

Figure 1. Image captured with the AiDx Assist showing *Loa loa* microfilaria (Image provided by AiDx Medical).

Table 2. summary of diagnostic performance of the Schistoscope and AiDx Assist for schistosomiasis and other helminthiases reported within this thesis.

Device/Validation year/ Chapter #	Setting	Parasite target	Sample type	Device Mode	Reference test	Sensitivity % (95% CI)	Specificity % (95% CI)
Schistoscope/2022/3	Nigeria	*S. haematobium*	Fresh urine	Semi-automated Schistoscope	Conventional microscopy (UF)	80.1 (73.2–86.0)	95.3 (92.4–97.4)
				Fully-automated Schistoscope		87.3 (81.3–92.0)	48.9 (43.3–55.0)
Schistoscope/2022/4	Netherlands	*S. haematobium*	Fresh urine	Fully-automated Schistoscope	Semi-automated Schistoscope	93.75 (-)	93.94 (-)
Schistoscope/2024/5	Gabon	*S. haematobium*	Fresh urine	Fully-automated Schistoscope	Conventional microscopy (UF) real time-PCR/UCP-LF CAA	83.1 (75.5-89.1)	77.0 (70.7-82.5)
						62.9 (55.8-69.6)	78.8 (71.0-85.3)
	Gabon		Banked slides	Fully-automated Schistoscope	Conventional microscopy (UF) real-time PCR/UCP-LF CAA	96.3 (92.6-98.5)	86.8 (80.5-91.6)
						78.0 (72.3-83.0)	90.9 (83.4-95.8)
AiDx Assist/2024/6	Nigeria	*S. mansoni*	Fresh stool	Semi-automated AiDx Assist	Conventional microscopy (KK)	86.8 (80.2-91.9)	81.4 (75.8-86.2)
				Fully-automated AiDx Assist		56.9 (48.4-65.2)	86.8 (80.2-91.9)
		S. haematobium	Fresh urine	Semi-automated AiDx Assist	Conventional microscopy (UF)	94.6 (91.1-97.0)	90.6 (84.4-94.9)
				Fully-automated AiDx Assist		91.9 (87.9-94.9)	91.3 (85.3- 95.4)
		T. trichiura	Fresh stool		-		
		A.lumbricoides	Fresh stool		-		
AiDx Assist/2023/7	Gabon	*Loa loa*	Blood	Semi-automated AiDx Assist	Conventional microscopy	93.8 (79.2-99.2)	99.4 (98.2-99.9)
				Fully-automated AiDx Assist	Conventional microscopy	96.9 (83.8-99.9)	76.8 (72.7-80.5)

UF= urine filtration, KK=Kato-Katz

Therefore, the capabilities of the Schistoscope and the AiDx Assist goes beyond analysing urine or stool samples and could be further explored for blood samples and potentially even be extended to the diagnosis of non-infectious diseases. On the other hand, with these prototypes challenges were encountered in effectively identifying relatively small parasites, such as *Entamoeba coli* cysts in fresh stool smears and *P. falciparum* trophozoites in Giemsa thick blood smears. To address this issue, more robust optical systems are needed. Nevertheless, this versatility renders the Schistoscope and the AiDx Assist customizable and promising for screening multiple parasites in endemic field settings. Other researchers have demonstrated or validated DODDs for the detection of multiple parasitic infections [31, 35, 39-41].

Furthermore, DODDs are currently being exploited by other companies and research groups for diagnostic application on infectious as well as non-infectious disease. For example the group of SpotLab (https://spotlab.ai/) have developed platforms for haematology analysis, differential cell counting in cerebrospinal fluid for meningitis diagnosis in new born, detection and quantification of lung lesions in COVID-19 patients. The group of enaiblers (https://www.enaiblers.com/team) has recently developed a platform to support monitoring of NTD control programs in resource limited settings. Other groups are currently applying DODDs for the detection and characterisation of non-infectious diseases such as cancer [42] and cardiovascular disease (https://medisimaging.com/, https://www.digitaldiagnostics.com/). However, the applicability of these systems in poor resource settings needs to be further explored.

Moving beyond test performance and readiness for LMIC: Economic considerations and accessibility (A Cost-Benefit Analysis and Stakeholder Engagement Perspective)

The Schistoscope and AiDx Assist have shown promising diagnostic performance for schistosomiasis and STH infections across various endemic settings. However, there is still need for a comprehensive cost-benefit analysis to support their implementation and integration into large-scale mapping and impact assessment surveys for national control programs in LIMCs, along with digital health initiatives [43]. This analysis should consider factors concerning the laboratory and case management efficiency gains inherent to the devices' based on the WHO's Target Product Profile (TPP). These factors include the capital cost per device, throughput, cost per test, analysis time per test run, personnel requirements for sample preparation/analysis, quality assurance needs, infrastructure requirements, consumables, repair feasibility, and associated costs compared to conventional microscopy. Also, the impact of DODDs on compliance to MDA programs and the costs associated with unnecessary rounds of annual MDA of praziquantel should be considered. For example, feedback from end-users, including laboratory technicians, community health workers, and final year medical students, regarding both the Schistoscope and AiDx Assist has indicated increased awareness and ease of use with minimal training [16, 44], potentially enhancing capacity building for implementation in LIMCs. Additionally, using the AiDx Assist for on-site analysis of urine samples in communities has led to improved compliance with praziquantel treatment (Personal communication Temitope E. Agbana). This improvement is attributed to dispelling local superstitions surrounding sample

collection for sorcery, due to on-site sample collection and processing, which in turn has augmented participation in surveys and subsequent treatments.

Furthermore, while the WHO TPP does not specify the minimum capital cost per device required for control and elimination of these diseases, several research efforts have developed DODDs ranging in price from US$465 to US$5000 [31-33, 41]. The current prototypes of the Schistoscope and AiDx Assist cost in all approximately US$1000 and US$2000 respectively. This is significantly lower than the AI-based digital microscope developed by Wards et al costing ~US$5000. Although comparable to the Newton Nm1 microscope (commercially available) in terms of price ranging from US$465 to US$1000 [45] depending on the series, the Schistoscope and AiDx Assist offer integrated AI for automated detection, enhancing their diagnostic capabilities. Also, upon mass production of these devices for commercialisation, the price would be expected to decrease.

In field experiences with DODDs

The operation of the Schistoscope encountered several challenges during its deployment, ranging from damages due to transportation to technical malfunctions within the equipment. These challenges included problems with auto-focus, defective membrane detection algorithms, loose screws during long transportation on bumpy roads, and vibrations from nearby instruments such as centrifuge affecting image quality. Additionally, lengthy slide capture and analysis time were noted compared to conventional microscopy which was dependent on the size of the membrane used as well as the infection intensity of the sample. Despite these obstacles, practical solutions were identified, such as implementing robust packaging for transportation, conducting regular maintenance checks, exploring software enhancements to improve efficiency and programming sample analysis to stop when a threshold of parasite count is reached. Addressing these challenges and implementing recommended solutions will be crucial for optimizing the performance and usability of the Schistoscope in field settings, ultimately facilitating more accurate and efficient sample analysis.

Advancements of AI-powered DODDs for human helminthiasis diagnosis: from development to field application

Important advancements have been made in the clinical sector with DODDs for automated malaria parasite detection [46-52]. Comparatively, the automated optical detection of human stool and urine parasites such as schistosomes and STHs was still in its early stages and has now gained momentum. With advancing technology, optical devices could be developed to have a fully functioning computing system, with the potential to accommodate specific features such as imaging sensors, Global Positioning System (GPS) navigation, internet access, data storage, and high processing power, each with added values for different stakeholders in the health system. This would facilitate data generation and distribution making it useful for mapping of *Schistosoma* spp. and other NTDs [53], and impact assessment of MDA programs.

Several DODDs have been developed for the diagnosis of schistosomiasis and STHs [54-59]. While most prototypes require human expertise for image interpretation before conclusive decisions could be reached (semi-automation), the fully-automated devices that's is, with integrated AI models could potentially mitigate the chances of human error and reduce the

need for human training. Complete automation of such devices makes them comparatively easy to use and facilitates multitasking during sample analysis. In this thesis we carried out validation of the AiDx Assist for the detection and quantification of stool parasites. Through digital imaging we also demonstrated the possibility of detecting multiple parasite species in stool (chapter 6). The presence of stool artifacts was found to interfere with AI detection. Some researchers have attempted to customised sample processing method for their devices in an effort to resolve this challenge [30, 60, 61]. However, maintaining the same sample workflow for DODDs as conventional microscopy was observed to not disrupt the workflow of laboratory technicians for processing and may facilitate acceptance in field settings. Also, certain sample processing methods developed by other researchers require high laboratory infrastructure, resenting a constraint on the application of the device in resource-limited settings. Additionally, some of these methods require further validation.

A standardised approach to guide the development of DODD technology for NTDs towards field readiness and application is needed. The proposed modified TRL scale presented in the introduction of this thesis could be a possible solution towards this goal. This scale highlights aspects including small scale and in-field validation of DODDs as well stakeholder engagement in the research and development of these devices to meet required recommendations and context specific needs respectively [62]. Engaging stakeholders provides further information on desired products and context specific needs, that in turn accelerate its readiness, acceptability and enable local productivity.

Conclusion

The development and validation of innovative diagnostic tools such as the Schistoscope and AiDx Assist represent significant strides towards addressing the pressing need for simple, inexpensive, portable, and robust (semi-) automated diagnostic solutions for NTDs like schistosomiasis, STHs and other helminthiases such as filariasis, where conventional diagnostic methods often face limitations. Through preclinical and extensive field validation in comparison with conventional microscopy and other reference tests, the Schistoscope and AiDx Assist have demonstrated promising diagnostic performance in detecting these diseases. While both devices exhibit certain strengths and limitations, particularly in terms of sensitivity, specificity, and parasite quantification, they represent valuable additions to the diagnostic toolkit for NTDs. Moving forward, it is imperative to conduct comprehensive cost-benefit analyses to support the integration of these diagnostic tools into large-scale mapping and impact assessment surveys for national control programs in LMICs. Engaging stakeholders, including developers, end-users, healthcare managers, and policymakers, is essential to ensure that these tools are not only affordable and accessible but also effectively address the specific needs and challenges of endemic regions. Moreover, ongoing research and development efforts should focus on refining the performance and usability of these devices, leveraging advancements in AI and digital imaging technology. Standardized approaches, such as the modified TRL scale proposed in introduction chapter, can guide the development of digital diagnostic technologies for NTDs, facilitating their readiness and application in field settings. Ultimately, the successful implementation of these innovative digital diagnostic tools has the potential to revolutionize

disease surveillance, control, and treatment efforts, ultimately contributing to the control and advancement of NTDs towards elimination in endemic settings.

References

1. Chesnais CB, Vlaminck J, Kunyu-Shako B, Pion SD, Awaca-Uvon NP, Weil GJ, et al. Measurement of Circulating Filarial Antigen Levels in Human Blood with a Point-of-Care Test Strip and a Portable Spectrodensitometer. Am J Trop Med Hyg. 2016;94(6):1324-9.
2. Krauth SJ, Greter H, Stete K, Coulibaly JT, Traoré SI, Ngandolo BNR, et al. All that is blood is not schistosomiasis: experiences with reagent strip testing for urogenital schistosomiasis with special consideration to very-low prevalence settings. Parasites & Vectors. 2015;8(1):584.
3. Greter H, Krauth SJ, Ngandolo BN, Alfaroukh IO, Zinsstag J, Utzinger J. Validation of a Point-of-Care Circulating Cathodic Antigen Urine Cassette Test for Schistosoma mansoni Diagnosis in the Sahel, and Potential Cross-Reaction in Pregnancy. Am J Trop Med Hyg. 2016;94(2):361-4.
4. Mewamba EM, Tiofack AAZ, Kamdem CN, Ngassam RIK, Mbagnia MCT, Nyangiri O, et al. Field assessment in Cameroon of a reader of POC-CCA lateral flow strips for the quantification of Schistosoma mansoni circulating cathodic antigen in urine. PLoS Neglected Tropical Diseases. 2021;15(7):e0009569.
5. Tchuem Tchuenté L-A, Kueté Fouodo CJ, Kamwa Ngassam RI, Sumo L, Dongmo Noumedem C, Kenfack CM, et al. Evaluation of Circulating Cathodic Antigen (CCA) Urine-Tests for Diagnosis of Schistosoma mansoni Infection in Cameroon. PLOS Neglected Tropical Diseases. 2012;6(7):e1758.
6. Casacuberta M, Kinunghi S, Vennervald BJ, Olsen A. Evaluation and optimization of the Circulating Cathodic Antigen (POC-CCA) cassette test for detecting Schistosoma mansoni infection by using image analysis in school children in Mwanza Region, Tanzania. Parasite Epidemiology and Control. 2016;1(2):105-15.
7. Siqueira LMV, Couto FFB, Taboada D, Oliveira ÁAd, Carneiro NFdF, Oliveira E, et al. Performance of POC-CCA® in diagnosis of schistosomiasis mansoni in individuals with low parasite burden. Revista da Sociedade Brasileira de Medicina Tropical. 2016;49.
8. Straily A, Kavere EA, Wanja D, Wiegand RE, Montgomery SP, Mwaki A, et al. Evaluation of the Point-of-Care Circulating Cathodic Antigen Assay for Monitoring Mass Drug Administration in a Schistosoma mansoni Control Program in Western Kenya. Am J Trop Med Hyg. 2021;106(1):303-11.
9. Sanneh B, Joof E, Sanyang AM, Renneker K, Camara Y, Sey AP, et al. Field evaluation of a schistosome circulating cathodic antigen rapid test kit at point-of-care for mapping of schistosomiasis endemic districts in The Gambia. PLOS ONE. 2017;12(8):e0182003.
10. Ochodo EA, Gopalakrishna G, Spek B, Reitsma JB, Van Lieshout L, Polman K, et al. Circulating antigen tests and urine reagent strips for diagnosis of active schistosomiasis in endemic areas. Cochrane Database of Systematic Reviews. 2015(3).
11. Coulibaly JT, N'gbesso YK, Knopp S, N'guessan NA, Silué KD, van Dam GJ, et al. Accuracy of urine circulating cathodic antigen test for the diagnosis of Schistosoma mansoni in preschool-aged children before and after treatment. PLoS neglected tropical diseases. 2013;7(3):e2109.
12. Kamgno J, Pion SD, Chesnais CB, Bakalar MH, D'Ambrosio MV, Mackenzie CD, et al. A Test-and-Not-Treat Strategy for Onchocerciasis in Loa loa-Endemic Areas. N Engl J Med. 2017;377(21):2044-52.
13. Mbong Ngwese M, Prince Manouana G, Nguema Moure PA, Ramharter M, Esen M, Adégnika AA. Diagnostic Techniques of Soil-Transmitted Helminths: Impact on

Control Measures. Trop Med Infect Dis. 2020;5(2).
14. Söderberg I, Calissendorff B, Elofsson S, Knave B, Nyman K. Investigation of visual strain experienced by microscope operators at an electronics plant. Applied ergonomics. 1983;14(4):297-305.
15. Ngakhushi R, Kaiti R, Bhattarai S, Shrestha G. Prevalence of myopia and binocular vision dysfunctions in microscopists. Int Eye Sci. 2018;18(7):1180-3.
16. Onasanya A, Bengtson M, Agbana T, Oladunni O, van Engelen J, Oladepo O, et al. Towards Inclusive Diagnostics for Neglected Tropical Diseases: User Experience of a New Digital Diagnostic Device in Low-Income Settings. Tropical Medicine and Infectious Disease. 2023;8(3):176.
17. Hoekstra PT, van Dam GJ, van Lieshout L. Context-Specific Procedures for the Diagnosis of Human Schistosomiasis – A Mini Review. Frontiers in Tropical Diseases. 2021;2.
18. Utzinger J, Becker S, Van Lieshout L, Van Dam G, Knopp S. New diagnostic tools in schistosomiasis. Clinical microbiology and infection. 2015;21(6):529-42.
19. Makau-Barasa L, Assefa L, Aderogba M, Bell D, Solomon J, Urude RO, et al. Performance evaluation of the AiDx multi-diagnostic automated microscope for the detection of schistosomiasis in Abuja, Nigeria. Sci Rep. 2023;13(1):14833.
20. Lin L, Dacal E, Díez N, Carmona C, Martin Ramirez A, Barón Argos L, et al. Edge Artificial Intelligence (AI) for real-time automatic quantification of filariasis in mobile microscopy. PLOS Neglected Tropical Diseases. 2024;18(4):e0012117.
21. Wiegand RE, Secor WE, Fleming FM, French MD, King CH, Deol AK, et al. Associations between infection intensity categories and morbidity prevalence in school-age children are much stronger for Schistosoma haematobium than for S. mansoni. PLoS Negl Trop Dis. 2021;15(5):e0009444.
22. Abudho BO, Guyah B, Ondigo BN, Ndombi EM, Ireri E, Carter JM, et al. Evaluation of morbidity in Schistosoma mansoni-positive primary and secondary school children after four years of mass drug administration of praziquantel in western Kenya. Infect Dis Poverty. 2020;9(1):67.
23. World Health Organisation. Soil-transmitted helminth infections fact sheeet World Health Organisation,; 2023 [Available from: https://www.who.int/news-room/fact-sheets/detail/soil-transmitted-helminth-infections.
24. Kabatende J, Mugisha M, Ntirenganya L, Barry A, Ruberanziza E, Mbonigaba JB, et al. Prevalence, Intensity, and Correlates of Soil-Transmitted Helminth Infections among School Children after a Decade of Preventive Chemotherapy in Western Rwanda. Pathogens. 2020;9(12).
25. World Health Organization. Prevention and control of schistosomiasis and soil-transmitted helminthiasis: report of a WHO expert committee 2002 [Available from: https://apps.who.int/iris/handle/10665/42588.
26. Gray DJ, Ross AG, Li YS, McManus DP. Diagnosis and management of schistosomiasis. Bmj. 2011;342:d2651.
27. Keiser J. Present drugs and future perspectives in treating soil-transmitted helminthiasis. Frontiers in Tropical Diseases. 2023;4:1282725.
28. Van GY, Onasanya A, van Engelen J, Oladepo O, Diehl JC. Improving Access to Diagnostics for Schistosomiasis Case Management in Oyo State, Nigeria: Barriers and Opportunities. Diagnostics (Basel). 2020;10(5).
29. Onasanya AA. Designing for Neglected Tropical Diseases: Co-creating digital diagnostic devices for Low-Resource Settings: Delft University Of Technology 2023.
30. Ayana M, Vlaminck J, Cools P, Ame S, Albonico M, Dana D, et al. Modification and optimization of the FECPAKG2 protocol for the detection and quantification of soil-transmitted helminth eggs in human stool. PLOS Neglected Tropical Diseases. 2018;12:e0006655.
31. Bogoch II, Andrews JR, Speich B, Ame SM, Ali SM, Stothard JR, et al. Quantitative evaluation of a handheld light microscope for field diagnosis of soil-transmitted helminth infection. The American journal of tropical medicine and hygiene. 2014;91(6):1138.

32. Boonyong S, Hunnangkul S, Vijit S, Wattano S, Tantayapirak P, Loymek S, et al. High-throughput detection of parasites and ova in stool using the fully automatic digital feces analyzer, orienter model fa280. Parasites & Vectors. 2024;17(1):13.
33. Dacal E, Bermejo-Peláez D, Lin L, Álamo E, Cuadrado D, Martínez Á, et al. Mobile microscopy and telemedicine platform assisted by deep learning for the quantification of Trichuris trichiura infection. PLoS Negl Trop Dis. 2021;15(9):e0009677.
34. Sangameswaran R. MAIScope: A low-cost portable microscope with built-in vision AI to automate microscopic diagnosis of diseases in remote rural settings. arXiv preprint arXiv:220806114. 2022.
35. Yang A, Bakhtari N, Langdon-Embry L, Redwood E, Grandjean Lapierre S, Rakotomanga P, et al. Kankanet: An artificial neural network-based object detection smartphone application and mobile microscope as a point-of-care diagnostic aid for soil-transmitted helminthiases. PLoS Negl Trop Dis. 2019;13(8):e0007577.
36. Oyibo P, Jujjavarapu S, Meulah B, Agbana T, Braakman I, van Diepen A, et al. Schistoscope: An Automated Microscope with Artificial Intelligence for Detection of Schistosoma haematobium Eggs in Resource-Limited Settings. Micromachines (Basel). 2022;13(5).
37. Kamgno J, Nana-Djeunga HC, Pion SD, Chesnais CB, Klion AD, Mackenzie CD, et al. Operationalization of the test and not treat strategy to accelerate the elimination of onchocerciasis and lymphatic filariasis in Central Africa. International Health. 2018;10(suppl_1):i49-i53.
38. Hasanah A, Nurdian Y. Use of Loa Scope as a Proper Identification and Treatment in Loiasis Disease. 2017.
39. Lundin J, Suutala A, Holmström O, Henriksson S, Valkamo S, Kaingu H, et al. Diagnosis of soil-transmitted helminth infections with digital mobile microscopy and artificial intelligence in a resource-limited setting. PLOS Neglected Tropical Diseases. 2024;18(4):e0012041.
40. Ward P, Dahlberg P, Lagatie O, Larsson J, Tynong A, Vlaminck J, et al. Affordable artificial intelligence-based digital pathology for neglected tropical diseases: A proof-of-concept for the detection of soil-transmitted helminths and Schistosoma mansoni eggs in Kato-Katz stool thick smears. PLoS Neglected Tropical Diseases. 2022;16(6):e0010500.
41. Holmström O, Linder N, Ngasala B, Mårtensson A, Linder E, Lundin M, et al. Point-of-care mobile digital microscopy and deep learning for the detection of soil-transmitted helminths and Schistosoma haematobium. Global health action. 2017;10(sup3):1337325.
42. Sufyan M, Shokat Z, Ashfaq UA. Artificial intelligence in cancer diagnosis and therapy: Current status and future perspective. Computers in Biology and Medicine. 2023;165:107356.
43. Ho J, Ahlers S, Stratman C, Aridor O, Pantanowitz L, Fine J, et al. Can Digital Pathology Result In Cost Savings? A Financial Projection For Digital Pathology Implementation At A Large Integrated Health Care Organization. Journal of pathology informatics. 2014;5:33.
44. Bengtson M, Onasanya A, Oyibo P, Meulah B, Samenjo KT, Braakman I, et al., editors. A usability study of an innovative optical device for the diagnosis of schistosomiasis in Nigeria. 2022 IEEE Global Humanitarian Technology Conference (GHTC); 2022: IEEE.
45. Meulah B, Bengtson M, Van Lieshout L, Hokke CH, Kreidenweiss A, Diehl J-C, et al. A review on innovative optical devices for the diagnosis of human soil-transmitted helminthiasis and schistosomiasis: From research and development to commercialisation. Parasitology. 2022:1-41.
46. Agbana TE, Diehl JC, van Pul F, Khan SM, Patlan V, Verhaegen M, et al. Imaging & identification of malaria parasites using cellphone microscope with a ball lens. PLoS One. 2018;13(10):e0205020.
47. Coulibaly JT, N'Goran EK, Keiser J, Ouattara M, Bogoch II, Andrews JR, et al. Evaluation of Malaria Diagnoses Using a Handheld Light Microscope in a Community-Based Setting in Rural Côte d'Ivoire. The American Journal of Tropical Medicine and Hygiene. 2016;95(4):831-4.
48. de Melo GC, Netto RLA, Mwangi VI, Salazar YEAR, de Souza Sampaio V, Monteiro WM, et al. Performance of a sensitive haemozoin-based malaria

diagnostic test validated for vivax malaria diagnosis in Brazilian Amazon. Malaria Journal. 2021;20(1).
49. Frean J. Improving quantitation of malaria parasite burden with digital image analysis. Transactions of the Royal Society of Tropical Medicine and Hygiene. 2008;102(11):1062-3.
50. Hashimoto M, Yatsushiro S, Yamamura S, Tanaka M, Sakamoto H, Ido Y, et al. Hydrophilic-treated plastic plates for wide-range analysis of Giemsa-stained red blood cells and automated Plasmodium infection rate counting. Malaria Journal. 2017;16(1).
51. Kaewkamnerd S, Uthaipibull C, Intarapanich A, Pannarut M, Chaotheing S, Tongsima S. An automatic device for detection and classification of malaria parasite species in thick blood film. BMC Bioinformatics. 2012;13(S17).
52. Kumar R, Verma AK, Shrivas S, Thota P, Singh MP, Rajasubramaniam S, et al. First successful field evaluation of new, one-minute haemozoin-based malaria diagnostic device. EClinicalMedicine. 2020;22.
53. Tilahun B, Gashu KD, Mekonnen ZA, Endehabtu BF, Angaw DA. Mapping the role of digital health technologies in the case detection, management, and treatment outcomes of neglected tropical diseases: a scoping review. Trop Med Health. 2021;49(1):17.
54. Agbana TE, Nijman P, Hoeber M, van Grootheest D, van Diepen A, van Lieshout L, et al. Detection of Schistosoma haematobium using lensless imaging and flow cytometry, a proof of principle study. Optical Diagnostics and Sensing XX: Toward Point-of-Care Diagnostics2020.
55. Armstrong M, Harris AR, D'Ambrosio MV, Coulibaly JT, Essien-Baidoo S, Ephraim RKD, et al. Point-of-Care Sample Preparation and Automated Quantitative Detection of Schistosoma haematobium Using Mobile Phone Microscopy. American Journal of Tropical Medicine and Hygiene. 2022;106(5):1442-9.
56. Dacal E, Bermejo-Peláez D, Lin L, Álamo E, Cuadrado D, Martínez Á, et al. Mobile microscopy and telemedicine platform assisted by deep learning for the quantification of Trichuris trichiura infection. PLOS Neglected Tropical Diseases. 2021;15(9):e0009677.
57. Holmstrom O, Linder N, Ngasala B, Martensson A, Linder E, Lundin M, et al. Point-of-care mobile digital microscopy and deep learning for the detection of soil-transmitted helminths and Schistosoma haematobium. Glob Health Action. 2017;10(sup3):1337325.
58. Linder E, Grote A, Varjo S, Linder N, Lebbad M, Lundin M, et al. On-chip imaging of Schistosoma haematobium eggs in urine for diagnosis by computer vision. PLOS Neglected Tropical Diseases. 2013;7(12):e2547.
59. Oyibo P, Jujjavarapu S, Meulah B, Agbana T, Braakman I, van Diepen A, et al. Schistoscope: An Automated Microscope with Artificial Intelligence for Detection of Schistosoma haematobium Eggs in Resource-Limited Settings. Micromachines. 2022;13(5).
60. Sukas S, Van Dorst B, Kryj A, Lagatie O, De Malsche W, Stuyver LJ. Development of a Lab-on-a-Disk Platform with Digital Imaging for Identification and Counting of Parasite Eggs in Human and Animal Stool. Micromachines. 2019;10(12):852.
61. Levecke B, Behnke JM, Ajjampur SS, Albonico M, Ame SM, Charlier J, et al. A comparison of the sensitivity and fecal egg counts of the McMaster egg counting and Kato-Katz thick smear methods for soil-transmitted helminths. PLoS Neglected Tropical Diseases. 2011;5(6):e1201.
62. Levecke B, Coffeng LE, Hanna C, Pullan RL, Gass KM. Assessment of the required performance and the development of corresponding program decision rules for neglected tropical diseases diagnostic tests: Monitoring and evaluation of soil-transmitted helminthiasis control programs as a case study. PLoS Neglected Tropical Diseases. 2021;15(9):e0009740.

Appendix

Summary

Neglected tropical diseases (NTDs) is a diverse range of infections primarily found in tropical and subtropical regions, and despite their significant impact on health and socio-economic well-being, NTDs have historically received less attention compared to other infectious diseases. The World Health Organization (WHO) has recognized the urgency of addressing NTDs and has developed a roadmap to combat them. Timely diagnosis is crucial for effective management and control of the debilitating life-long disease associated with these infections. Among the major NTDs, schistosomiasis, soil-transmitted helminth (STH) and filariasis are particularly prevalent, causing widespread morbidity with a substantial public health burden, especially in low- and middle-income countries (LMICs). Schistosomiasis, transmitted through contact with contaminated water, can lead to severe urogenital and intestinal complications. Similarly, STH infections, acquired through ingestion of parasite eggs or skin penetration by parasite larvae, contribute to anaemia, malnutrition, and developmental impairments, particularly in children. Lymphatic filariasis and onchocerciasis need proper diagnosis, not only for accurate case management, but also to determine co-infections, specifically with *Loa loa*. Addressing the burden of these diseases requires concerted efforts to enhance diagnosis, treatment, and prevention strategies, ultimately promoting health equity and improving the lives of millions worldwide.

In LMICs, the diagnosis of NTDs such as schistosomiasis, STH and several types of filariasis predominantly relies on conventional microscopy, which involves identifying and quantifying parasite-derived products in urine, stool and blood samples. However, this method is labour-intensive, requires skilled personnel, and often lacks the necessary infrastructure in resource-limited settings. Alternative diagnostic approaches for microscopy include urine-based point-of-care tests (POC-CCA) for detecting circulating cathodic antigens, and up-converting particle lateral flow (UCP-LF) assays for detecting circulating anodic antigens (CAA) in urine and serum for schistosomiasis and blood circulating antigen test for lymphatic filariasis. Nucleic acid amplification tests (NAATs) have also been utilized for detecting parasite-specific nucleic acid sequences in urine and serum for both schistosomiasis and STH infections, even though primarily in research settings in LIMCs. While these alternative methods offer higher accuracy, they are still undergoing validation and standardization for routine clinical use in LMICs. Additionally, they require trained personnel and for most of these tests, a well-equipped laboratory infrastructure posing challenges for widespread implementation in resource-limited settings. Further efforts are needed to validate and standardize these diagnostic techniques to improve their accessibility and utility in field settings.

Innovative digital optical diagnostic devices (DODDs) have been developed to automatically detect parasites in clinical samples, utilizing technical modifications of smartphone optical systems or off-the-shelf optical components. These devices leverage the integrated sensors and processing power of smartphones, as well as simple computer units like Raspberry Pi and Jetson Nano, to run artificial intelligence (AI) algorithms for image analysis. While promising for automated medical diagnosis in endemic settings, these devices are currently insufficiently available for LMICs. Despite their potential, the readiness of DODDs for field

applications in LMICs remains limited. A modified version of the technology readiness level (TRL) scale, incorporating the WHO's Target Product Profile (TPP) and context-specific needs, revealed that the majority of DODDs are not yet ready for field deployment. Meeting the WHO TPP, particularly during field validation stages (TRL 5, 6, and 7), was found to be a significant bottleneck, highlighting the need for further research, development, and validation studies in diverse endemic settings. Two notable AI-powered DODDs, the Schistoscope and AiDx Assist devices, initiatives of the Technical University of Delft, have been developed for diagnosing schistosomiasis, STH infections and other parasitic infections. Both devices feature custom-designed optical bright-field illumination and movement systems, differing primarily in their electronic and computing modules, including the AI framework used. In this thesis preclinical and in-field validations of these devices have been conducted across various iterations of their development in different settings.

The primary objective of this thesis was to, through research and development, validate the diagnostic performance of the Schistoscope and AiDx Assist as morphology (egg and/or larvae)-based detection methods for schistosomiasis and STHs and loiasis through preclinical and in-field studies across different endemic and/or settings. **In Chapter 1**, an overview of the thesis is provided, highlighting the challenges encountered in the research and development leading to the commercialization of DODDs as morphology-based parasite detection methods. **Chapter 2** focuses on demonstrating the context-specific needs for different diagnostic methods, emphasizing the limitations of POC-CCA and haematuria rapid tests in diagnosing schistosomiasis in a setting (community in Tanzania) co-endemic with *S. haematobium* and *S. mansoni* infections, and the need for egg-based detection methods to accurately assess the prevalence of *Schistosoma* spp in a specific endemic setting.

Chapter 3 evaluated the Schistoscope as both a semi-automated and fully-automated digital microscope with AI algorithms, for detecting and quantifying *S. haematobium* eggs in urine in Nigeria, comparing its performance to conventional microscopy. The sensitivity of the semi- and fully -automated mode of the Schistoscope was found to be comparable to that of conventional microscopy. However, the specificity of the fully-automated Schistoscope was significantly inferior to conventional microscopy. The fully-automated Schistoscope also underestimating egg count associated to the AI algorithm, specifically in the high egg count excretion range. In **chapter 4**, the enhancement of the AI algorithm of the Schistoscope through a two-stage automated diagnosis framework for detecting and quantifying *S. haematobium* eggs is described and validated using microscopy images obtained from low-resource settings. Improved performance in terms of sensitivity and specificity was achieved requiring thorough validation in a field setting. **Chapter 5** presented a follow-up validation of the Schistoscope in Lambaréné, Gabon, comparing its performance in detecting and quantifying *S. haematobium* eggs in fresh urine (as well as banked filters) to conventional microscopy and a more sensitive composite reference standard including a urine-based real-time PCR and the UCP-LF-CAA test.

Chapter 6 validated the AiDx Assist digital microscope as a diagnostic tool for *Schistosoma* spp. in urine and stool while exploring its potential for detecting other helminths in stool under field conditions in Nigeria. The AiDx Assist was found to meet the WHO TPP in terms of diagnostic performance for *S. haematobium.* However, for the detection of *S. mansoni* eggs, the

performance was found to be modest and would require further optimisation. **Chapter 7** summarized and discussed the results within this thesis including outcome from our unpublished data of the AiDx Assist performance for the detection and quantification of *Loa loa* microfilaria on 514 Giemsa thick blood smears collected from the field settings. We also highlighted the progress made in the development of DODDs beyond diagnostic performance, considering context-specific needs, and exploring the prospects of DODDs for diagnosing schistosomiasis, STHs and filariasis in endemic settings as well as its usability in diagnosing other infectious and non-infectious diseases.

The Schistoscope and AiDx Assist represent important advancements in NTD diagnosis, offering simple, portable solutions for diseases like schistosomiasis, STHs and filariasis where traditional methods fall short. Through rigorous validation studies, both devices have shown promising performance compared to conventional microscopy. While they have strengths and limitations, their integration into national control programs in LMICs could potentially revolutionize disease surveillance and treatment efforts. Future efforts should focus on conducting thorough cost-benefit analyses to support their integration into large-scale mapping and impact assessment surveys for national control programs in LMICs. Furthermore, continued research and development should focus on improving performance and usability, guided by standardized approaches like the modified TRL scale, facilitating their readiness and deployment in field settings. Ultimately, successful implementation of these tools could greatly impact NTD control and elimination efforts in endemic areas.

Nederlandse samenvatting

Verwaarloosde tropische ziekten, bekend onder de afkorting NTD's (Neglected Tropical Diseases), vormen een groep van ziekten die hoofdzakelijk in lage- en middeninkomenslanden (vaak afgekort als LMIC's, low and middle income countries) voorkomen. NTD's omvatten vooral infectieziekten en de meesten komen praktisch uitsluitend voor in tropische en subtropische gebieden, onder meer omdat ze geassocieerd worden met armoede en slechte hygiënische omstandigheden, maar ook omdat veel van deze infecties door vectoren (meestal insecten) worden overgebracht. Ondanks hun significante impact op de gezondheid en het sociaaleconomisch welzijn van de aangedane populatie, hebben NTD's historisch gezien altijd minder aandacht gekregen dan andere belangrijke infectieziekten, zoals bijvoorbeeld malaria, tuberculose en HIV. De WHO (de wereldgezondheidsorganisatie van de Verenigde Naties) erkent de urgentie van het bestrijden van NTD's en zij hebben een routekaart ontwikkeld met aanwijzingen hoe de bestrijding van NTD's aan te pakken. Daarin wordt ook aangegeven dat tijdige diagnose cruciaal is voor een effectieve behandeling en dat daarmee langdurige fysieke schade, die veelal met deze chronische aandoeningen gepaard gaat, voorkomen kan worden. Goede diagnostiek is ook van belang voor het in kaart brengen van de prevalentie en de verspreiding van deze infecties alsook voor het monitoren van bestrijdingsmaatregelen.

De belangrijkste NTD's zijn schistosomiasis, infecties met wormen die via de bodem worden overgebracht (vaak afgekort als STH, soil-transmitted helminths) en filariasis. Deze drie aandoeningen zijn wijdverspreid en leiden tot een aanzienlijke morbiditeit en aantasting van de volksgezondheid, vooral in de afgelegen en armere gebieden van LMIC's. Schistosomiasis, een ziekte die wordt overgedragen door contact met besmet water, kan leiden tot ernstige urogenitale en intestinale complicaties. STH-infecties, die - afhankelijk van de soort - worden opgelopen door het oraal binnenkrijgen van parasieteneieren of door huidpenetratie van parasietenlarven, leveren vooral bij kinderen een belangrijke bijdrage aan bloedarmoede, ondervoeding en ontwikkelingsstoornissen. Ook lymfatische filariasis en onchocerciasis (rivierblindheid) vereisen een juiste diagnose, niet alleen voor het bepalen van de juiste behandelingsstrategie, maar ook om co-infecties, in het bijzonder met *Loa loa*, te kunnen uitsluiten. Om de wereldwijde ongelijkheid in ziektelast aan te pakken en de gezondheidssituatie van miljoenen mensen over de wereld te verbeteren, is het van belang dat er een gecoördineerde strategie wordt uitgerold voor de diagnose, behandeling en preventie van NTDs.

In LMIC's is het stellen van de diagnose bij NTD's zoals schistosomiasis, STH en verschillende soorten filariasis vooral gebaseerd op een klassieke vorm van laboratoriumonderzoek, waarbij parasietenstadia worden geïdentificeerd en gekwantificeerd doormiddel van microscopisch onderzoek van urine-, ontlasting- en bloedmonsters. Deze methode is niet alleen arbeidsintensief, het vereist ook geschoold personeel. Daarnaast ontbreekt het veelal aan de noodzakelijke laboratoriummiddelen en de juiste infrastructuur. Alternatieve diagnostische benaderingen voor microscopie bestaan onder meer uit het toepassen van een urine sneltest genaamd POC-CCA, voor de detectie van het *Schistosoma* circulerend antigen CCA, een laterale flow (UCP-LF CAA) test voor de detectie van het *Schistosoma* circulerend antigen CAA in serum of urine en een bloedcirculatie-antigeentest voor lymfatische filariasis. Daarnaast

wordt er voor schistosomiasis en STH-infecties ook wel gebruik gemaakt van nucleïnezuur-amplificatietests (NAAT's) zoals PCR, waarbij parasiets-specifiek DNA wordt gedetecteerd in urine of ontlasting. Deze testen worden binnen LMIC's voornamelijk toegepast in het kader van wetenschappelijk onderzoek. Ondanks de hogere diagnostische nauwkeurigheid die deze alternatieve methoden bieden, worden ze in LMIC's nog niet routinematig klinisch toegepast. Daarvoor is eerst meer validatieonderzoek en verdere standaardisatie nodig. Daar komt ook bij dat de meeste van deze testen een goede laboratoriuminfrastructuur en specifiek getraind personeel vereist zijn en dat weerhoudt een brede implementatie in gebieden met beperkte economische middelen. Er is meer onderzoek nodig om dit soort diagnostische testen verder te verbeteren en toegankelijker te maken voor toepassingen onder veldomstandigheden in LMIC's.

Vernieuwend is de ontwikkeling van digitale optische diagnostische apparaten (DODD's). Deze apparaten kunnen op geautomatiseerde wijze parasieten in klinische monsters detecteren. Dit kan met behulp van technische aanpassingen van optische systemen van mobiele telefoons of door het gebruik van kant-en-klare optische componenten. Daarbij wordt ook gebruik gemaakt van kunstmatige intelligentie (AI) algoritmen voor beeldanalyse op basis van geïntegreerde sensoren en dataprocessors van mobiele telefoons, in combinatie met eenvoudige computerunits zoals Raspberry Pi en Jetson Nano. Hoewel veel van deze apparaten veelbelovend zijn voor geautomatiseerde medische diagnostiek, zijn ze veelal onvoldoende beschikbaar voor LMIC's. Dit terwijl er daar ook vele potentieel interessante toepassingen lijken te zijn. Door het gebruiken van een aangepaste versie van het technologie gereedheidsniveau (TRL) inschalingssysteem in combinatie met de Target Product Profile (TPP) van de WHO en een inventarisatie van context-specifieke behoeften is aangetoond dat de meerderheid van de DODD's nog niet klaar is voor implementatie in rurale gebieden in LMIC's. De voorwaarden die worden gesteld in de TPPs blijken daarbij een significant struikelblok te vormen, vooral als het gaat om verdere validatie in de praktijk (TRL 5, 6, en 7). Dit geeft tevens aan hoe belangrijk het is dat er meer onderzoek wordt uitgevoerd binnen endemische gebieden naar de ontwikkeling en validatie van dergelijke apparaten.

In de afgelopen jaren zijn er op initiatief van Technische Universiteit Delft twee opmerkelijke AI-gestuurde DODD's ontwikkeld voor het diagnosticeren van schistosomiasis, STH-infecties en andere parasitaire infecties, genaamd de Schistoscope en de AiDx Assist. Beide apparaten zijn voorzien van speciaal ontworpen optische bright-field verlichtingssysteem en bewegingssystemen, maar verschillen in enkele elektronische en computer-gerelateerde componenten, waaronder het gebruikte AI-framework. In dit proefschrift wordt beschreven hoe diverse preklinische en in-het-veld validatie studies zijn uitgevoerd waarbij verschillende ontwikkelingsstadia van deze twee apparaten onder verschillende veldomstandigheden zijn toegepast.

De voornaamste doelstelling van het onderzoek beschreven in dit proefschrift is om de diagnostische prestaties van de Schistoscope en AiDx Assist te valideren als een optische detectiemethode op basis van de morfologie van de eieren en/of larven en daarmee de diagnostiek van schistosomiasis, STH's en loiasis te vereenvoudigen, in zowel preklinische als in-het-veld studies in verschillende endemische gebieden in Afrika. **Hoofdstuk 1** is een algemene inleiding waarbij een overzicht wordt gegeven van het proefschrift. Ook worden de specifieke

uitdagingen belicht die duidelijk zijn geworden bij het ontwikkelen van DODD's en wordt beschreven welke ontwikkeling hebben geleid tot commercialisering van DODD's als morfologie-gebaseerde parasietdetectiemethoden. **Hoofdstuk 2** richt zich op het in kaart brengen van de context-specifieke behoeften voor verschillende diagnostische methoden voor schistosomiasis. Hierbij wordt omschreven wat de diagnostische beperkingen zijn van de urine POC-CCA- en haematurie-sneltesten in een gemeenschap in Tanzania waar twee verschillende *Schistosoma* soorten tegelijkertijd (zowel *S. haematobium* als *S. mansoni*) voorkomen. Ook wordt beargumenteerd dat in specifieke endemische gebieden ei-gebaseerde optische detectiemethoden noodzakelijk zijn om de prevalentie van *Schistosoma* soorten nauwkeuriger in kaart te brengen.

Hoofdstuk 3 beschrijft een in Nigeria uitgevoerde evaluatie waarbij voor het detecteren en kwantificeren van *S. haematobium* eieren in urine de prestatie van de Schistoscope wordt vergeleken met traditionele microscopie. Hierbij is er ook nog een onderscheid gemaakt tussen een semi-geautomatiseerd systeem en een volledig geautomatiseerde digitale microscoop met AI-algoritmen. Uit deze studie blijkt de gevoeligheid van de semi- en volledig-geautomatiseerde modus van de Schistoscope vergelijkbaar met die van traditionele microscopie. Echter, de specificiteit van de volledig-geautomatiseerde Schistoscope was significant lager dan die van traditionele microscopie. Bij de volledig-geautomatiseerde Schistoscope werd bij een hoge ei-uitscheiding ook het aantal eieren in de telling onderschat door het AI-algoritme. In **Hoofdstuk 4** wordt een verbetering van het AI-algoritme van de Schistoscope beschreven door middel van een twee-staps geautomatiseerd diagnosekader voor het detecteren en kwantificeren van *S. haematobium* eieren en deze werd gevalideerd met behulp van microscopieopnames verzameld in een endemische populatie. Het nieuwe AI-algoritme resulteerde in een betere prestatie op het gebied van gevoeligheid en specificiteit, maar verdere validatie in het veld was nog noodzakelijk. Dit wordt vervolgens beschreven in **Hoofdstuk 5**. Hier wordt de prestatie van de Schistoscope beschreven, uitgevoerd in Lambaréné, Gabon, waarbij niet alleen een vergelijking werd gemaakt de traditionele microscopie uitgevoerd op verse urine monsters, maar ook op urinefilters die enkele maanden tot jaren werden opgeslagen. In de vergelijking werd ook gebruik gemaakt van een samengestelde en meer gevoelige referentie waarin additionele diagnostische testen werden meegenomen zoals een urine-gebaseerde real-time PCR en de UCP-LF-CAA test.

Hoofdstuk 6 richt zich op de validatie van de AiDx Assist digitale microscoop als diagnostisch hulpmiddel voor *Schistosoma* spp In urine en ontlasting onder veldomstandigheden in Nigeria, waarbij ook is gekeken naar de diagnostische mogelijkheden voor het detecteren van andere soorten worminfecties. De AiDx Assist bleek te voldoen aan de door de WHO opgestelde TPP met betrekking tot de diagnostische prestatie voor *S. haematobium* ei-detectie in urine. Echter, voor de detectie van *S. mansoni*-eieren in ontlasting bleek de prestatie nog onvoldoende en is een verdere optimalisatie nodig. **Hoofdstuk 7** bespreekt de samenhang van de onderzoeksresultaten binnen dit proefschrift. Ook wordt nog aandacht besteed aan een serie niet gepubliceerde gegevens van de AiDx Assist waarbij onder veldomstandigheden 514 Giemsa gekleurde dikke druppel preparaten zijn geanalyseerd op de kwantitatieve aanwezigheid van *Loa loa* microfilaria. In dit hoofdstuk benadrukken we de vooruitgang die de laatste jaren is geboekt in de ontwikkeling van DODD's. Dit is niet alleen op het gebied van de technische diagnostische karakteristieken. Er wordt namelijk ook steeds meer rekening gehouden met de context-

specifieke behoefte, wat zijn weerslag heeft in de operationele en logistieke eigenschappen van de apparaten. Dit komt de toepasbaarheid van DODD's in LMIC's ten goede, niet alleen voor de diagnostiek van schistosomiasis, STH infecties en filariasis, maar ook van andere infectieuze en niet-infectieuze ziekten.

De ontwikkeling van de Schistoscope en de AiDx Assist laten zien dat er belangrijke vooruitgang is geboekt in de diagnose van NTD's. Deze apparaten bieden een eenvoudig en mobiele oplossing voor het aantonen van ziekten zoals schistosomiasis, STH infecties en filariasis, waar traditionele microscopische methoden veelal tekortschieten. Beide apparaten hebben laten zien onder veldomstandigheden uitstekend te kunnen presteren en ondanks het feit dat ze nog enkele beperkingen hebben, zijn ze in potentie geschikt voor verdere integratie in nationale controleprogramma's voor NTD's in LMIC's. DODD's kunnen relevante veranderingen teweegbrengen in de uitvoering en monitoring van dergelijke programma's. Toekomstig onderzoek zou zich vooral moeten richten op het uitvoeren van grondige kosten-batenanalyses, om daarmee verdere integratie in grootschalige bevolkingsonderzoeken te ondersteunen en de apparaten in het bijzonder voor LMIC's geschikt te maken. Daarnaast zou toekomstig onderzoek aandacht moeten besteden aan een verdere verbetering van de prestatie en toepasbaarheid van de DODD's, maar dit zou zoveel mogelijk moeten gebeuren op een gestandaardiseerde wijze en op geleide van een aangepaste TRL-schaal om daarmee inzetbaarheid onder veldomstandigheden beter te garanderen. Uiteindelijk kan een succesvolle implementatie van DODD's van grote invloed zijn op het efficiënt bestrijden, en zelfs elimineren, van NTD's in endemische gebieden.

Appendix

Curriculum Vitae

Brice Meulah, born on the 3rd of April 1993 in Buea Cameroon and an alumnus of Lycee Bilingual Grammar School Buea, obtained his Bachelor's degree in Biochemistry with a Minor in Medical Laboratory Technology and a Master's degree in Biochemistry and Molecular Biology from the University of Buea in 2015 and 2018 respectively. During his Master research he worked at the Molecular and cell Biology Laboratory (MCBI) where he focused on investigating the genetic polymorphism and identifying the allelic variants of domain 1 of *P. falciparum* AMA-1 gene for its implication in malaria vaccine design. For this research he conducted blood sampling at different hospitals in Buea and performed microscopy and different types of PCR and restriction fragment length polymorphism. After defending his Master thesis and while waiting for a new academic year to begin his PhD research, he continued working at Molecular and Cell Biology Laboratory for a few months as a graduate researcher on elucidating the function of OVOC5284 gene homologues in *Onchocerca ochengi* worm, to identify novel biomarkers using knockdown experiments. He later began a PhD training at the University of Buea where he took a year course on advance methods in Molecular Biology and Functional Genomics. Uncertain about the source of funding for his PhD research, he got offered a year later the opportunity of a new PhD position through Centre de Recherches Médicales de Lambaréné to study at Leiden University Medical Center. He joined the department of Parasitology, Leiden University Center for Infectious Disease as well as Centre de Recherches Médicales de Lambaréné working under the INSPiRED-project: Inclusive diagnosis of poverty related parasitic disease with the aim to test and validate novel diagnostics for NTDs, Schistosomiasis, Filariasis and Malaria in Nigeria and Gabon (http://inspired-diagnostics.info/about/).

List of publications

In this thesis

Meulah, B., Bengtson, M., Van Lieshout, L., Hokke, C. H., Kreidenweiss, A., Diehl, J. C., Adegnika A.A., and Agbana, T. E. (2023). A review on innovative optical devices for the diagnosis of human soil-transmitted helminthiasis and schistosomiasis: from research and development to commercialization. *Parasitology*, *150*(2), 137-149.

Pyuza, J. J., **Meulah, B.**, Hoekstra P. T., Mdende, N., Mvilli E., van Lieshout, L., Hilt, S.T., Corstjens, P.L.A.M., Yazdanbakhsh, M., Msuya, S.E., and van Dam, G.J. (2024). Current status of schistosomiasis in school-aged children in Mwanga district Tanzania; impact of two decades of annual Mass Drug Administration programme. *Parasitology* 1-6.

Meulah, B., Oyibo, P., Bengtson, M., Agbana, T., Lontchi, R. A. L., Adegnika, A. A., Oyibo W., Hokke C. H., Diehl J. C., and van Lieshout, L. (2022). Performance evaluation of the Schistoscope 5.0 for (semi-) automated digital detection and quantification of Schistosoma haematobium eggs in urine: A field-based study in Nigeria. *The American Journal of Tropical Medicine and Hygiene*, *107*(5), 1047.

Oyibo, P., **Meulah, B.**, Bengtson, M., van Lieshout, L., Oyibo, W., Diehl, J. C., Vdovine, G and Agbana, T. E. (2023). Two-stage automated diagnosis framework for urogenital schistosomiasis in microscopy images from low-resource settings. *Journal of Medical Imaging*, *10*(4), 044005-044005.

Meulah, B., Oyibo, P., Hoekstra, P. T., Moure, P. A. N., Maloum, M. N., Laclong-Lontchi, R. A., Honkpehedji Y. J., Bengtson M., Hokke C. H., Corstjens P. L .A .M., Agbana T .E., Diehl, J. C., Adegnika A.A., and van Lieshout, L. (2024). Validation of artificial intelligence-based digital microscopy for automated detection of Schistosoma haematobium eggs in urine in Gabon. *PLoS neglected tropical diseases*, *18*(2), e0011967.

Meulah, B, Hoekstra, P. T., Popoola S., Jujjavarapu, S., Aderogba, M., Fadare, J. O., Omotayo, J. A., Bell, D., Hokke, C. H., van Lieshout, L., Vdovine, G., Diehl, J C., Agbana, T. E., Makau-Barasa, L., Solomon, J. **(**2024). Validation of AiDx Assist device for automated detection of *Schistosoma* eggs in stool and urine samples in Nigeria. *Under review Frontiers. Parasitology.*

Other publications

Oyibo, P., Jujjavarapu, S., **Meulah, B**., Agbana, T. E., Braakman, I., van Diepen, A., Bengtson, M., van Lieshout, L., Oyibo, W., Vdovine, G., and Diehl, J. C. (2022). Schistoscope: an automated microscope with artificial intelligence for detection of Schistosoma haematobium eggs in resource-limited settings. *Micromachines*, *13*(5), 643.

Bengtson, M., Onasanya, A., Oyibo, P., **Meulah, B.**, Samenjo, K.T., Braakman, I., Oyibo, W., Diehl, J. C. (2022, September). A usability study of an innovative optical device for the diagnosis of schistosomiasis in Nigeria. In *2022 IEEE Global Humanitarian Technology Conference (GHTC)* (pp. 17-22). IEEE.

Nguema Moure, P. A., Nzamba Maloum, M., Manouana, G. P., Laclong Lontchi, R. A., Mbong Ngwese, M., Edoa, J. R., Fréjus Zinsou, J., **Meulah, B**., Mahmoudou, S., N'noh Dansou, EM.,

Appendix

Honkpehedji, J. Y., Adegbite, B. R., Agnandji, S. T., Ramharter, M., Lell, B., Borrmann, S., Kremsner, P. G., Dejon-Agobé, J. C., and Adegnika, A. A. (2024). A randomized assessors-blind clinical trial to evaluate the safety and the efficacy of albendazole alone and in combination with mebendazole or pyrantel for the treatment of Trichuris trichiura infection in school-aged children in Lambaréné and surroundings. *Antimicrobial Agents and Chemotherapy*, *68*(5), e01211-23.

Nguema Moure, P. A., Dejon-Agobé, J. C., Laclong Lontchi, R. A., Manouana G. P., Nzamba Maloum, N. M., **Meulah, B**., Mabicka .D C. M., Ngome M. E. N., Kremsner, P. G., and Adegnika, A. A. (accepted 2024). Effect Of Anthelmintic Treatment On The Agreement Between Real-Time Polymerase Chain Reaction (RT-PCR) And Kato-Katz Microscopic Technique In The Diagnosis Of Soil-Transmitted Helminth Infections. *Parasitologia* 4, no. 4: 345-357

Gerstenberg, J., Honkpehedji, Y. J., Dejon-Agobe, J. C., Mahmoudou, S., Recker, M., Mba, R, B., Maloum, M. N., Laclong-Lontchi, R.., Nguema Moure, P. A., **Meulah, B**., Zinsou J. F., Edoa, J. R.., Adegbite, B. R., Ramharter, M., Lell, B., Agnandji, S.T., Kremsner, P. G., Corstjens, P. L. A. M., Hoekstra P. T., van Dam, G. J., Kreidenweiss, A., Adegnika A. A., for the freeBILy Consortium. (2024). Safety and Efficacy of Praziquantel in Pregnant Women Infected with Schistosoma haematobium in Lambaréné, Gabon - Clinical Results from the Randomized, Single-Blinded, Controlled freeBILy-Gabon Trial. *International journal of infectious diseases.* 107253

Acknowledgements

I would like to thank you all who helped and supported me in one way or the other throughout my PhD research.

First of all, I'd like to offer my sincere gratitude to Lisette van Lieshout for the thorough supervision and guidance from the conception of this journey till the end. I have learnt so much from your expertise and ways of executing things. Also, thank you for your dedication and care you extended towards me throughout this period. Thank you, Ron Hokke, for your supervision and guidance throughout my journey. Your pragmatic and rationale way of working smoothened my work-life. Thank you Jan-Carel Diehl for your supervision, guidance and positivity even when situations looked less bright. You brightened up the environment with your humour and enthusiastic energy. Thank you Ayola Akim Adegnika for giving me this opportunity to embark on this PhD research and for the support and supervision in Gabon.

Govert van Dam, it was a pleasure working with you towards the last year of my study. Thank you Tope for the opportunity you gave me to work with AiDx as well as the supervision you provided to see this journey through. Thank you Michel for your supervision and support throughout and for the nice moments you made available to decompressing. Thank you Pytsje for the supervision and support you provided towards the last year of my PhD. Thank you Prosper for your support and friendship throughout this journey. It was a pleasure working with you. Thank you Angela for all the *Schistosoma* eggs you provided during the early phases of my research (pre-validation) and for the questions in the corridor regarding my thesis defence date which fuelled my stamina and zeal to work towards the finish line. Thanks to Wellington Oyibo for the supervision and support in Nigeria.

Thanks to those who welcomed me and showed me around in the Aquarium office (Rike, Miriam) and also to get started in the department (Miriam, Maryam and Pytsje). Gratitude to my office colleagues (Maaika, Noor, Iris, Sanne, Claudia, Michel) for the nice moments shared with chocolates, tea or coffee breaks. Special thanks to Maaika for the extra words of encouragement during my down moments and Claudia for the life cycle drawings. To other colleagues from the department (Diksha, Rike, Jan Pieter, Louis, Nikolas, Stan, Koen, Yoanne, Eunice and Yu): thank you all for the insightful conversations, drinks and cakes shared. Special thanks also goes CERMEL for making the resources available that led to a huge milestone in my research in the field. Thanks to my colleagues at CERMEL especially the parasitology laboratory; Alvyn, Moustapha, Romeo, Mermoz, Carel, Massande and Maximilian for your support in field sampling, laboratory analysis and fun moments we shared. Other CERMEL colleagues, Prof. Lell, Dr. Rafiou, Dr. Ronald, Dr. Dejon, Dr. Josiane, Elsy, Anita, Ulrich, Emma, Ayo, for your support during the field study. Special thanks to Mirabeau for the warm welcome and supervision during the first few months at CERMEL. I will also like to thank my colleagues from TU Delft (Gleb, JC, Tope, Prosper) as well as the TU Delft Admin for the warm environment made available during our pre-validation phases of our research at the University. Special thanks to my new colleagues (Eric, Justin, Krishna, Nomchit, Julien, Niko) for the support and friendly environment made available for a nice and smoothy transition into my next career path while concluding my PhD.

Appendix

To my family, mama Pauline, big mami Theresa, Siani (Manyi and Tanyi). Thank you for your support, patience and for believing in me. Thank you Leticia, Thierry Miguel, Kamani and Alain for your moral support through this process. To my friends Fabrice, Finley for your moral support through this journey of mind. Friends from LTV de Merewijk Loek, Leanne, Remco, Twan for the extra-curricular activities (including the tennis competitions and tournaments) we had together during my PhD journey. Finally to almighty God for life and good health throughout this period.